Calhoun: The NPS Institutional Archive
DSpace Repository

Theses and Dissertations 1. Thesis and Dissertation Collection, all items

1968

Load test analysis at Toa Industrial Site, Kawasaki, Japan.

Donnelly, William Patrick

Massachusetts Institute of Technology

http://hdl.handle.net/10945/40064

This publication is a work of the U.S. Government as defined in Title 17, United States Code, Section 101. Copyright protection is not available for this work in the United States.

Downloaded from NPS Archive: Calhoun

Calhoun is the Naval Postgraduate School's public access digital repository for research materials and institutional publications created by the NPS community. Calhoun is named for Professor of Mathematics Guy K. Calhoun, NPS's first appointed -- and published -- scholarly author.

Dudley Knox Library / Naval Postgraduate School
411 Dyer Road / 1 University Circle
Monterey, California USA 93943

http://www.nps.edu/library

NPS ARCHIVE
1968
DONNELLY, W.

Master of Science

LOAD TEST ANALYSIS AT TOA INDUSTRIAL SITE, KAWASAKI, JAPAN

by

WILLIAM PATRICK DONNELLY

Course I September 1968

DUDLEY KNOX LIBRARY
NAVAL POSTGRADUATE SCHOOL
MONTEREY CA 93943-5101

LOAD TEST ANALYSIS AT
TOA INDUSTRIAL SITE, KAWASAKI, JAPAN

BY

WILLIAM PATRICK DONNELLY
BS, U. S. Naval Academy
(1965)

Submitted in partial fulfillment
of the requirements for the degree of
Master of Science
at the
Massachusetts Institute of Technology
(September 1968)

Signature of Author . . . William Patrick Donnelly . . . . . .
Department of Civil Engineering, 19 August 1968

Certified by . . . T. William Lambe . . . .
Thesis Supervisor

Accepted by . . . .
Chairman, Departmental Committee on Graduate Students

ABSTRACT

LOAD TEST ANALYSIS AT
TOA INDUSTRIAL SITE, KAWASAKI, JAPAN

by

WILLIAM PATRICK DONNELLY

Submitted to the Department of Civil Engineering on 19 August 1968 in partial fulfillment of the requirements for the degree of Master of Science.

Heavy loads on soft soil layers are becoming a common problem as good available sites are used up. Much of the industrial land around Tokyo has been reclaimed by pumping fill hydraulically over soft clay layers which underly Tokyo Bay. The weight of the fill and deep pumping of water in the area are causing area-wide compression of the clay layers. This settlement, combined with settlement under the weight of tanks on the reclaimed sites, is enough to cause serious problems.

A test embankment was placed on the Toa Industrial Site 400 in order to evaluate these settlements. Carrier (1966) attempted to predict before-hand, by one-dimensional analysis, the Skempton-Bjerrum method and by the Lambe Stress Path method, the initial excess pore pressure and settlement due to this test load. The predictions were compared with actual field data and the differences rationalized by considering the methods of prediction. It was found that the stress path method gave the most reasonable results and that all methods of prediction improved when stress increments calculated by the finite element technique rather than elastic theory were used.

Thesis Supervisor: T. William Lambe

Title: Professor of Civil Engineering

ACKNOWLEDGEMENTS

The author wishes to thank for his advice and encouragement, Professor T. W. Lambe, Head of the Soil Mechanics Division, who supervised this thesis.

Appreciation is also expressed for the help of R. H. McGillvary who made many suggestions concerning the laboratory work necessary for the completion of this thesis.

Acknowledgement is due to many others, both staff and students, of the Soil Mechanics Division for their help in various areas of the thesis.

Finally, the author wishes to express his appreciation to his wife Mary-Anne whose patience, encouragement, corrections and meticulous typing of the manuscript were essential to its completion.

TABLE OF CONTENTS

PAGE

Title Page 1
Abstract 2
Acknowledgements 3
Table of Contents 4

Chapter I Introduction 6

Chapter II Description of the Toa Industrial Site and Load Test 8
- A. Site History 8
- B. Soil Profile 8
- C. Site Settlement 9
- D. The Load Test 10

Chapter III Performance of the Load Test 13
- A. Horizontal Movement 13
- B. Vertical Movement 13
- C. Pore Pressures 14
- D. Immediate Settlements 15
- E. Initial Excess Pore Pressures 16
- F. Percent of Consolidation 16

Chapter IV Comparison of Predicted and Measured Performance of the Load Test 19
- A. Introduction 19
- B. Discussion of the Results of Comparison 20

Chapter V Stress Calculations 29
- A. Introduction 29
- B. Moduli Used 29
- C. Stress Increments 31

PAGE

Chapter VI Revised Predictions of Initial Excess Pore Pressures and Compressions of Soil Layers 33
- A. Introduction 33
- B. One-Dimensional Analysis 33
- C. Skempton-Bjerrum Method 34
- D. Lambe Stress Path Method 35

Chapter VII Conclusions 41
- A. Introduction 41
- B. Areas of Greatest Uncertainty 42
- C. Suggestions for Future Work 42

List of Figures 44
List of Tables 96
List of References 116

CHAPTER I

INTRODUCTION

Heavy loads placed on soft soil layers constitute a problem area of soil mechanics. It is difficult to predict to what degree and how rapidly the load will settle. The purpose of this thesis is to analyze an actual case illustrating this problem by comparing predicted and measured performances. From this comparison, tentative conclusions are reached regarding the actual mechanism of settlement and true soil parameters. This comparison also allows evaluation of prediction techniques used for load settlement.

Settlement under a load test on an industrial site in Kawasaki, Japan is the case to be analyzed. The soil profile of the site shows approximately 39 meters of soft clay overlaid by 11.4 meters of hydraulic fill. These two layers in turn rest on a rigid base of dense sand and stiff clay. An abundance of field data showing movements and pore pressures in each of the soil layers is available.

Predictions of pore pressures and settlements under the load test were made by Carrier (1966) and by the author. Carrier used three methods to predict pore pressures and settlements: One-Dimensional Analysis, Skempton-Bjerrum Method, and the Lambe Stress Path Method. The stresses and stress increments used in the soil tests associated with these methods were obtained from elastic theory. The author, after studying the field data and comparing it with Carrier's predictions, used for his predictions the same three methods but with different soil parameters and stress increments obtained by the finite element technique.

Comparisons were then made between the settlements and pore pressures, both predicted and actual, to determine which soil parameters and prediction technique best described the actual case.

CHAPTER II.

DESCRIPTION OF THE TOA INDUSTRIAL SITE AND LOAD TEST

A. Site History

A severe shortage of industrial land in Japan has necessitated hydraulic reclamation of land, especially in the Tokyo area. The site under consideration in this thesis is owned by Toa Nenryo Kogyo K.K., situated in Kawasaki City, and was made by reclaiming land in Tokyo Bay. Figure II-1 shows the location of the site (Site 400) which was filled during the period of April 1959 through January 1963 in two distinct phases. Using fill from both the canal and Bay, the northern and western sections were filled first, followed by the remaining portions.

B. Soil Profile

The soil profile of Site 400 is shown in Figure II-2. The base rock is mudstone overlaid with diluvial sediments extending upward to an elevation of about -50 meters. Desication and overburden removal overconsolidated the diluvial soils. They are therefore relatively strong and incompressible, having little effect on the foundation engineering problems at the site. The only complication resulting from the diluvium concerns the sand-gravel layer which is an aquifer. Inland from Site 400, water for industrial use is pumped from deep wells extending down to this aquifer.

The soils extending from an elevation of approximately -50 meters up to the surface are alluvial sediments. The 39 meters of soft clay have been divided into three layers on the basis of their engineering properties: Clay I, Clay II, and Clay III. The top stratum of Site 400 is the hydraulic fill, a clay-sand-silt mixture dredged from the Bay and canal.

Study of the field data and tests run in the Soil Mechanics laboratory at M.I.T. indicate that surface loads will affect only the fill and the three soft clays. Figure II-3 shows a generalized soil profile of these soil strata and their properties as determined from the laboratory tests. It is emphasized that the laboratory test results for permeability and coefficient of consolidation of the fill are higher than those of the clay layers. It is expected that consolidation of the fill under a load would occur more quickly than would take place in the clay.

C. Site Settlement

The reclamation area including Site 400 is settling, without structural weight being imposed, for two reasons. Water is being pumped from the sand-gravel aquifer, causing excess pore pressure in the soft clay, which results in consolidation of these layers as the pore pressure dissipates. The second reason is that consolidation of the same clay layers is still occurring under the weight of the placed fill.

Verification of these reasons can be obtained through examination of the piezometer data in the form of measured total head versus elevation as presented in Figure II-4. The pumping has caused the total head to drop below static head in the soil beneath Clay III while the addition of the fill has caused excess head above static in the clay layers. As these layers drain and consolidate, the total head will finally reach the line labelled steady state pumping. Site settlement will be complete at that time.

These two factors (consolidation due to pumping and consolidation under the fill) have resulted in 0.5 to 1.0 meters of settlement to date around Site 400. Figure II-5a shows the whole area settlement and Figure II-5b gives the true rate of settlement at Site 400.

Predictions have been made for the magnitude and rate of settlement caused by the two factors (Wong 1968, Lambe 1968). It is estimated that more than three meters of settlement of the ground surface will take place due to consolidation of the clay layers; consolidation will not be complete until after 1990. Comparisons of the predicted and actual rates of settlement are in very close agreement to date.

D. The Load Test

A test embankment was constructed on Site 400, as shown in Figure II-6, in order to gather data concerning bearing capacity and settlement as they relate to the subsoils in that area. The theory was that the data could be used to predict the performance of structures (such as oil tanks) to be built on the site at a later date.

The embankment was constructed in circular lifts of one meter in height to a final height of 6 meters and having a bottom diameter of 54.4 meters and top diameter of 40 meters. Construction of the test embankment commenced on 19 October 1966 and was completed 16 November 1966, each lift being placed over approximately four working days. Before construction of the embankment began, special treatment was given to soil sections which were to underly the embankment. One third of the area was treated with 85 triangularly spaced sand drains, each 40 centimeters in diameter and extending to a depth of 15 meters from the surface. In another third of the area, 235 paper drains were installed, also spaced triangularly and extending to a depth of 15 meters. No treatment was given to the remaining third portion of the area.

In order to observe and monitor the effects of the test embankment on the underlying soil layers, instrumentation was installed. A total of 14 settlement plates, 10 piezometers, and 3 inclinometers were positioned as shown in Figure II-7. Settlement plates S-2, 3, 4, 5, 7, 8, 10, 11, 13, and 14 are screw type while the remaining settlement plates (S-1, 6, 9, and 12) are plate type. Piezometers P-6 and P-7 are the Casagrande type (open-standpipe porous tube). Piezometers

P-1, 2, 3, 4, 5, 8, 9, and 10 are open-standpipe piezometers of the Geonor type. Inclinometer I-1 uses a stationary pendulum and electrical resistance. Inclinometers I-2 and I-3 are the Wilson type, employing electrical resistance and a pendulum which slides up and down the pipe.

CHAPTER III

PERFORMANCE OF THE LOAD TEST

A. Horizontal Movement

A great deal of instrumentation was installed under the test embankment in order to measure both vertical and horizontal movements of and pore pressures in the soil layers. The inclinometer readings measuring horizontal soil movement did not fluctuate from their initial values, indicating invalid readings or no horizontal displacement, probably invalid readings.

B. Vertical Movement

From the movement of the settlement plates it is possible to determine the compression of each of the soil layers and to compare these compressions with those of the same layer in an area with different treatment. Figures III-la, b, c, and d show the compression of the soil layers in each of the different areas. It is seen that the compression of Clay I, II, and III in Figures III-la and III-ld differ markedly from the compression of the same layers in Figures III-lb and III-lc. This difference is so great that it cannot reasonably be attributed solely to actual compression differences in the different sections. Based on soil properties and predictions from soil mechanics theory, it is concluded that the settlement curves showing compressions in the untreated and paper drain sections shown in Figures III-1b and III-1c represent actual movements and that settlement plates S-3 and S-14 (under the center and in the sand drain section) are reading incorrectly. The reason for the suspected error in settlement of these plates is that they were probably carried down by friction. Therefore, settlement curves based on compression of soil layers in the center and sand drain sections measured by these plates are not used, except to illustrate the large differences.

Figures III-2a, b, and c compare the compressions of the same soil layers in the paper drain and untreated sections; also, it is seen how much difference is caused by the faulty settlement plates (S-3 and S-14) in the center and sand drained sections. These figures indicate that special draining treatment has little effect on the magnitude or rate of settlement in any of the soil layers.

C. Pore Pressures

Piezometers were installed to measure pore pressures under the center and in each of the treated sections under the load test. (Piezometers P-5 and P-6 were either suspected damage during construction or ceased functioning on their own and were replaced by piezometers P-5a and P-6a. Piezometer P-10 was also discontinued but was not replaced.) Figures III-3a and III-3b show the pore pressures (as measured by these piezometers) versus time from date test embankment was placed.

It can be seen from these plots that the piezometers in the clay have a time lag of two months or more (from the time of embankment placement) before pore pressure buildup is registered. Also, piezometer P-5a has given very erratic readings which indicate it may be unreliable.

D. Immediate Settlements

Soft soil layers, when subjected to a heavy load, will undergo immediate settlement which is caused by a change in shape but not in volume of a soil element; there is no drainage or consolidation involved. It is possible, in this case, to estimate the magnitude of immediate settlement or compression of each of the soil layers by determining, from settlement plots such as Figures III-1b and III-1c, the compression of these layers at the middle of the loading period of the test embankment. Figures III-4a and III-4b show the same figures replotted to a larger time scale where 0 time is the middle of the loading period.

The drawback to this method of estimating immediate settlements is that the choice of the middle of the loading period as the point of average immediate settlement is somewhat arbitrary. In this case it is based on the assumption that a load placed uniformly over a specific period of time can be closely approximated by the full load placed instantly at the middle of the period (Taylor 1948). A slightly different choice of the time of average immediate settlement causes a large difference in magnitude of the estimates due to rapid compression of the soil layers during this time. However, in Figures III-4a and III-4b the curves have been extrapolated back to zero time rather than forward from the beginning of placement of the embankment. Therefore, the trend of the curves is due to consolidation and the immediate settlement, as shown by the intersection of these curves with zero time, should be more accurate. The results are shown in Table III-1.

E. Initial Excess Pore Pressure

From the piezometer data, it is possible in this case to make an estimate of initial excess pore pressures. Before this can be done, the pore pressure curves as shown in Figures III-3a and III-3b (since there is a time lag) must be extrapolated back to zero time. Again, the zero time is chosen as the middle of the loading period. As a first estimate, straight lines are used in the extrapolation. The initial excess pore pressures are the differences between the piezometer readings at the end of September 1966 and the extrapolated values at the middle of the loading period. They have been tabulated in Table III-2.

F. Percent of Consolidation

The pore pressure distribution due to the load test in the soil layers over a period of a year, as determined from the straight line extrapolation in Figure III-3a, has been plotted in Figure III-5. Using these figures, it is possible to determine (as shown in Table III-3) the degree of consolidation for every three months throughout the first year.

In this case, the extrapolation also has been up to the judgement of the individual. A slightly different angle of the straight line approximation can result in large differences in initial excess pore pressure.

One method of checking the reliability of the piezometer data and the accuracy of the straight line extrapolations to zero time is to compare the percentage of consolidation values during the year period to the actual settlement curves. For example, Clay I in the untreated section has compressed 57 centimeters in a year. If 57 centimeters less immediate settlement represents 69% of the consolidation under the test embankment as suggested by Figure III-5 and Table III-3, then the settlement curve based on the percent consolidation values for Clay I would appear as shown in Figure III-6a. Also shown in Figure III-6a is an actual curve for Clay I. The same procedure has been carried out for Clay II and III and the results are shown in Figure III-6b. It is seen that consolidation as determined from the straight line extrapolation does not occur as rapidly as indicated by the actual curve. The most probable reason is that a straight line extrapolation is not a good approximation of the actual case.

The extrapolations are probably more like those shown in

Figures III-7a and III-7b. (It was decided from Figure III-5 that the data from piezometer P-5a was too high and that P-5 gave a better representation of the actual case.) Using these figures to find new values for percent consolidation and applying them to a settlement curve results in the third curve shown in Figure III-6a and III-6b. Clearly, this curve is much closer to the actual settlement curve. Therefore, the curved line extrapolations in Figures III-7a and III-7b are closer to reality. Tables III-4 and III-5 give new values of initial excess pore pressures and percent consolidation based on the revised extrapolations in Figures III-7a and III-7b. Figure III-8 shows the revised pore pressure distribution under the center of the load test.

CHAPTER IV

COMPARISON OF PREDICTED AND MEASURED PERFORMANCE OF THE LOAD TEST

A. Introduction

Carrier (1966) predicted settlements and pore pressures along the center line under the test embankment by four methods: field data from embankments on Site 200, one-dimensional analysis, the Skempton-Bjerrum method, and the Lambe Stress Path method. He assumed that excess pore pressures comparable to those in the clays were also built up in the fill layer (undrained loading) and used this fact in his predictions. However, it was seen in Chapter III and Figure III-8 that there was no registered pore pressure build-up in the fill and therefore a drained loading probably more closely approximated the actual case. For these reasons the author directed most of his attention to a comparison of predicted and measured performance in the clay layers. Carrier's predictions, by the three theoretical methods, of amount and rate of compression of the soil layers are compared with the actual compressions in Figures IV-1a, b, and c. Shown in Figure IV-2 is the comparison of Carrier's predictions of initial excess pore pressure and the author's estimation of the actual initial excess pore pressures (Chapter III). Finally, Table IV-1 is a comparison of the predicted and measured immediate settlements.

B. Discussion of the Results of Comparison

1. Rate of Compression

The most obvious difference between the predicted and measured values of compression is the rate of compression in the clay layers. The predicted rates were based on a laboratory coefficient of consolidation c_v determined under one-dimensional conditions. Since the predicted rates were much slower than the measured rates of compression, it is certain that radial drainage plays a large role and the one-dimensional role does not come close to approximating the actual consolidation.

Unfortunately, the theory of three-dimensional consolidation is not satisfactorily advanced to be of use in this case. One method of overcoming this problem is to use a higher value of c_v than obtained in the one-dimensional case. Wong (1968) backfigured from the load test a c_v approximately 8 times greater than the c_v obtained in the laboratory. Further proof that the settlement under the test embankment is not one-dimensional is the fact that the rate of area-wide settlement, which is likely to be one-dimensional, compares closely with the rate predicted on the basis of one-dimensional consolidation.

2. Magnitude of Compression

Since the test embankment has been in place less than two years, and primary consolidation is probably not yet complete, an extrapolation must be used to estimate the final amount of compression of each clay layer. This was done by determining the percentage dissapation of excess pore pressure at a certain time from Figures III-7a, III-7b and III-8 as listed in Table III-5. With the percentage dissapation and measured amount of compression at the same time, it is possible to estimate the amount of compression at 100% dissapation of excess pore pressure. This has been done for each clay layer and the estimated values are compared with Carrier's predicted values in Table IV-2.

In order to establish reasons for the differences between the predicted and estimated final values of compression, the methods of prediction must be examined in more detail.

In Carrier's one-dimensional analysis, he used the following formula for primary consolidation:

$$\rho_c = \int \frac{c_c}{1+e_o} \log \frac{\bar{\sigma}_{vf}}{\bar{\sigma}_{vo}} \, dH$$

To determine values of $\bar{\sigma}_{vf}$, he added a vertical stress increment $\Delta\bar{\sigma}_v = 10.93 \text{ t/m}^2$ to $\bar{\sigma}_{vo}$ for each clay layer. This stress increment is greater than those determined by elastic theory and by the finite element technique, especially in the lower layers of Clay II and III. A graphical representation of the vertical stress increments determined by these three methods is given in Figure IV-3. Certainly the stress increments determined by elastic theory and the finite element technique are more realistic; this is supported by the comparison of predicted and estimated values of compression. The compression predicted for Clay I by one-dimensional means is slightly higher than the estimated value, while the compression predicted for Clay II and III is almost twice as great. The much larger value predicted for Clay II and III is probably largely due to the greater stress increments predicted by this method and used in consolidation tests on samples from these layers.

The Skempton-Bjerrum method (1957), developed for evaluating settlement in clays, is a semi-empirical method but is more realistic than one-dimensional analysis. This method recognizes that in settlement problems in clay, the total settlement has three components:

$$\rho = \rho_i + \rho_c + \rho_s$$

where ρ_i = initial settlement

ρ_c = primary consolidation settlement

ρ_s = secondary consolidation settlement

The initial (immediate) settlement is caused by a soil element changing shape but remaining at constant volume; the soil element undergoes undrained shear. Usually, ρ_i is computed by the theory of elasticity, assuming the soil mass to be isotropic and homogeneous. However, Carrier used a different method. He divided the soil profile into 26 layers, collected all the triaxial data available for these layers, normalized the data for each test, and prepared an average plot of strain from the undrained portions of the tests for each clay. He then determined the immediate settlement by multiplying each strain by the thickness of its corresponding layer. The results were shown in Table IV-1 and are good if the amount of settlement is considered.

For primary consolidation settlement, Skempton and Bjerrum used the same expression as for one-dimensional consolidation with the following modifications:

$$\rho_c = \int \frac{c_c}{1+e_o} \log \frac{\bar{\sigma}_{vf}}{\bar{\sigma}_{vo}} \, dH$$

or $$\rho_c = \int m_v \, \Delta\bar{\sigma}_v \, dH$$

where $$m_v = \frac{c_c}{1+e_o} \, \frac{\log \bar{\sigma}_{vf}/\bar{\sigma}_{vi}}{\Delta\bar{\sigma}_v}$$

and substituting Δu for $\Delta\sigma_v$

where Δu = initial excess pressure

$= \Delta\sigma_H + A(\Delta\sigma_v - \Delta\sigma_H)$

so that $$\rho_c = \int m_v \, \Delta u \, dH$$

This recognizes that settlements are controlled by $\Delta\sigma_H$ as well as $\Delta\sigma_v$.

The pore pressure parameter A is usually selected from a chart which gives a constant range of values of A for different types of clays. However, it has been shown that A is not constant for a given soil but depends on strain, amount of over-consolidation, anisotropic consolidation, type of shear, and environment.

Therefore, Carrier used a different method to select values of A . He calculated values for each of the original 26 layers from the normalized triaxial data. A comparison of his predictions of Δu for the Skempton-Bjerrum method and the measured values was shown in Figure IV-2 and will be discussed in the next section. It is seen that he under-predicted values of Δu for Clay I. If Clay II and Clay III are taken as one layer, and the predicted and measured values averaged, his prediction for Clay II and III is reasonably close to the measured value.

After determining u on a three-dimensional basis, the Skempton-Bjerrum method assumes the consolidation settlements are one-dimensional and uses the results of oedometer tests to determine the amount.

Thus:

$$m_v = \frac{c_c}{1+e_o} \; \frac{\log \bar{\sigma}_{vf}/\bar{\sigma}_{vi}}{\Delta\bar{\sigma}_v}$$

where $$\Delta\bar{\sigma}_v = \bar{\sigma}_{vf} - \bar{\sigma}_{vi}$$

and $\bar{\sigma}_{vi}$ is the vertical stress acting on the soil after undrained shear has occurred (Figure IV-4). It is not the same as $\bar{\sigma}_{vo}$, the in situ vertical stress used in the one-dimensional analysis.

Since $$\bar{\sigma}_{vf} - \bar{\sigma}_{vi} = \Delta u$$

then $$\Delta\bar{\sigma}_v = \Delta u$$

and the two cancel out in the formula for ρ_c , thus:

$$\rho_c = \int \frac{C_c}{1+e_o} \log \frac{\bar{\sigma}_{vf}}{\bar{\sigma}_{vi}} dH$$

Carrier used his predicted value of Δu for Clay I, which was lower than the field value as estimated by the author, in determining $\bar{\sigma}_{vf}$ for the preceding formula. This helps to explain why, using the Skempton-Bjerrum method, he predicted such a low value of compression for Clay I as compared to the field value estimated by the author (Figure IV-2).

Both the previous methods discussed, the one-dimensional analysis and the Skempton-Bjerrum method, have the same drawback: neither method really approximates what happens in the field. Figure IV-4 shows a first approximation of the actual stress path that is followed by a soil element under the load test. It also shows the stress paths that were followed in laboratory tests on soil samples for both methods of prediction discussed so far.

If the strains between the same vertical stresses were the same for different stress paths, the Skempton-Bjerrum method would be a simple and accurate way of determining settlements in clays if Δu could be predicted accurately. Unfortunately, the strains for two different stress paths between the same vertical stresses are not usually the same, as shown by Carrier (1966) in Figure IV-5.

The fact that different stress paths can result in large differences in strain, as seen in Figure IV-5, is another factor which contributed to the differences between actual and predicted values of magnitudes of compression.

In some cases, however, it is possible that this factor can compensate for the other errors. For example, in the Skempton-Bjerrum method where the Δu and thus $\bar{\sigma}_{vf}$ are under-predicted for Clay I, leading to a prediction of a smaller ρ_c, the larger strain given by the sample in the oedometer during the consolidation portion will lead to a larger prediction of strain than if the sample were run along the actual stress path.

To overcome these difficulties, Lambe (1967) developed the Stress Path method of predicting settlements where ρ_c is not based on oedometer tests but on three-dimensional triaxial tests which more accurately duplicate field conditions. An "average" soil sample is first consolidated to in situ stress conditions then loaded under the same stresses expected in the field at that depth (the stress increments are usually determined from elastic theory)--first in undrained shear, then consolidated at constant shear stress (Figure IV-4). The strain is then measured and multiplied by the thickness of the soil layer to determine settlement or compression.

In this case, Carrier determined initial excess pore pressure and immediate settlements in the same manner for both the Skempton-Bjerrum and Lambe methods.

Carrier selected the average soil samples, stresses, and stress increments on the basis of a 60-meter diameter embankment. After he completed his tests, the diameter of the proposed embankment was changed to 40 meters, making it necessary to normalize his data and assume the vertical strain was proportional to log $\bar{p}_f/\bar{p}_i$.

It is seen from Table IV-2 that the Lambe method gives prediction of magnitude of compression of the soil layers closest to the field values. Carrier (1966) lists the testing difficulties for this method which undoubtedly had some effect on the results.

3. Initial Excess Pore Pressure

Figure IV-2 compared Carrier's predicted values of initial excess pore pressure with those estimated by the author from field data. As was stated earlier and seen in Figure IV-2, the predicted value of excess pore pressure for Clay I is considerably lower than the field estimated value. There could be several reasons for this. The possibility of faulty piezometer data should not be ruled out, although the data for P-4 in Clay I is relatively consistent and the extrapolation to determine the initial excess pore pressure is supported by the field data for compression of Clay I. More likely, the error comes from the samples which were used in the triaxial tests upon which Carrier based his pore pressure predictions. Clay I appears to contain many small isolated pockets of sandy silt. When Clay I is taken as a whole, the pockets have little effect in decreasing pore pressure buildup or increasing dissapation. However, these pockets in a small triaxial sample do have the effect of decreasing initial excess pore pressure. Therefore, it is probable that initial pore pressures measured in the triaxial tests were low.

Another factor which can cause differences may be the fact that the stress increments in Clay I, due to the load test, bring Clay I under the center line very close, if not all the way, to failure (Chapter VI). If this happens in the field, the shear stresses are re-distributed along the center line, stopping further strain, and the pore pressures can continue to rise. In a triaxial sample reaching failure under undrained loading, pore pressures will stop rising and fall as the strain increases. Therefore, pore pressures obtained in the field in this way cannot be measured in the laboratory.

CHAPTER V

STRESS CALCULATIONS

A. Introduction

All of the methods which were used to predict settlements require that the stress increments due to the load test be estimated at various depths below ground surface. In the past, the most common way to do this has been by means of elastic theory in which the soil is assumed to be a homogeneous, isotropic, elastic halfspace. This assumption is invalid for most soils, thereby introducing errors into the calculation of stress increments, especially in the horizontal direction.

In the author's opinion, a better approach (which has been developed for use with computers) is the finite element technique because it can handle stratified soils whose layers have different moduli and Poisson's ratios. It therefore appears to be a much closer approximation to the actual case.

B. Moduli Used

Both elastic theory and the finite element technique require that Young's moduli and Poisson's ratios be determined in order to calculate the stress increments. Since elastic theory assumes that the soil is a homogeneous, isotropic, elastic halfspace, only a single value of Young's modulus and Poisson's ratio can be used.

For the finite element technique, a Young's modulus and Poisson's ratio is required for each different material used in the finite element analysis. The most significant errors which can occur using this technique are usually the result of incorrect moduli.

According to Ladd (1964, 1965), undrained moduli are dependent on several factors including stress level, anisotropy, and overconsolidation ratio. Wong (1968) discusses methods of obtaining undrained moduli for the soil layers under the load test considering these factors. He calculated undrained moduli by determining stress level and then using the finite element technique. He also backfigured them, using the immediate settlements of the load test and triaxial data on the Kawasaki clays reported by Lambe (1962).

In the field, the layer of fill drained much faster under the load test than the clay layers, as shown by the pore pressure data in the preceding chapters. Therefore, all shear which took place in the fill was considered drained shear and an undrained modulus was not determined for this layer.

Based on this assumption, Wong assigned to the fill a Poisson's ratio of 0.33 and backfigured from the load test a Young's modulus of 150 t/m^2.

Wong also obtained drained moduli for each of the clay layers using elastic theory and assuming one-dimensional loading.

Tables V-1a and V-1b summarize the values of moduli and

Poisson's ratio obtained by using the various techniques on the Kawasaki soils.

C. Stress Increments

In order to use elastic theory to determine stress increments, the soil layers must be lumped together so that a single average modulus and Poisson's ratio may be selected. Also, the test embankment must be replaced by an equivalent cylinder (Figure V-1). This was done for different values of Poisson's ratio. The stress distributions which result are seen in Figure V-1, showing that the vertical stress increment is independent of ν while the horizontal stress increment is not.

As stated before, the advantage of the finite element technique is its ability to handle problems involving soil layers having different moduli and Poisson's ratios. The input data for the computer is in the form of moduli and Poisson's ratio for each different material and numbers describing elements and nodal points of a mesh superimposed on the cross-section of the soil layers. The mesh used for this particular problem is shown in Figure V-2. A computer program called FEAST I was used which was developed by E. L. Wilson of the University of California in 1966 and modified by John Christian of M.I.T. The program allows close simulation of boundary conditions, such as the rigid layers under the soft clays.

The distribution of stress increments obtained by this method under undrained and drained conditions are shown in Figures V-3a and V-3b, respectively. Figure V-4 compares the elastic stress distribution with stress distributions obtained from the finite element technique, using both undrained and drained moduli and corresponding Poisson's ratio. Some important points to notice from this figure are the small differences in $\Delta\sigma_1$, as determined by the previously described methods, and the relatively large variance in $\Delta\sigma_3$. An error in calculating $\Delta\sigma_3$ will have no effect on the prediction of settlement by one-dimensional analysis. However, it will affect the determination of Δu needed in the Skempton-Bjerrum method of calculating settlements. The Lambe Stress Path method will be the most affected, however, since the terminating point of the stress path along which laboratory samples are taken in a triaxial test depends on both $\Delta\sigma_3$ and $\Delta\sigma_1$.

CHAPTER VI

REVISED PREDICTIONS OF INITIAL EXCESS PORE PRESSURES AND COMPRESSIONS OF SOIL LAYERS

A. Introduction

Analysis of the field data from the load test and comparison of these data with previously predicted performance illustrate what probably happens in the subsoil. Considering this, it is possible to revise certain aspects of the methods of prediction with new techniques (such as finite elements) in order to make better predictions. Suggestions are made for improvements of each of the three methods discussed previously. However, most of the effort has been spent on the Stress Path method since it is considered more realistic and straight-forward than the others and should eventually yield the best predictions.

B. One-Dimensional Analysis

If the diameter of the load test were large (relative to the thickness of the compressible strata), the one-dimensional method of prediction would be a good and simple approximation of the field case. This is not true in this example because consolidation has been shown to be three-dimensional. An improvement over Carrier's predictions, however, could be made in determining $\Delta\sigma_v$ by elastic theory or the finite element technique, rather than allowing $\Delta\sigma_v$, at all depths, to be equal to the stress increment added at the surface. This has been done for the load test with the results summarized in Table VI-1. These predictions are seen to be closer to the actual case than Carrier's original estimate. (Compare pore pressures with those in Table III-4 and settlements with those in Table IV-2.)

C. Skempton-Bjerrum Method

The Skempton-Bjerrum method of predicting settlements, as stated in Chapter III, is a better approximation of actual field conditions in this case. It considers immediate and secondary as well as primary compression, and comes closer to accounting for three-dimensional effects by using $\Delta\sigma_3$ in determining Δu and by using Δu in calculating settlements:

$$\Delta u = \Delta\sigma_3 + A(\Delta\sigma_1 - \Delta\sigma_3)$$

$$\rho_c = H\, m_v\, \Delta u$$

Skempton and Bjerrum recommend that parameter A be selected from a chart which, in the author's opinion, is very limited (especially for the inexperienced) since it neglects specifically the factors mentioned in Chapter III to which A is sensitive, and allows them only to be included intuitively. The author agrees with Carrier (1966) and Wong (1968) that the parameter A be determined from previous $\overline{\text{CIU}}$ and $\overline{\text{CAU}}$ tests on clay samples taken from Site 200. Values of A determined by this method are shown in Table VI-2.

Figure V-4 illustrated the relatively large differences in the Clay I layer between the $\Delta\sigma_3$ determined by elastic theory and the $\Delta\sigma_3$ determined by the finite element technique using undrained properties. The finite element technique gives higher values of $\Delta\sigma_3$ in Clay I, resulting in higher predicted values of Δu for that layer and bringing the predictions closer to the field measurement of Δu. This supports the author's belief that the finite element technique yields a better representation of stress distribution than does elastic theory. Use of a higher value of Δu in the one-dimensional formula employed by Skempton and Bjerrum for consolidation settlements should also give a larger value of compression in Clay I, bringing this prediction closer to the field data. A summary of the revised Skempton-Bjerrum predictions is given in Table VI-3.

The prediction of Δu and compression in Clay I is still lower than the field values. This may indicate that the A factor calculated for Clay I from triaxial tests on samples from Site 200 is not close to the A factor for Clay I in Site 400.

However, the predicted values of initial excess pore pressure, Δu, and compression for Clays II and III are relatively close especially using the A factor determined from $\overline{\text{CAU}}$ tests.

D. Lambe Stress Path Method

The stress path concept of predicting settlements and initial excess pore pressures uses tests which better duplicate field conditions than those used in the other methods. On this basis it is expected that the stress path method would yield better predictions. As was seen in Chapter IV, this was the case in Carrier's predictions. However, for the stress path method, stress increments determined by elastic theory were again used and, as noted previously, there are relatively large differences between horizontal stress increments calculated by the finite element technique. The stress path method will be the most affected by changes in $\Delta\sigma_3$ since the stress path along which samples are tested depends on $\Delta\sigma_3$ as well as $\Delta\sigma_1$.

Based on the assumption used in improving the previous prediction techniques (that the stress distribution determined by the finite element technique is more accurate than that provided by elastic theory), new effective stress paths for each of the clay layers were drawn. These are shown in Figures VI-1a, b, and c. The end points, E_c , were determined from the undrained stress increments $\Delta\sigma_1$ and $\Delta\sigma_3$, as shown in Figure V-4 and listed in Table VI-4. The undrained portions of the paths in Figure VI-1, E_o-E_i , were determined by estimating immediate strain for each layer under the load test, entering Carrier's curves of $q/\bar{\sigma}_{vc}$ versus axial strain at the appropriate strain to determine q , then from his normalized curves of $\bar{p}$ versus q , determining $\bar{p}$ for that q (Table VI-5). Carrier showed several normalized curves of q versus axial strain and $\bar{p}$ versus q for each clay layer. For the preceding manipulations, it was therefore necessary to determine from his data average curves for each layer; these are shown in Figures VI-2a, b, and c.

Carrier assumed that vertical consolidation strain at constant shear stress in a triaxial test could be normalized similarly to vertical strain in an oedometer test. Based on this assumption, he plotted curves of $\bar{p}_f/\bar{p}_i$ versus vertical strain from Kawasaki Site 400 clay samples. Using this data it is then possible to calculate strains for consolidation at constant shear stress as takes place in the proposed stress paths. The predictions of ρ_c and Δu based on these stress paths are given in Table VI-6. It is noticed that these predictions, when compared with the field data in Tables III-4 and IV-2, are closer than the predictions made by Carrier based on stress paths using stress increments determined from elastic theory.

An example of a field total stress path for the effective stress paths just constructed would be as shown in Figure VI-3 for Clay I, where both $\Delta\sigma_1$ and $\Delta\sigma_3$ increase during undrained shear and then remain constant during consolidation.

During the undrained portion of the stress path, the soil element (sample) changes shape but not volume (see Figure VI-4a). It is quite reasonable, therefore, to assume a Poisson's ratio of 0.5. However, during consolidation (the drained part of the stress path), the soil element changes shape and volume (see Figure VI-4b). Poisson's ratio decreases during consolidation to a value of less than 0.5; this causes a change in total stresses. These facts are reflected in the stress increments determined by the finite element technique (see Figure V-4). Assuming a Poisson's ratio of 0.33 gives a smaller value of $\Delta\sigma_3$ than for a Poisson's ratio of 0.5, especially in Clay I. Poisson's ratio, however, has comparatively little effect on the vertical stresses. The change, then, in vertical effective stress during consolidation is equal to the initial excess pore pressure while horizontal effective stress during consolidation decreases with the total horizontal stress. Probably a better representation of the effective and total stress paths for an element in the middle of the Clay I layer is as shown in Figure VI-5. The stress values are given in Table VI-7.

To test this theory, the author attempted to duplicate this stress path in triaxial tests on samples from near the middle of Clay I. The undisturbed samples came from boring I-16, located as shown in Figure II-6. The stress path tests were conducted according to the steps outlined by Guertin (1967) except that the stress-controlled K_o consolidation was carried out in a strain control loading frame so that the triaxial cell did not have to be moved between the stress-controlled and strain-controlled portions of the test. This modification eliminates disturbance to the sample caused by the move. The samples were consolidated anisotropically along the K_o line to three times the in situ vertical effective stress in order to eliminate the disturbance effects of sampling procedures and handling.

It was expected that effective stress paths for the undrained portion of the tests would roughly approximate those of Carrier's, as shown in Figures VI-3 and VI-5 (E_o-E_i). This, however, was not the case. Figure VI-6 (E_o-E_i) shows the undrained portion of the stress paths as recorded in these tests. There are two reasons which may account for the difference. First, as mentioned earlier, the layer of Clay I contains many small isolated pockets of sand. It is possible for a triaxial sample to consist of as much as 50% sand which is certainly not representative of Clay I. This may have been the case with Carrier's samples, causing his results to differ from the author's. The other reason for the difference may be the improvement of triaxial equipment in the M.I.T. laboratory between the time of Carrier's tests (1965-66) and the author's. The author feels that his results better approximate what actually happened in the field.

The results of these tests were normalized and are shown in Figures VI-6, VI-7 and VI-8, and summarized in Table VI-8.

The initial excess pore pressure obtained in these tests were much higher than expected from Carrier's data but very close to the estimated field value for Clay I. Strains in the samples tended to go slightly higher than would be expected on the basis of field measurement. This could be explained by the fact that the stress path comes very close to the failure envelope causing greater strains in a triaxial sample than in the field where the stresses probably redistributed, thereby retarding further strain.

It is felt that this stress path is more nearly correct than those previously discussed because it does consider the change in Poisson's ratio between drained and undrained shear. However, this type of stress path test must be carefully controlled, especially near failure, if it is to give accurate results.

CHAPTER VII

CONCLUSIONS

A. Introduction

Table VII-1 gives a summary of the predictions of initial excess pore pressures and compression due to primary consolidation in each of the soil layers. The same quantities determined from the field data are also shown.

It is seen that for each method, use of the finite element technique in determining stress increments produced an improvement in the predictions as compared with the field values. The author believes that the finite element technique is superior to elastic theory in calculating stress increments.

This table also shows that in using both elastic theory and the finite element technique, the Lambe Stress Path method gives predictions closest to the field values. The author feels that the stress path method is best because it is the only one of the three which attempts to duplicate field conditions. For this reason any improvements in techniques, such as in calculating stress increments, are adapted with more significance into the stress path method than into the others. As improvements such as these are added, predictions by the stress path method will converge on the true answer, while incorporation into the other methods may or may not. Certain aspects in the field, such as greater strains when a soil element nears the failure envelope, will not be reflected in tests used in the one-dimensional and Skempton-Bjerrum methods but will be included in the Stress Path method.

B. Areas of Greatest Uncertainty

As is evident throughout this thesis, the greatest uncertainty in predicting pore pressures and settlements under heavy loads in soft clay layers lies in the determination of stress increments in the subsoils. Although the finite element technique appears to be an improvement over elastic theory in this area, moduli (both drained and undrained) and Poisson's ratios are needed for each soil layer. Methods of determining these quantities are subject to error.

A danger in all soil tests, especially the stress path tests, is not choosing a representative soil sample. Therefore, care must be taken to insure that the soil profile is accurate (concerning relatively homogeneous layers) and that the samples to be tested are truly representative of these layers.

C. Suggestions for Future Work

1. Field Load Tests

When running a load test for the purpose of evaluating settlements and pore pressures, it is evident that great care must be taken in installing instruments (piezometers, settlement plates, and inclinometers) to give reliable data. Data from the inclinometers would have been valuable in evaluating horizontal stresses under the load. Even more valuable would be a load cell which could measure both vertical and horizontal total stress in the field without influencing them too much.

2. Laboratory Tests

The author believes that using a combination of drained and undrained stress increments to determine the stress paths, as was described in the final part of Chapter VI, gives a more accurate representation of field conditions and thus yields better predictions. The stress path tests conducted in this manner gave good results but more tests are needed to confirm this.

It is seen from Table VII-1 that all methods of predictions give reasonable results. For this reason it is felt that for simple, inexpensive jobs where the amounts of settlement are not critical, one-dimensional analysis and the Skempton-Bjerrum method may be preferred to the Stress Path method since stress path tests are more time consuming and expensive to run.

LIST OF FIGURES

FIGURE NO.		PAGE
II-1	Industrial Sites of Toa Nenryo, Kawasaki	47
II-2	Geological Profile	48
II-3	Generalized Soil Profile and Properties - Site 400	49
II-4	Measured Head on September 1966 - Site 400	50
II-5a	Kawasaki Site Settlement	51
II-5b	Settlement of Revetment - Site 400	52
II-6	Location of the Test Embankment - Site 400	53
II-7	Details and Instrumentation of Load Test	54
III-1a	Compression of Soil Layers - Center	55
III-1b	Compression of Soil Layers - No Treatment	56
III-1c	Compression of Soil Layers - Paper Drains	57
III-1d	Compression of Soil Layers - Sand Drains	58
III-2a	Compression of Fill	59
III-2b	Compression of Clay I	60
III-2c	Compression of Clay II and III	61
III-3a	Piezometer Readings and Straight Line Extrapolation Under Center of Load Test	62
III-3b	Piezometer Readings 12 Meters from Center of Load Test	63
III-4a	Compression of Soil Layers - No Treatment	64
III-4b	Compression of Soil Layers - Paper Drains	65
III-5	Pore Pressure Distribution under Center of Load Test (First Estimate)	66
III-6a	Comparison of Actual Settlement Curve and Curves Based on Percent Consolidation - Clay I	67

FIGURE NO.		PAGE
III-6b	Comparison of Actual Settlement Curve and Curves Based on Percent Consolidation - Clay II and III	68
III-7a	Piezometer Readings and Curved Line Extrapolation under Center of Load Test	69
III-7b	Piezometer Reading and Curved Line Extrapolation under Center of Load Test	70
III-8	Pore Pressure Distribution under Center of Load Test (Revised)	71
IV-1a	Comparison of Predicted and Measured Rate and Magnitude of Settlement - Clay I	72
IV-1b	Comparison of Predicted and Measured Rate and Magnitude of Settlement - Clay II and III	73
IV-1c	Comparison of Predicted and "Measured" Rate and Magnitude of Settlement - Fill	74
IV-2	Comparison of Predicted and "Measured" Initial Excess Pore Pressure	75
IV-3	Vertical Stress Increments Computed by Different Methods under Test Embankment	76
IV-4	Comparison of Stress Paths Used in Different Prediction Methods with Actual Field Stress Path	77
IV-5	Comparison of Strains along Different Stress Paths - Fill	78
V-1	Elastic Stress Distributions under Center-Line of Load Test	79
V-2	Mesh Used in Finite Element Analysis	80
V-3a	Stress Distribution under Centerline of Load Test Using Finite Element Technique and Undrained Moduli	81
V-3b	Stress Distribution under Centerline of Load Test Using Finite Element Technique and Drained Moduli	82
V-4	Comparison of Stress Distributions under Centerline of Load Test	83

FIGURE NO. PAGE

VI-1a Effective Stress Path in Center of Clay I under Centerline of Load Test 84

VI-1b Effective Stress Path in Center of Clay II under Centerline of Load Test 85

VI-1c Effective Stress Path in Center of Clay III under Centerline of Load Test 86

VI-2a Averages of Normalized Data for Clay I From Triaxial Tests Reported by Carrier (1966) 87

VI-2b Averages of Normalized Data for Clay II From Triaxial Tests Reported by Carrier (1966) 88

VI-2c Averages of Normalized Data for Clay III From Triaxial Tests Reported by Carrier (1966) 89

VI-3 Effective and Total Stress Paths for Middle of Clay I under Centerline of Load Test 90

VI-4a Soil Element under Undrained Shear 91

VI-4b Soil Element under Drained Consolidation 91

VI-5 Revised Effective and Total Stress Paths for Middle of Clay I under Centerline of Load Test 92

VI-6 Best Estimate of Effective and Total Stress Path in Field for Clay I and Lab Stress Path 93

VI-7 Normalized Stress Difference vs Vertical Strain Undrained Portion of Stress Path Test 94

VI-8 Normalized Stress Difference vs Vertical Strain Drained Portion of Stress Path Test 95

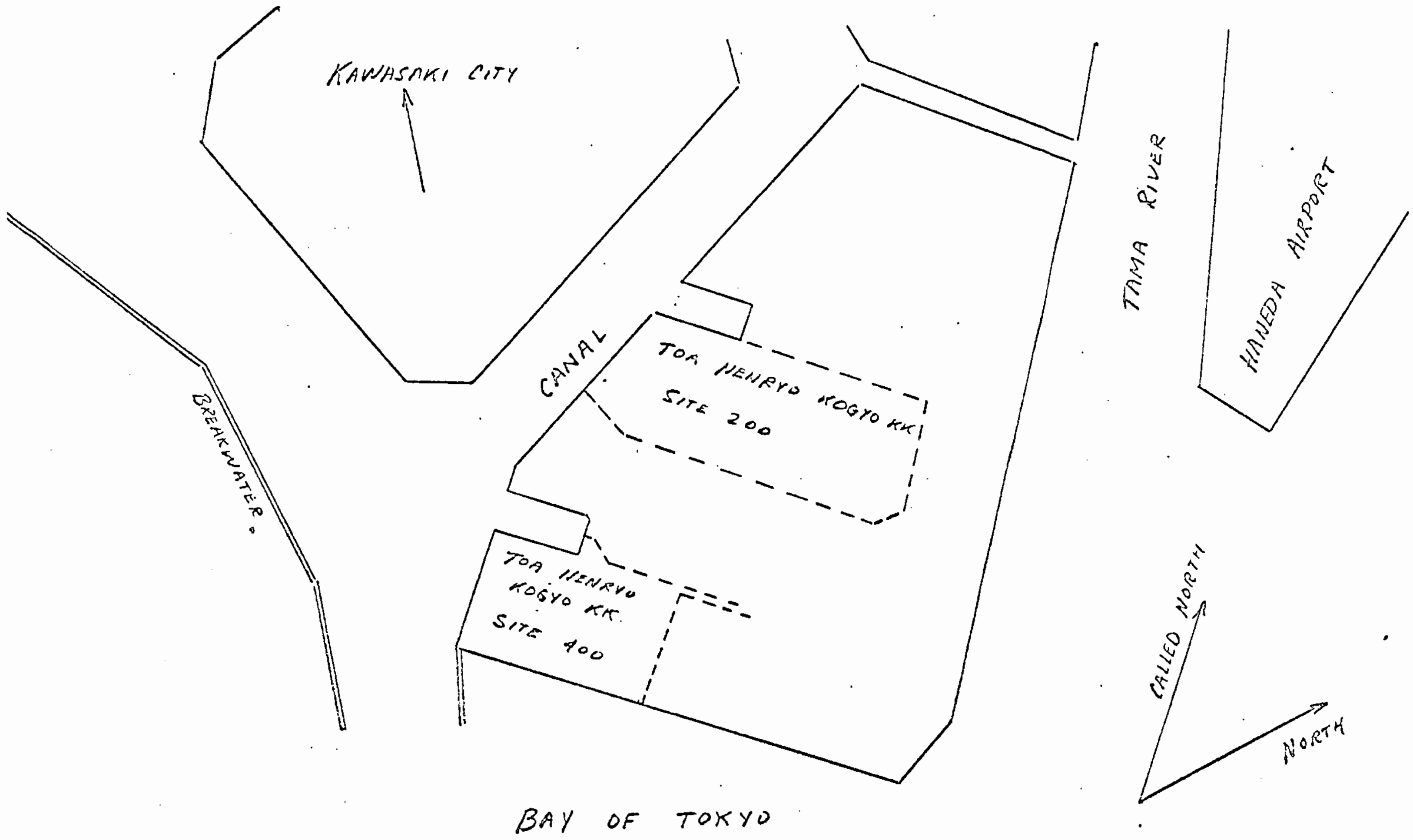

FIG. II-1 INDUSTRIAL SITES OF TOA NENRYO, KAWASAKI

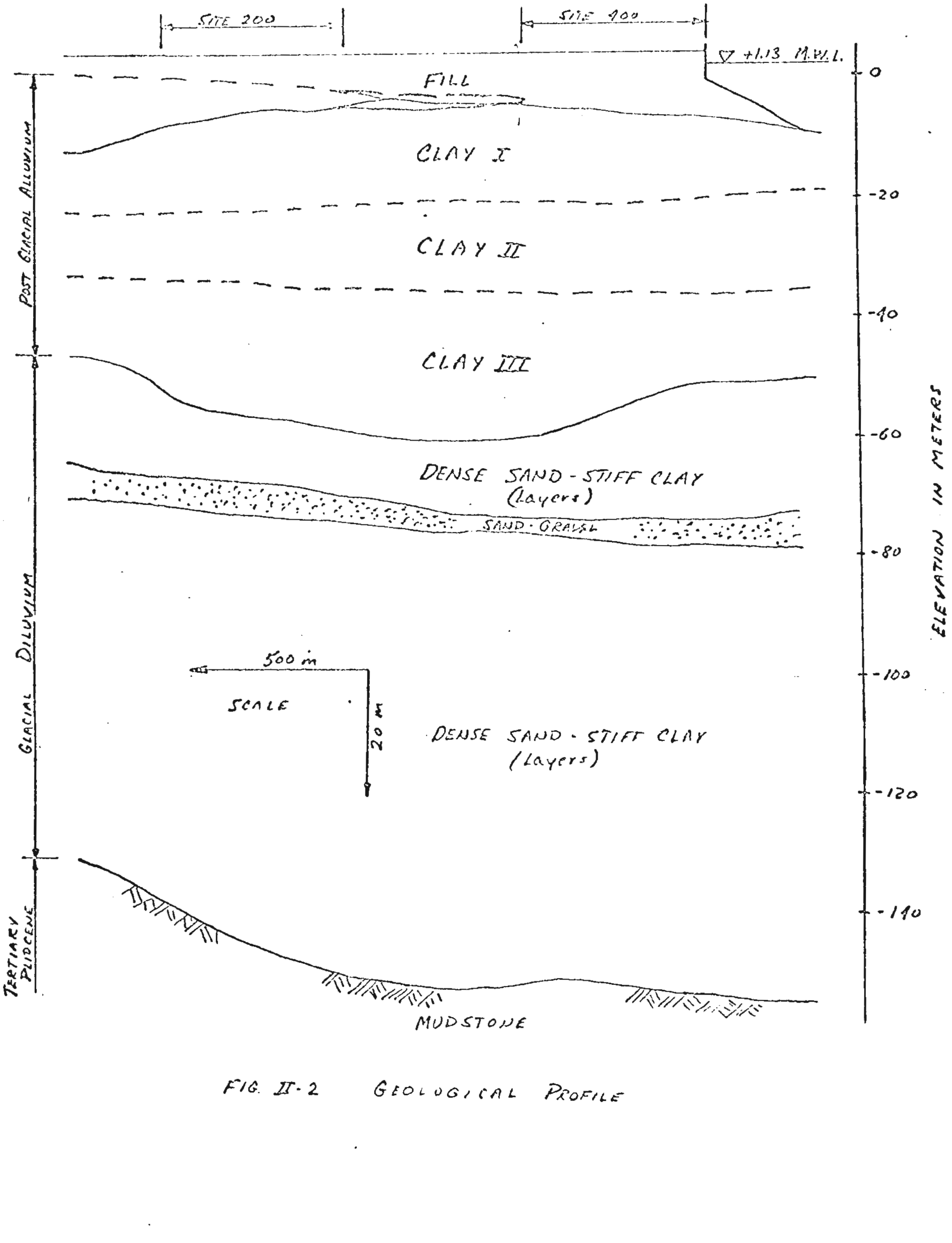

FIG. II-2 GEOLOGICAL PROFILE

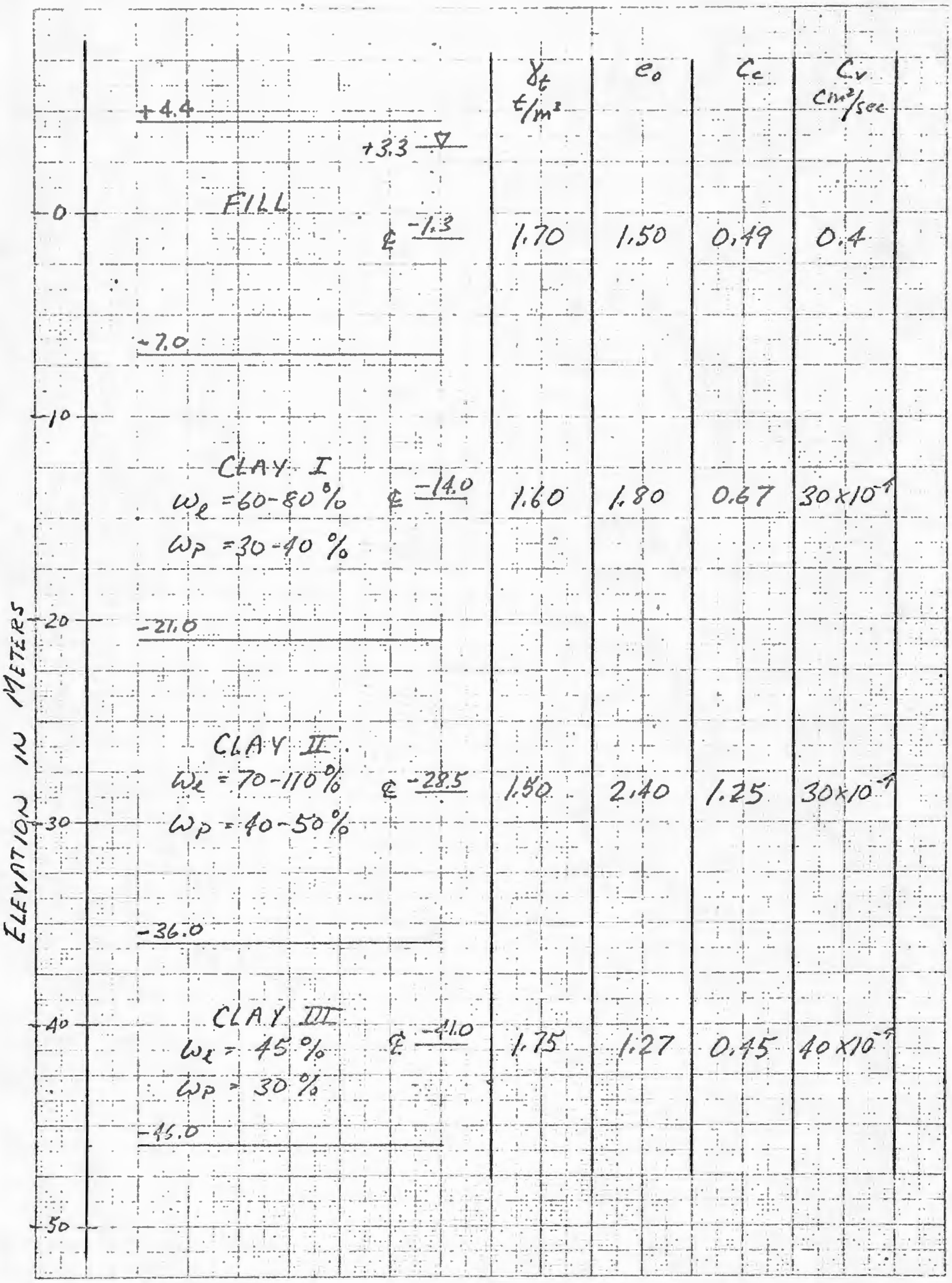

FIG II-3 GENERALIZED SOIL PROFILE AND PROPERTIES – SITE 400

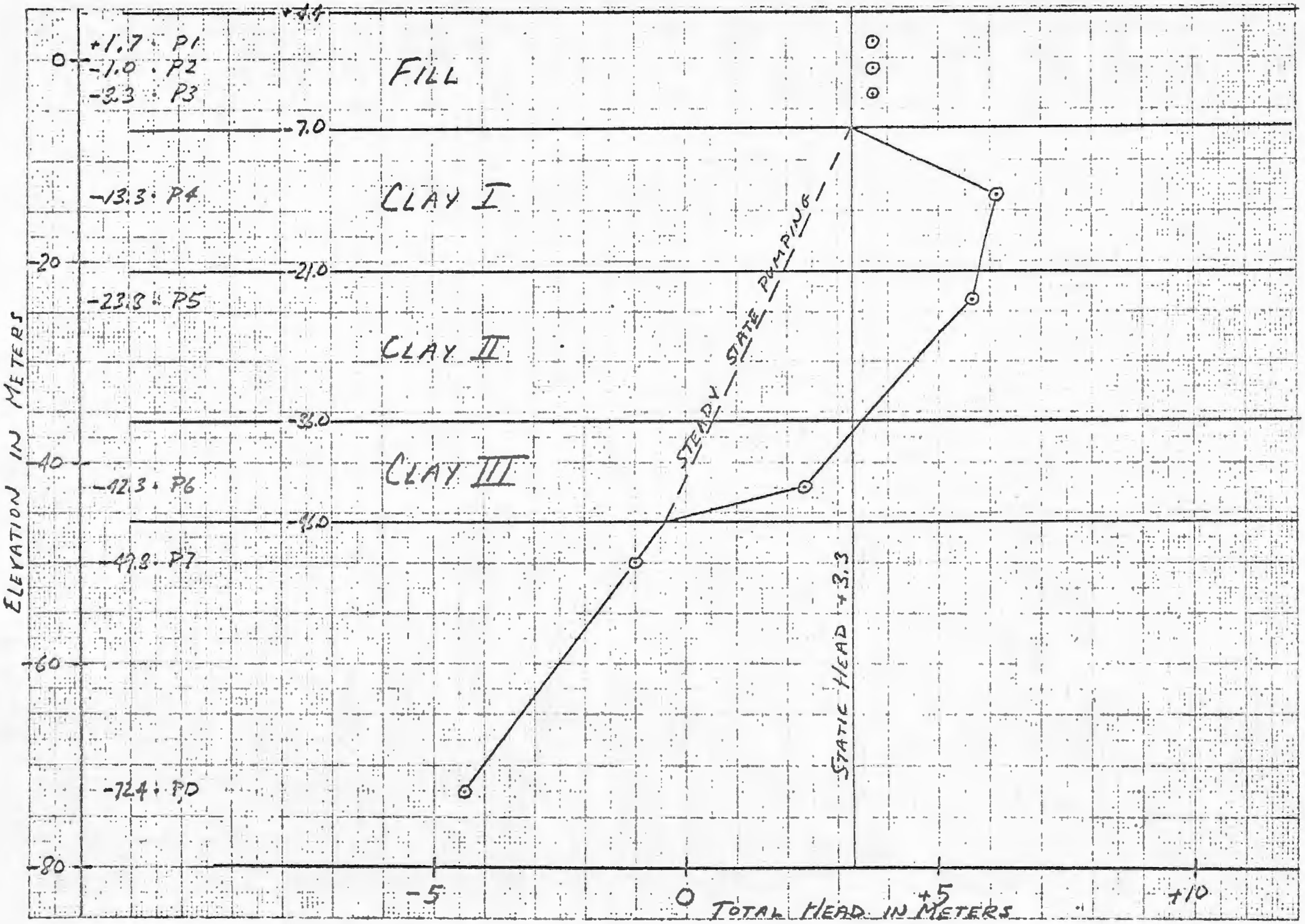

FIG. II-4 MEASURED HEAD ON SEPTEMBER 1966 SITE 400

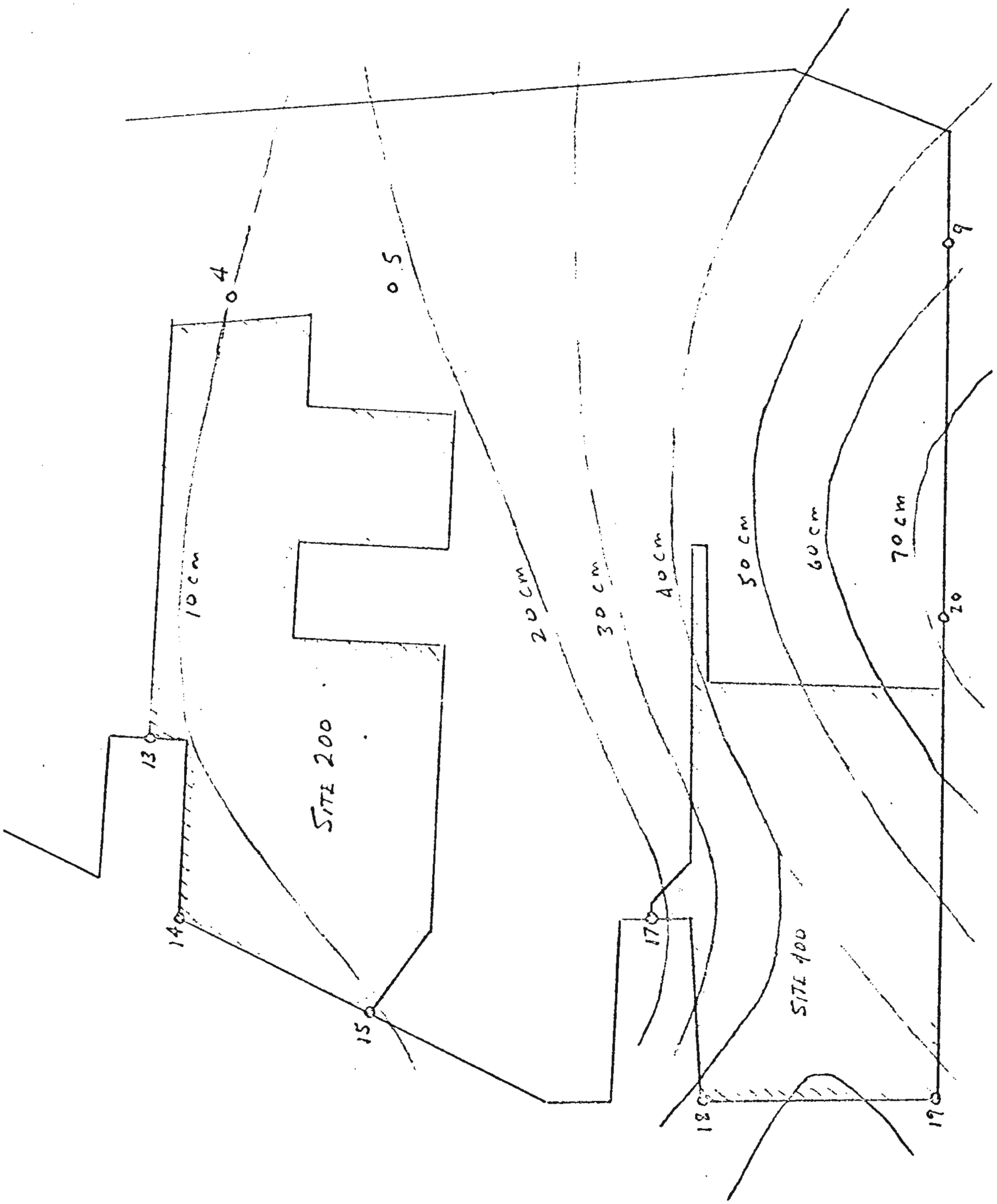

FIG. II-5a KAWASAKI SITE SETTLEMENT
July, 1963 to October, 1957

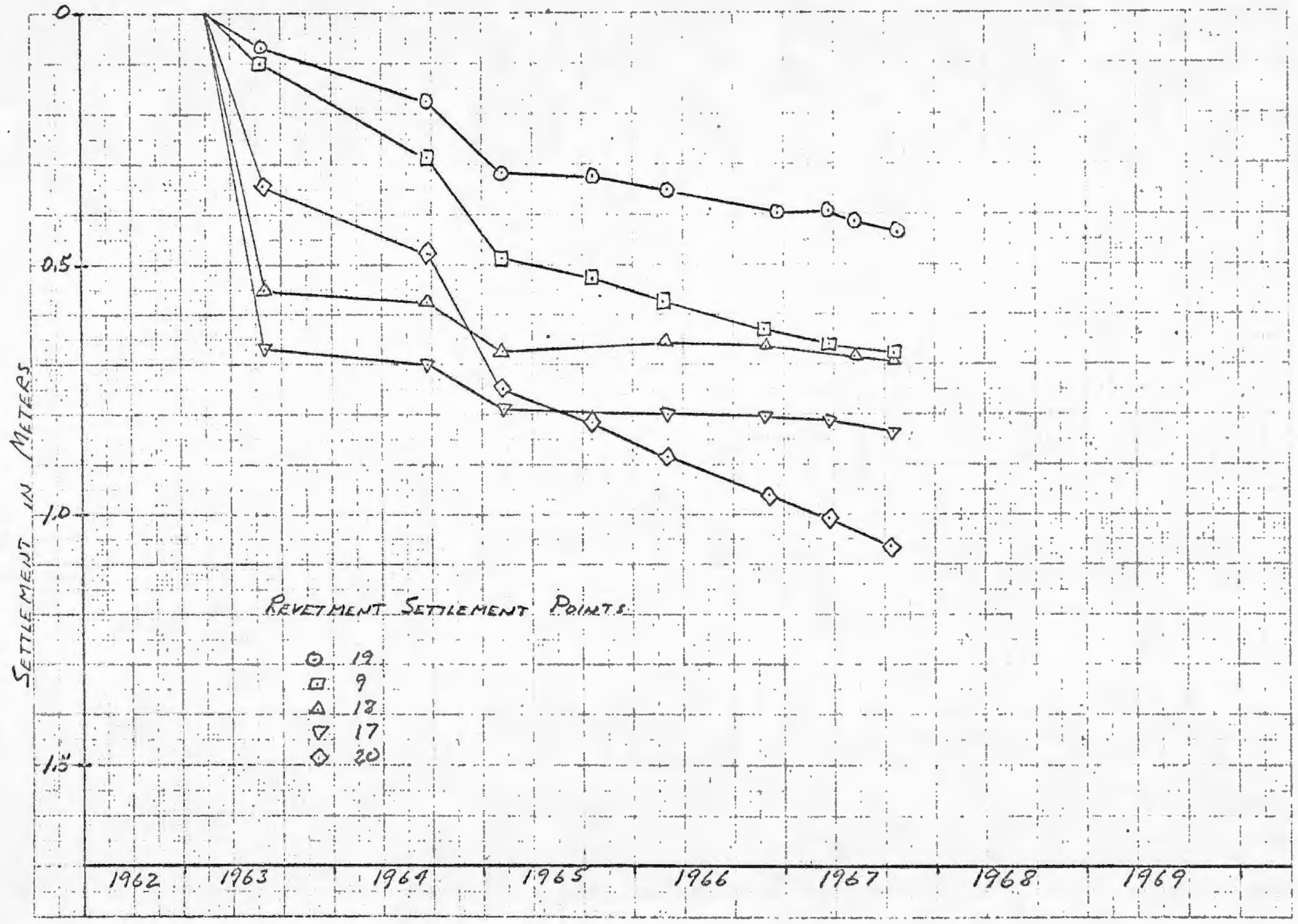

FIG II-5b SETTLEMENT OF REVETMENT SITE 400

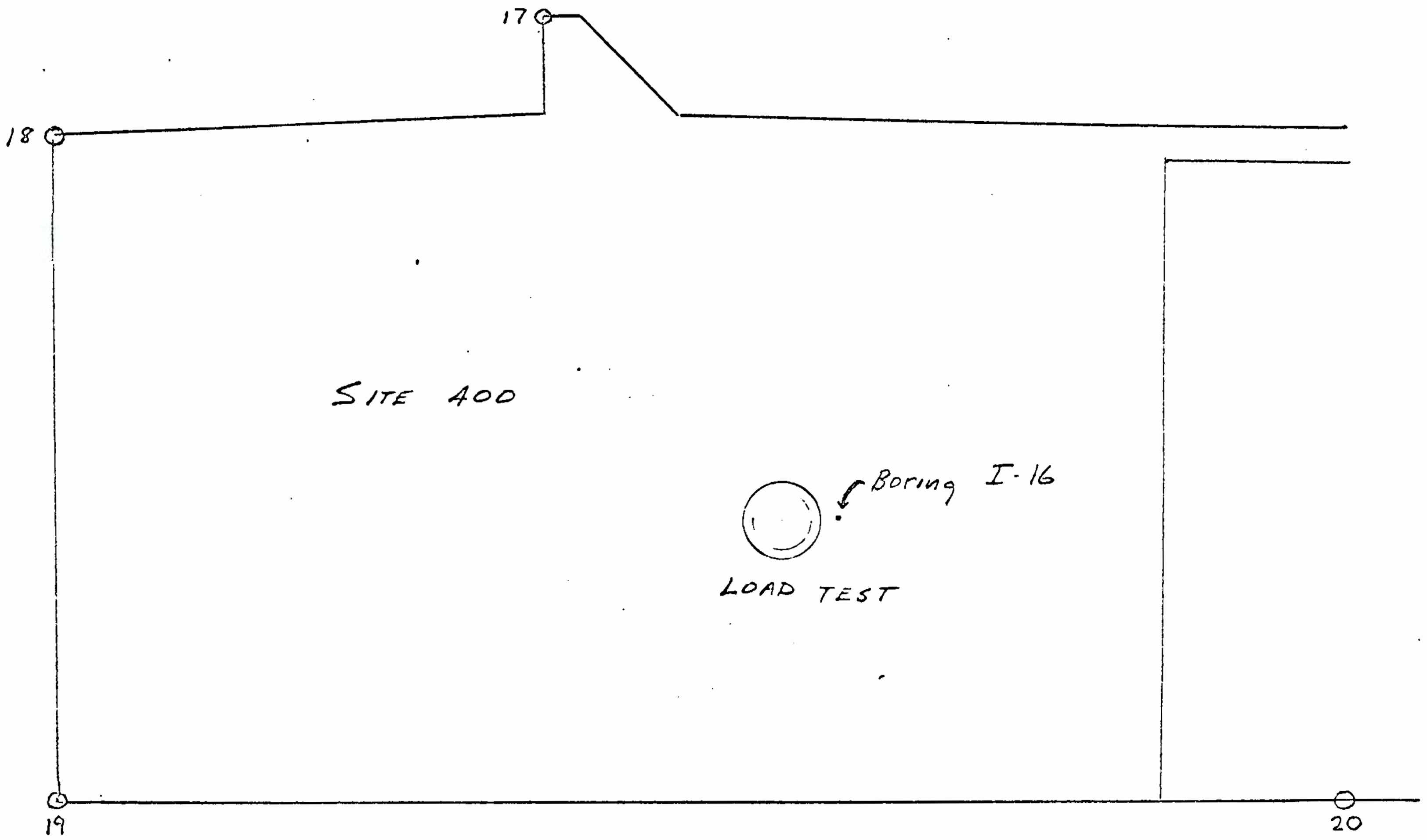

FIG II-6 LOCATION OF THE TEST EMBANKMENT SITE 400

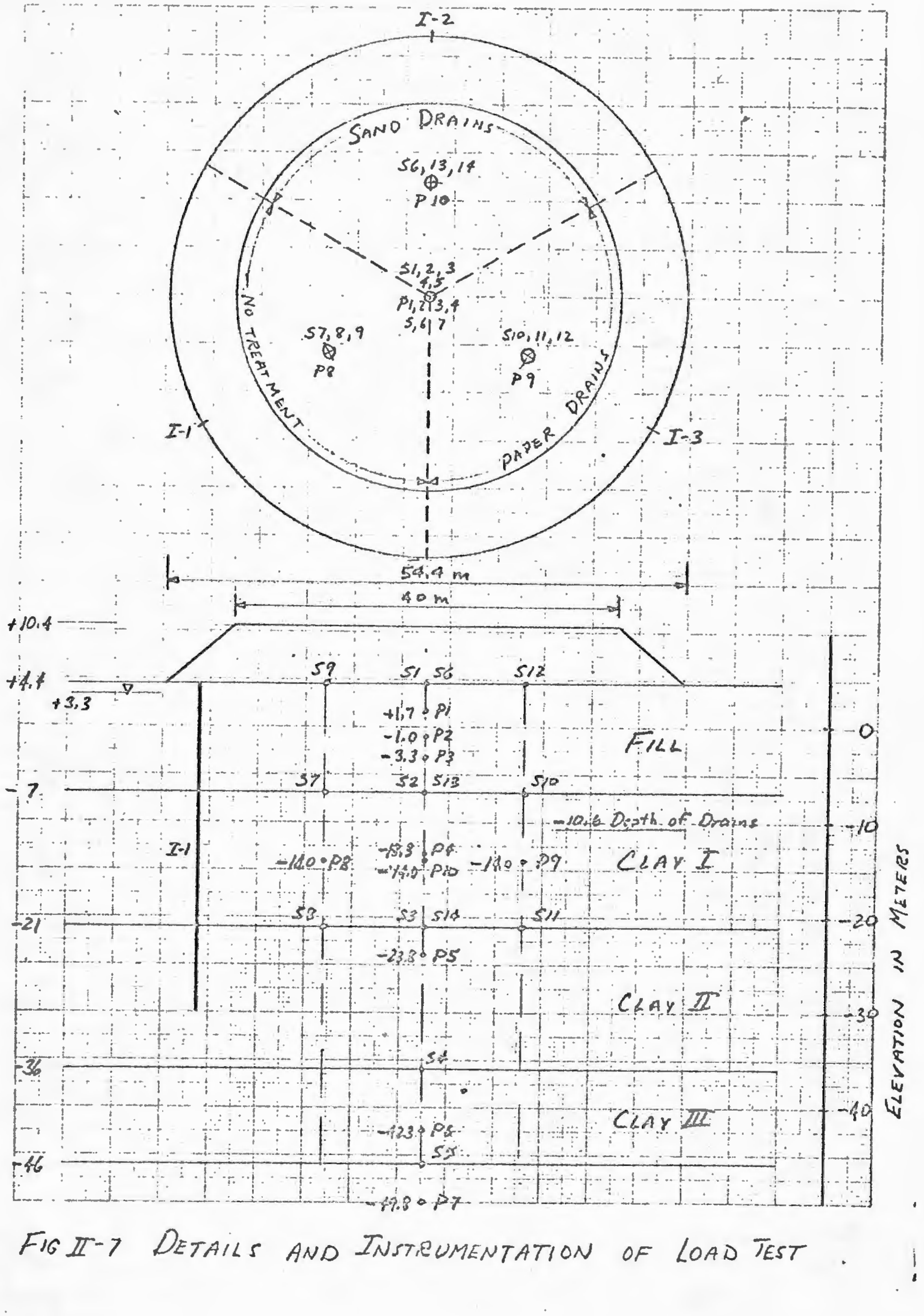

FIG II-7 DETAILS AND INSTRUMENTATION OF LOAD TEST

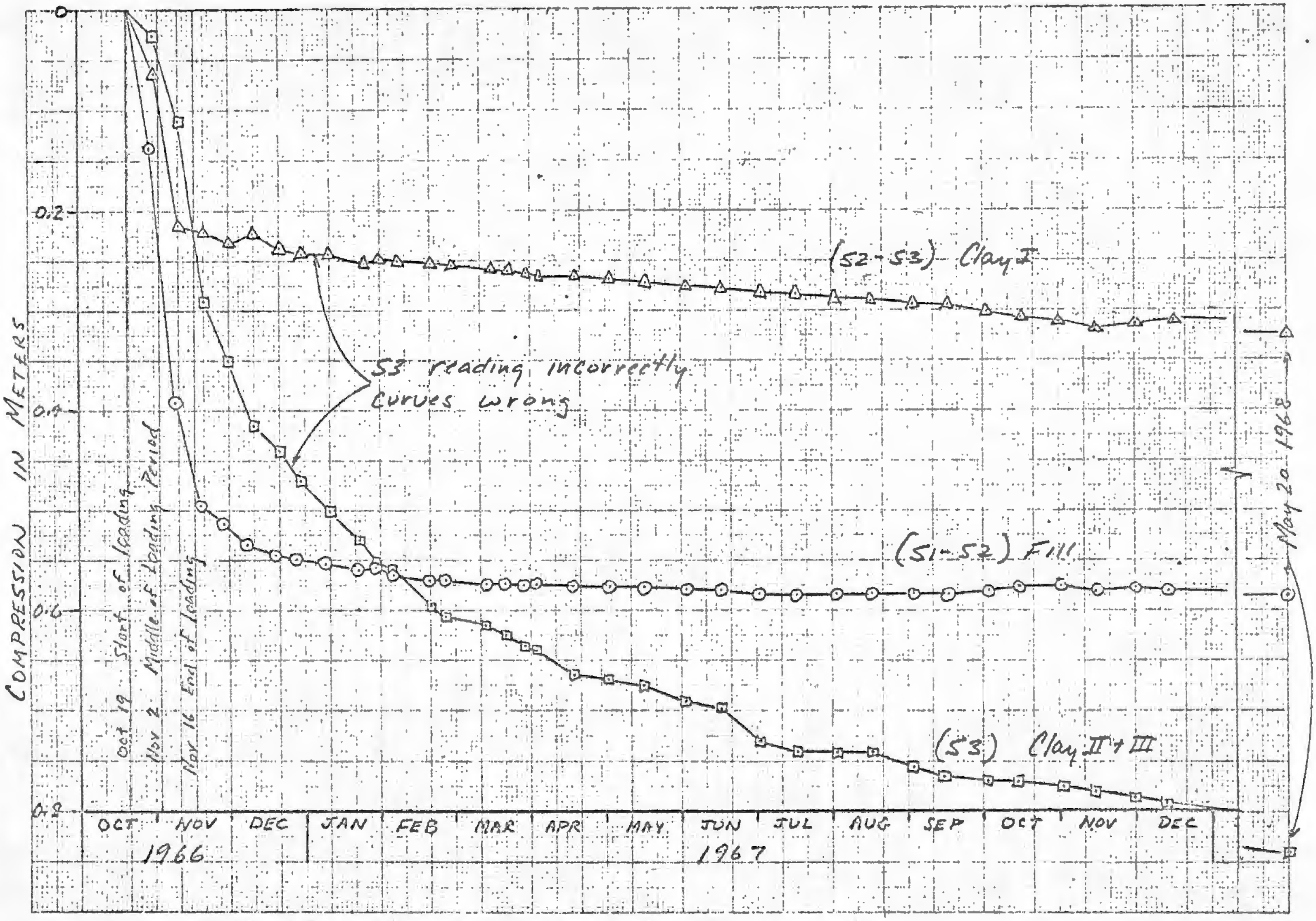

FIG III-1a COMPRESSION OF SOIL LAYERS - CENTER

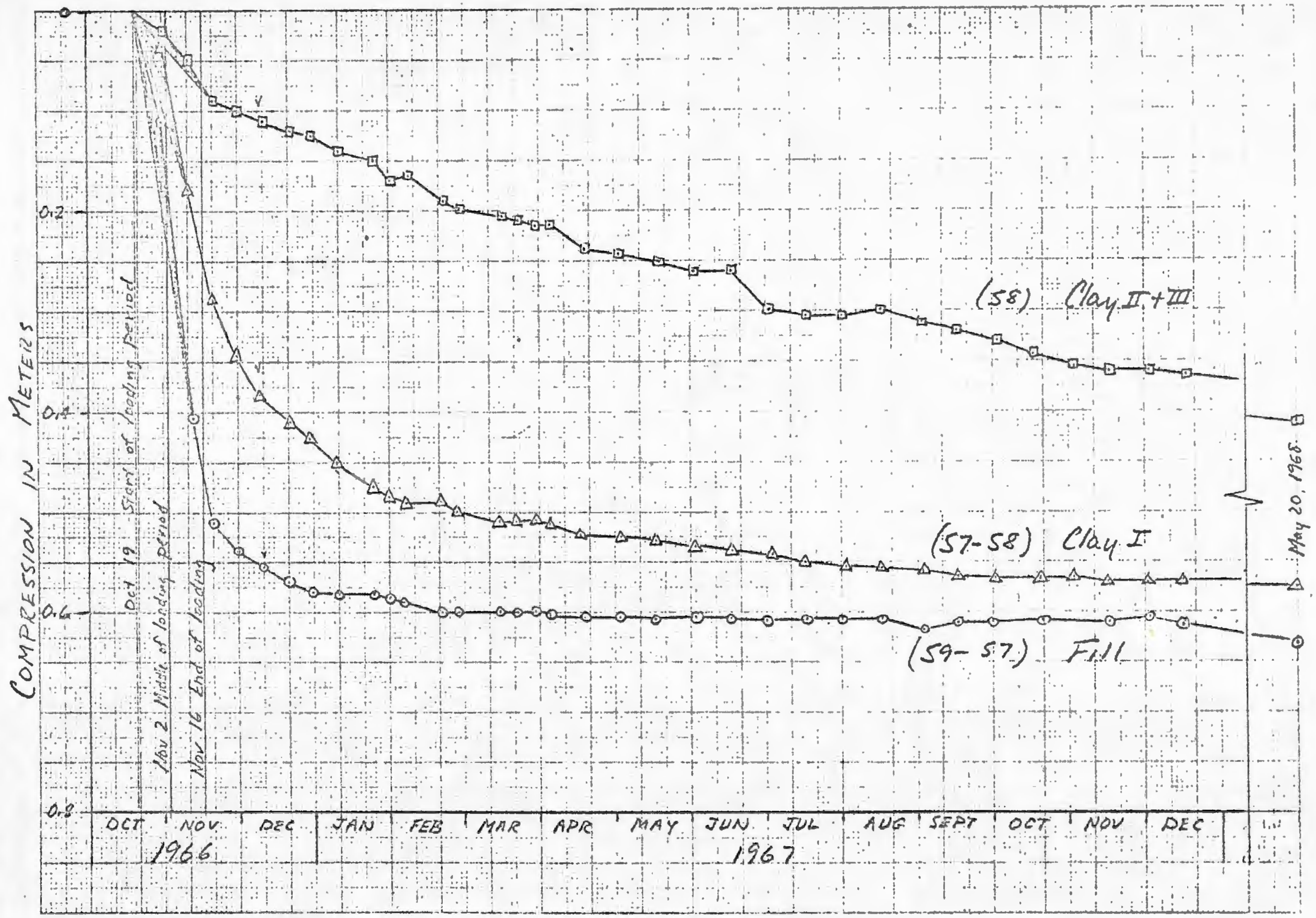

FIG III-16 COMPRESSION OF SOIL LAYERS - NO TREATMENT

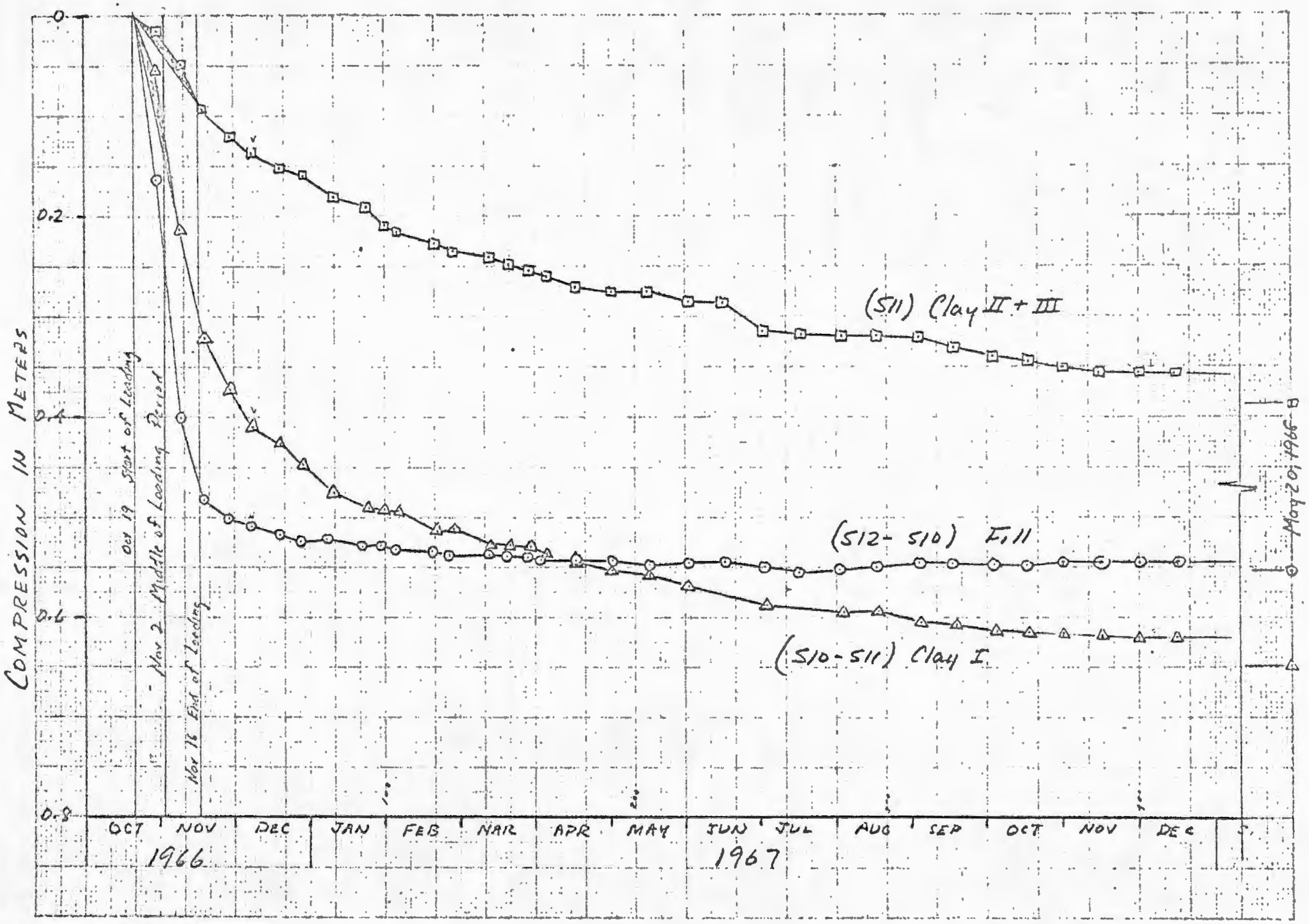

FIG III-1c COMPRESSION OF SOIL LAYERS - PAPER DRAIN SECTION

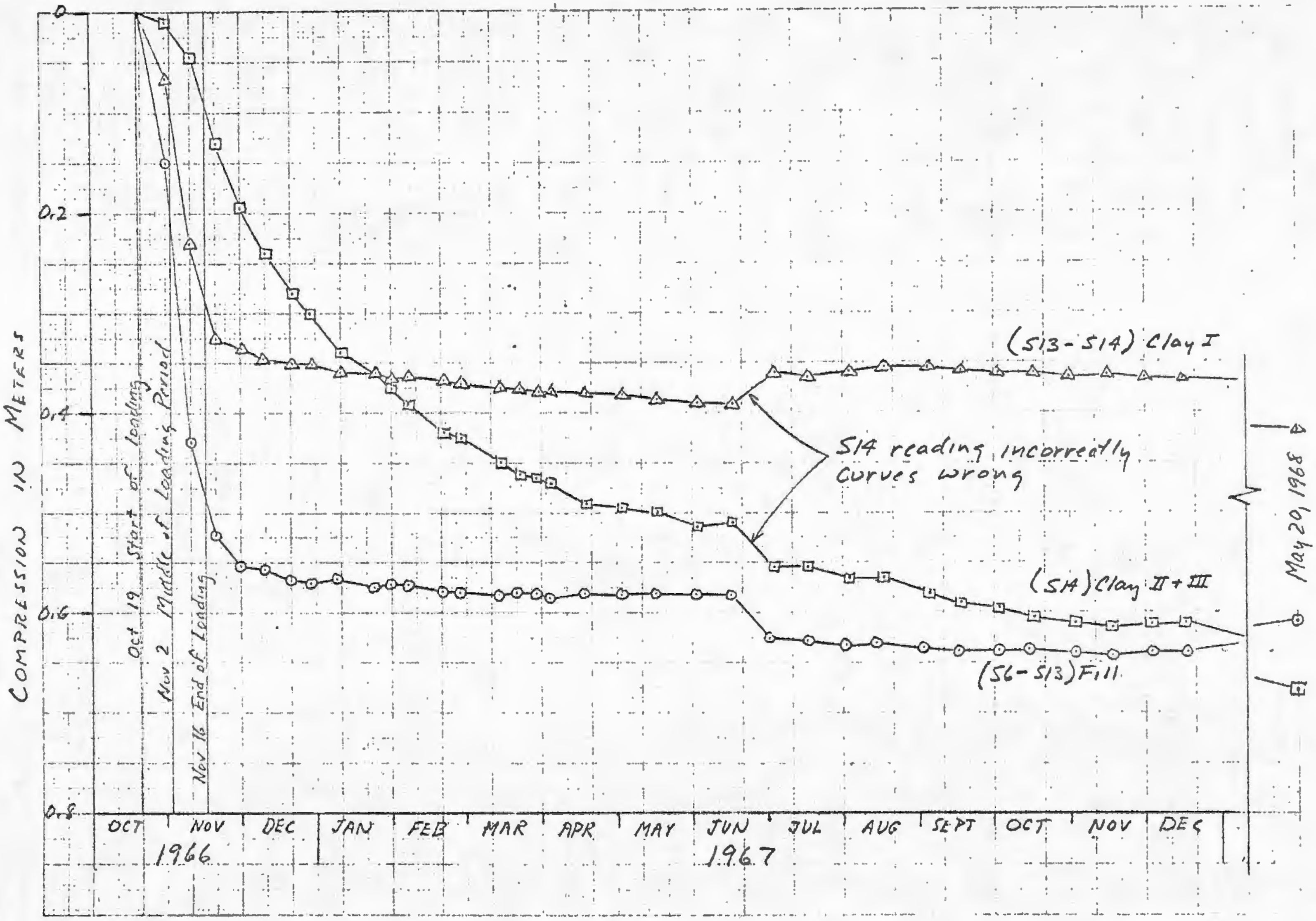

FIG III-1d COMPRESSION OF SOIL LAYERS - SAND DRAIN SECTION

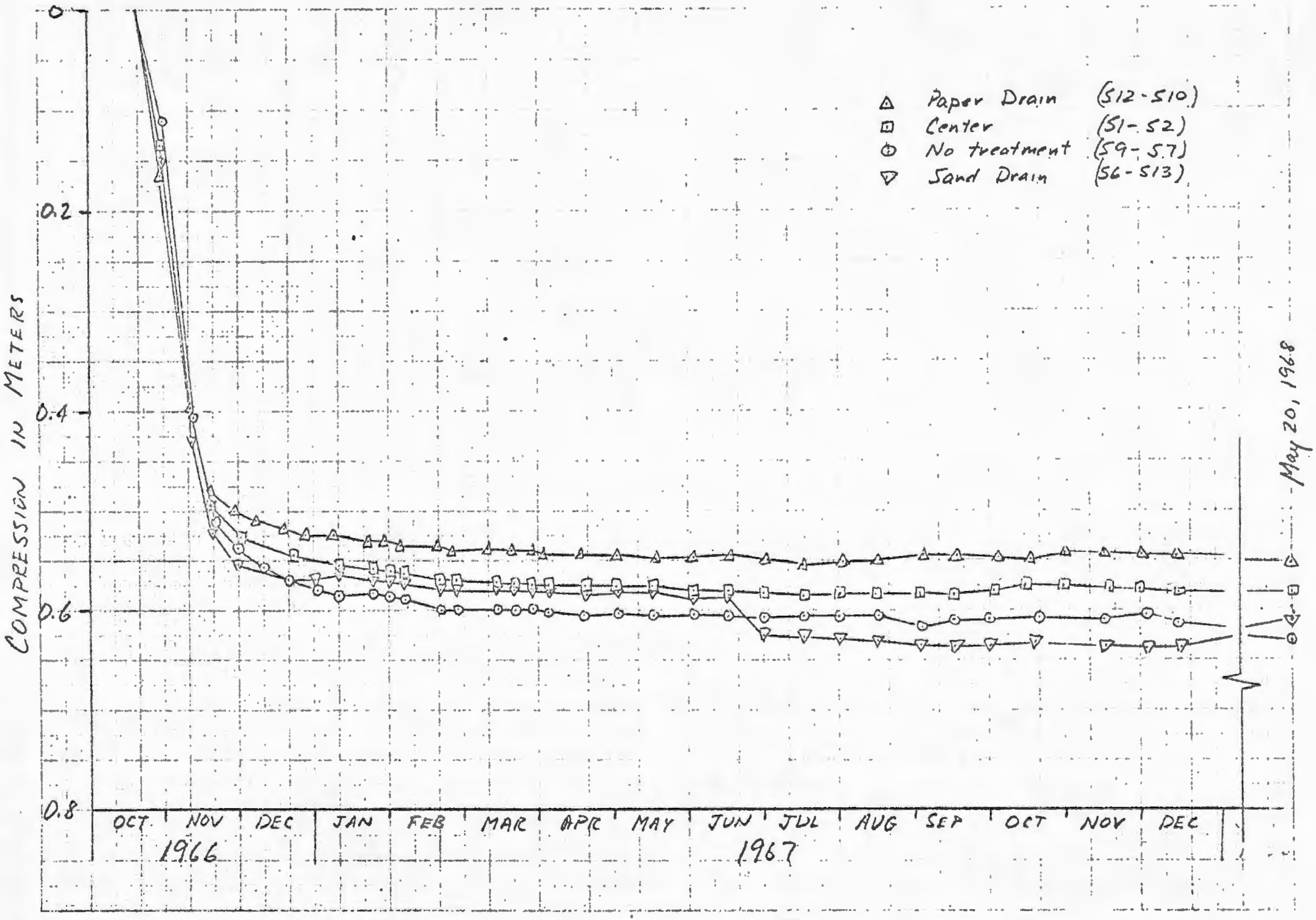

FIG III-2a COMPRESSION OF FILL

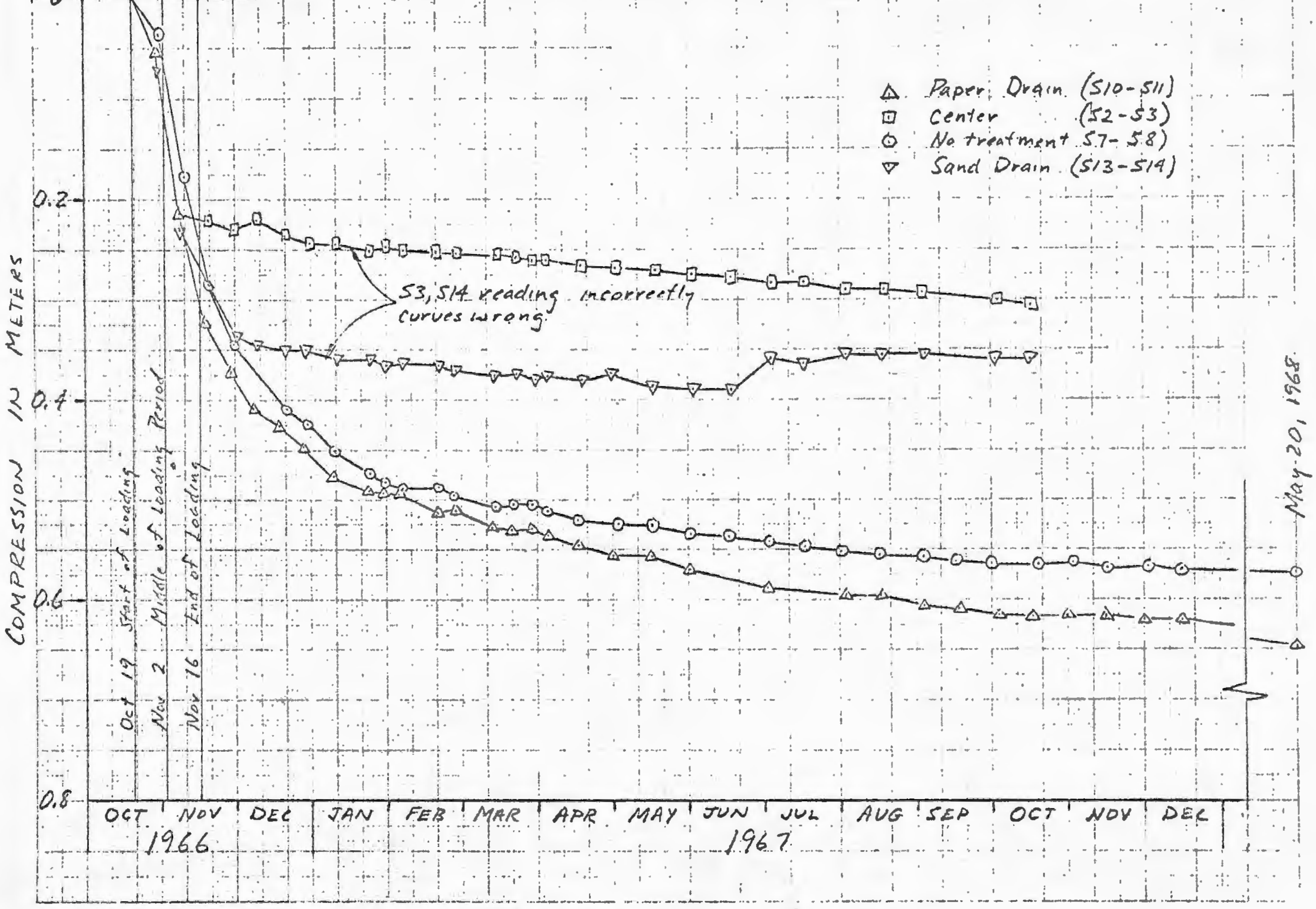

S3, S14 reading incorrectly curves wrong.

FIG III-26 COMPRESSION OF CLAY I

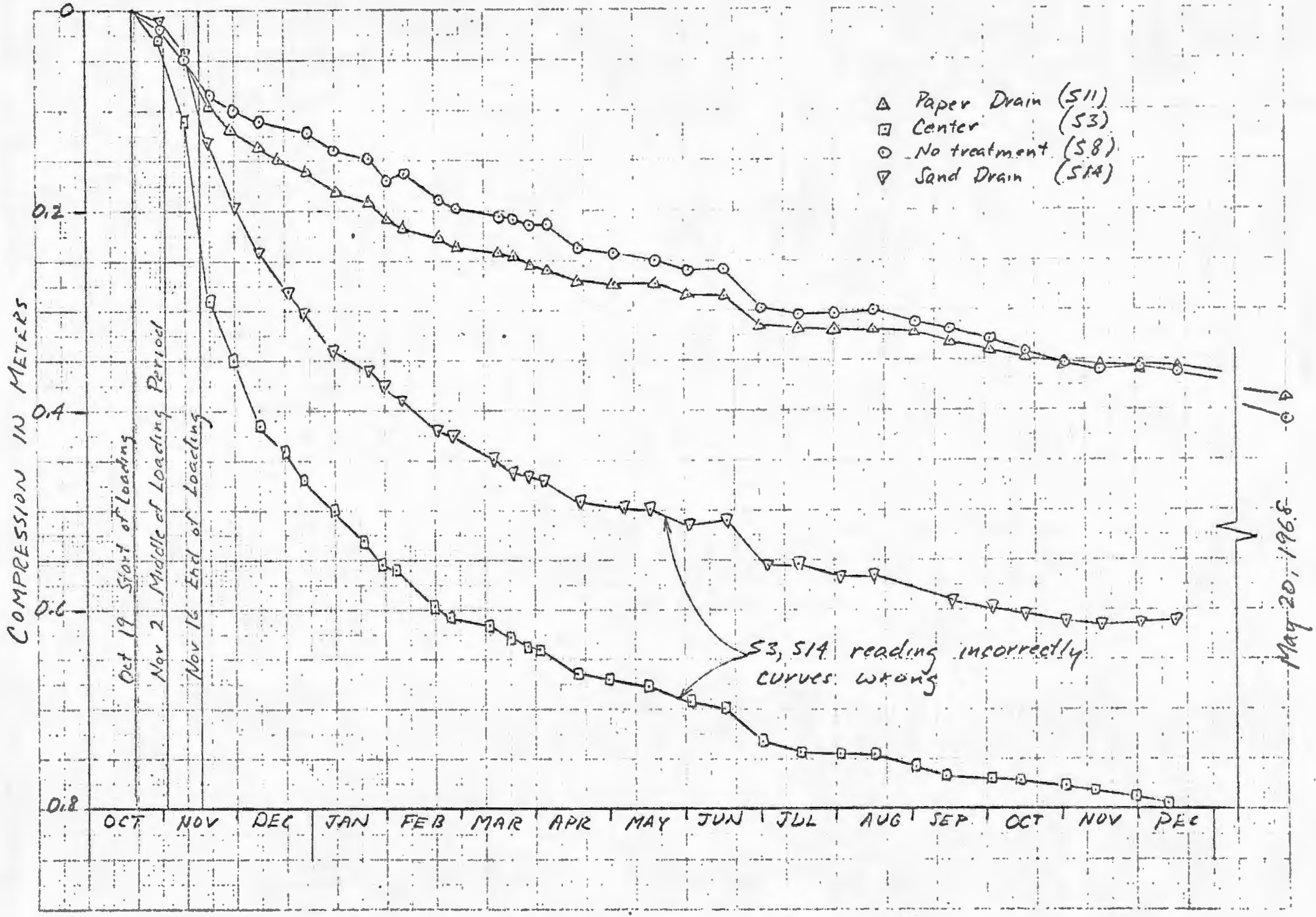

FIG III-2c COMPRESSION OF CLAY II + III

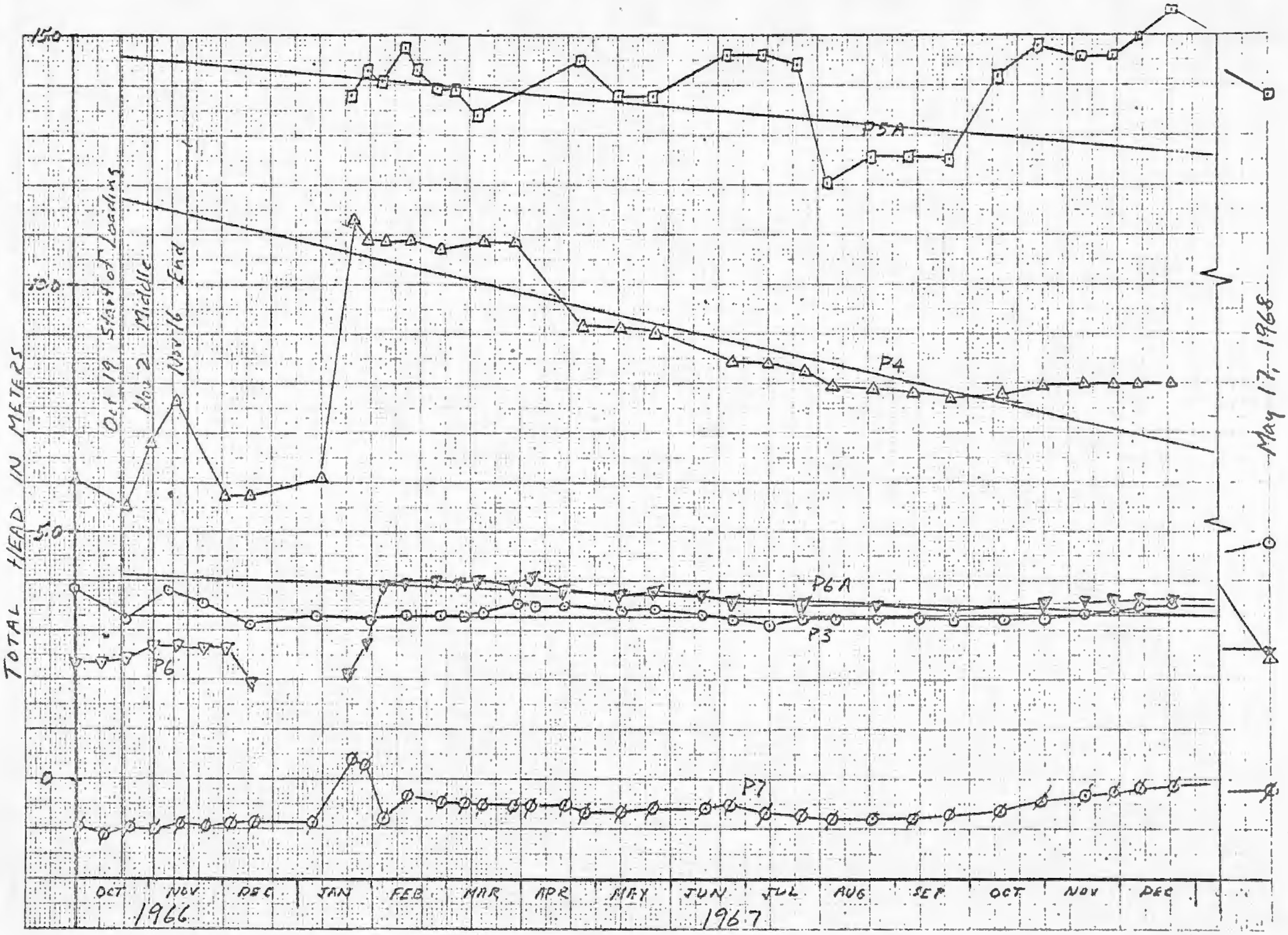

FIG III-3a PIEZOMETER READINGS AND STRAIGHT LINE EXTRAPOLATION UNDER CENTER OF LOAD TEST.

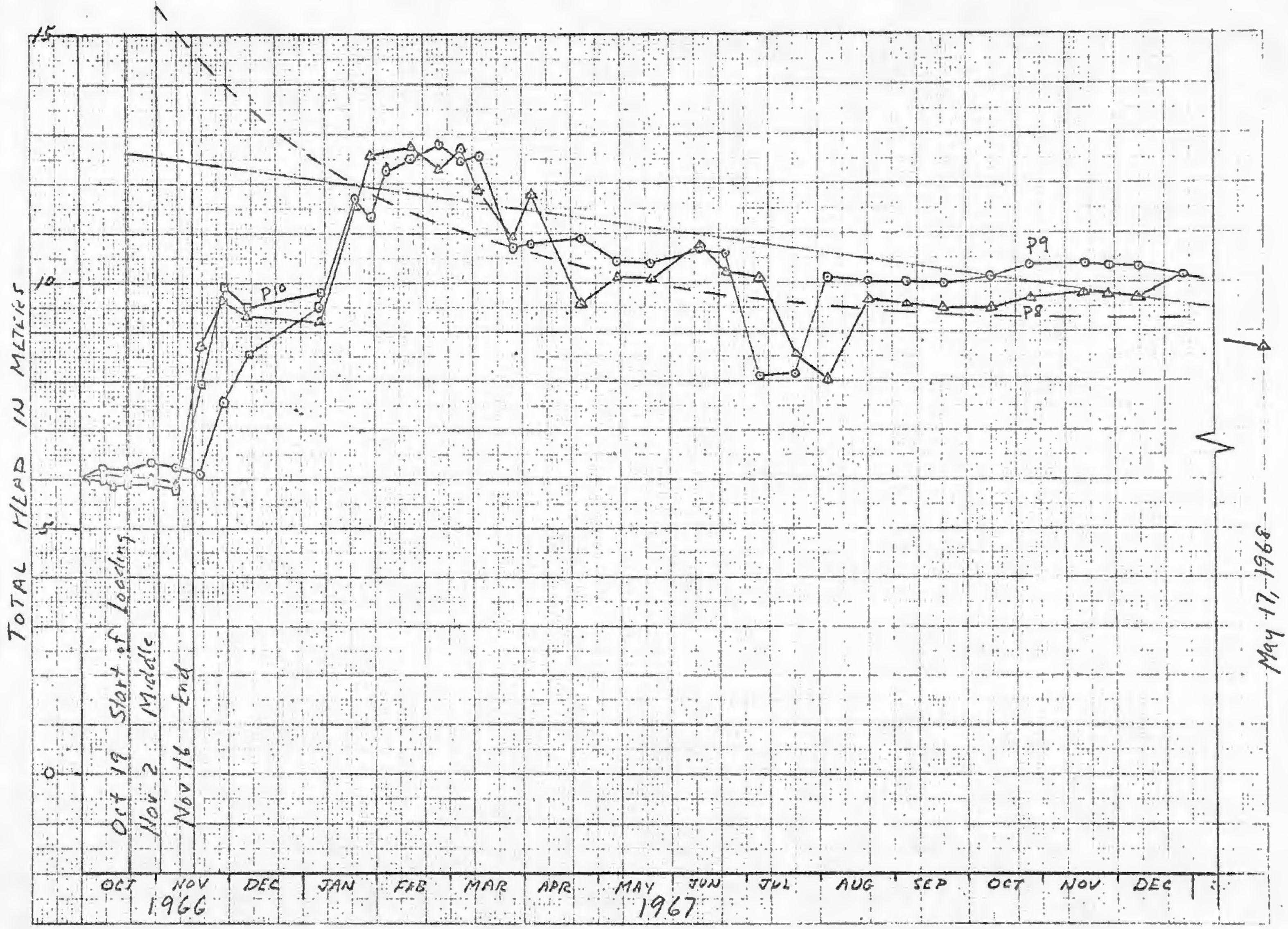

FIG III-3b PIEZOMETER READINGS 12 METERS FROM CENTER OF LOAD TEST

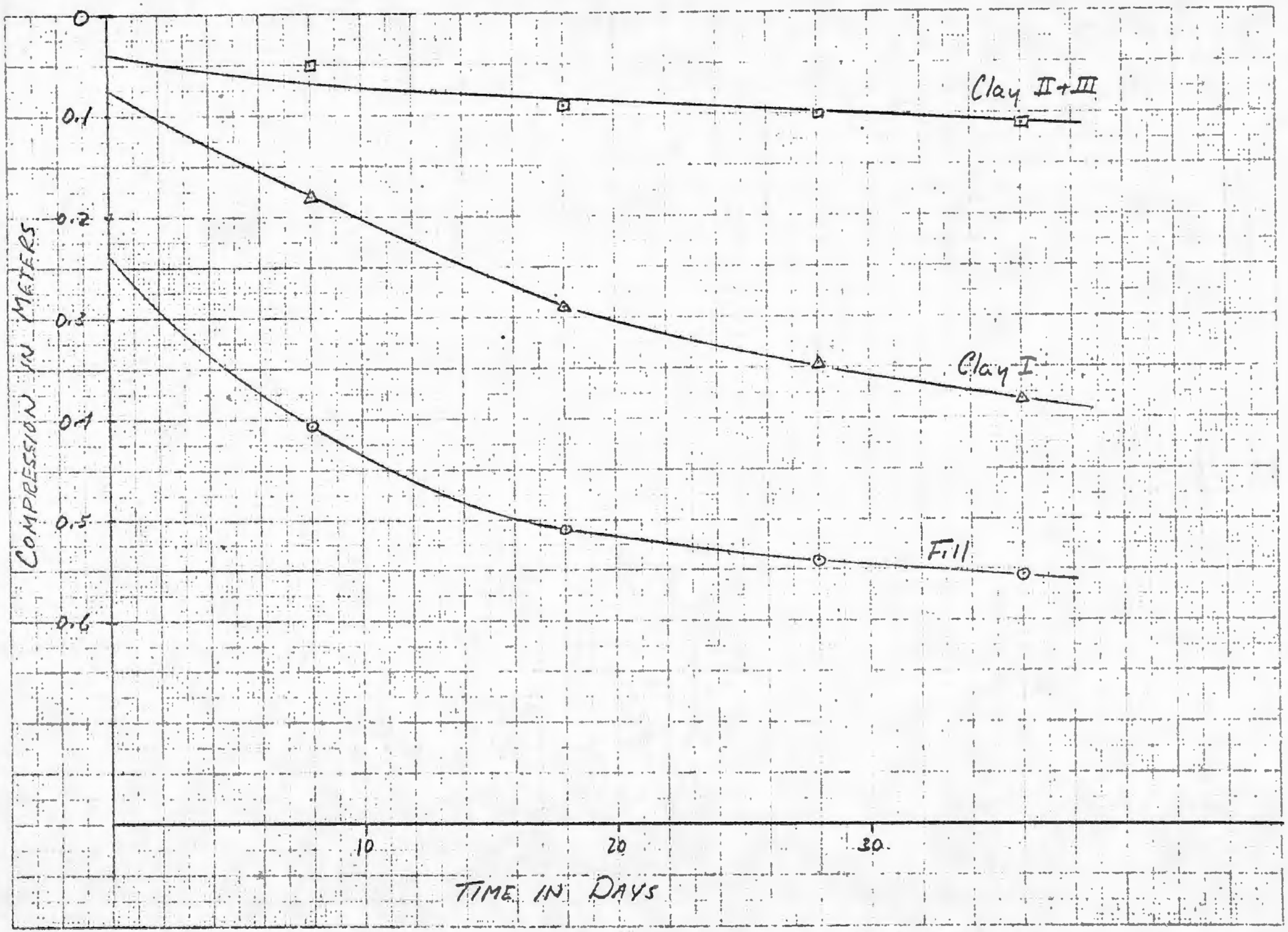

FIG III-4a COMPRESSION OF SOIL LAYERS - NO TREATMENT

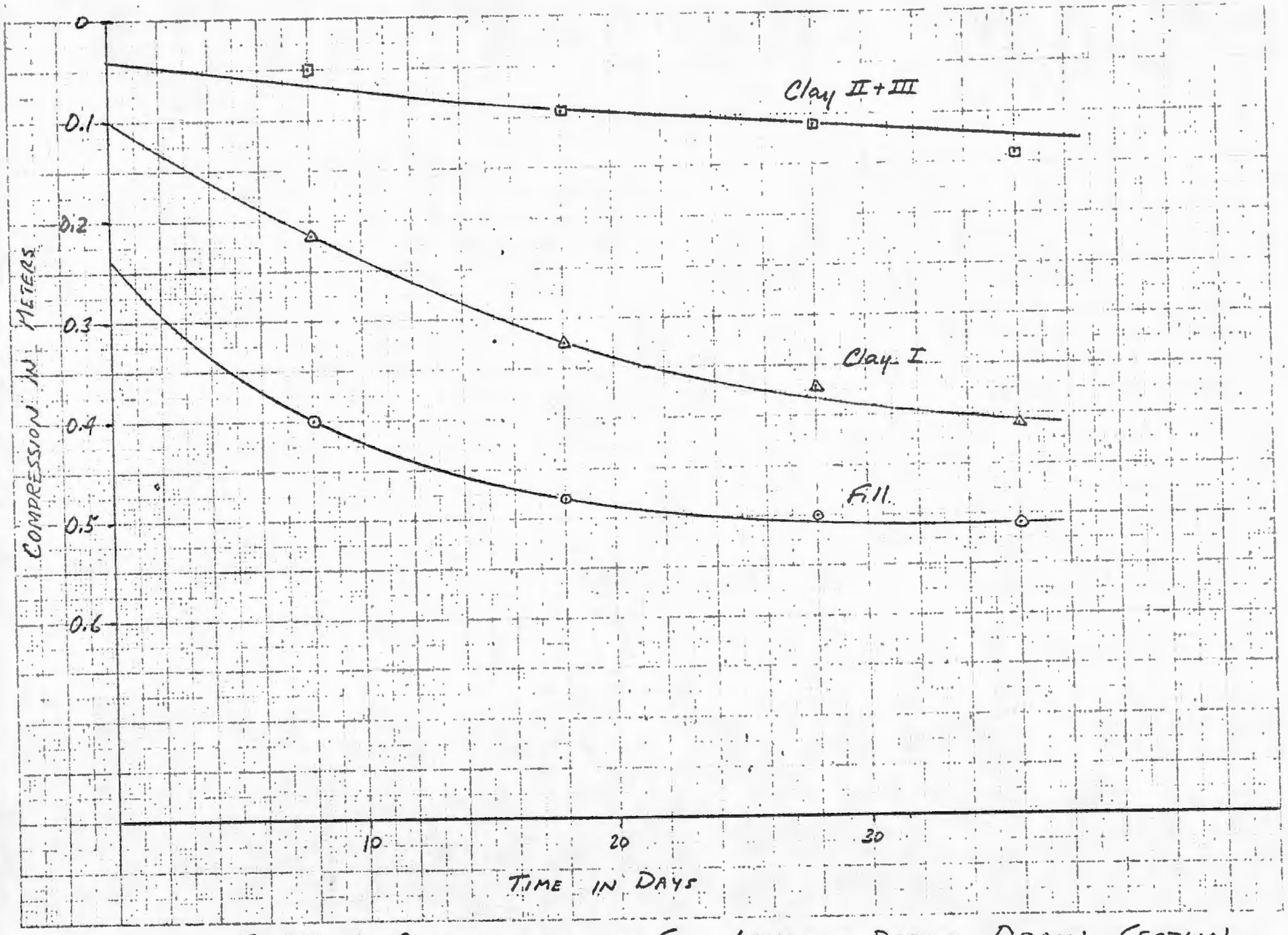

FIG III-4b COMPRESSION OF SOIL LAYERS - PAPER DRAIN SECTION

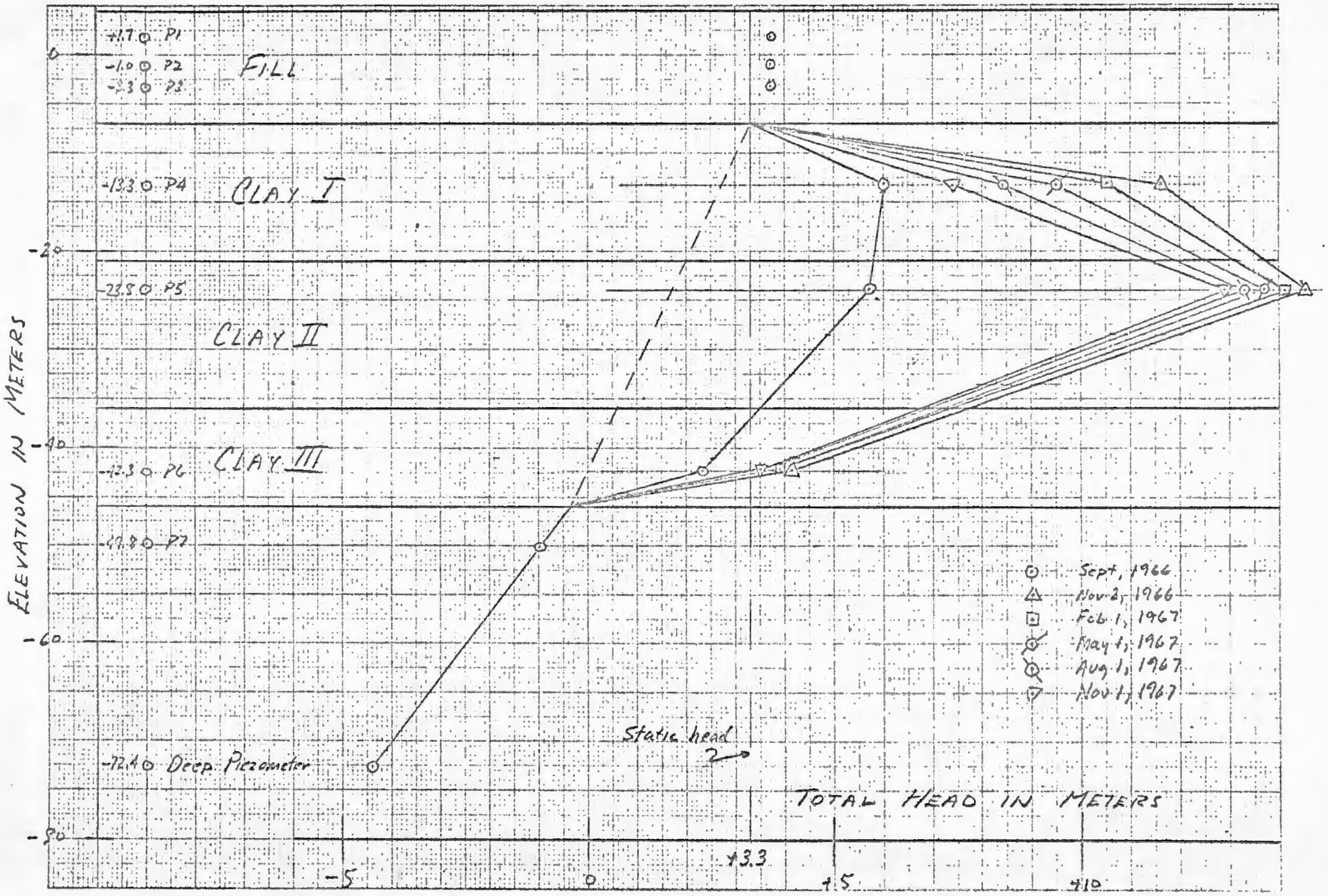

FIG III-5 PORE PRESSURE DISTRIBUTION UNDER CENTER OF LOAD TEST (FIRST ESTIMATE)

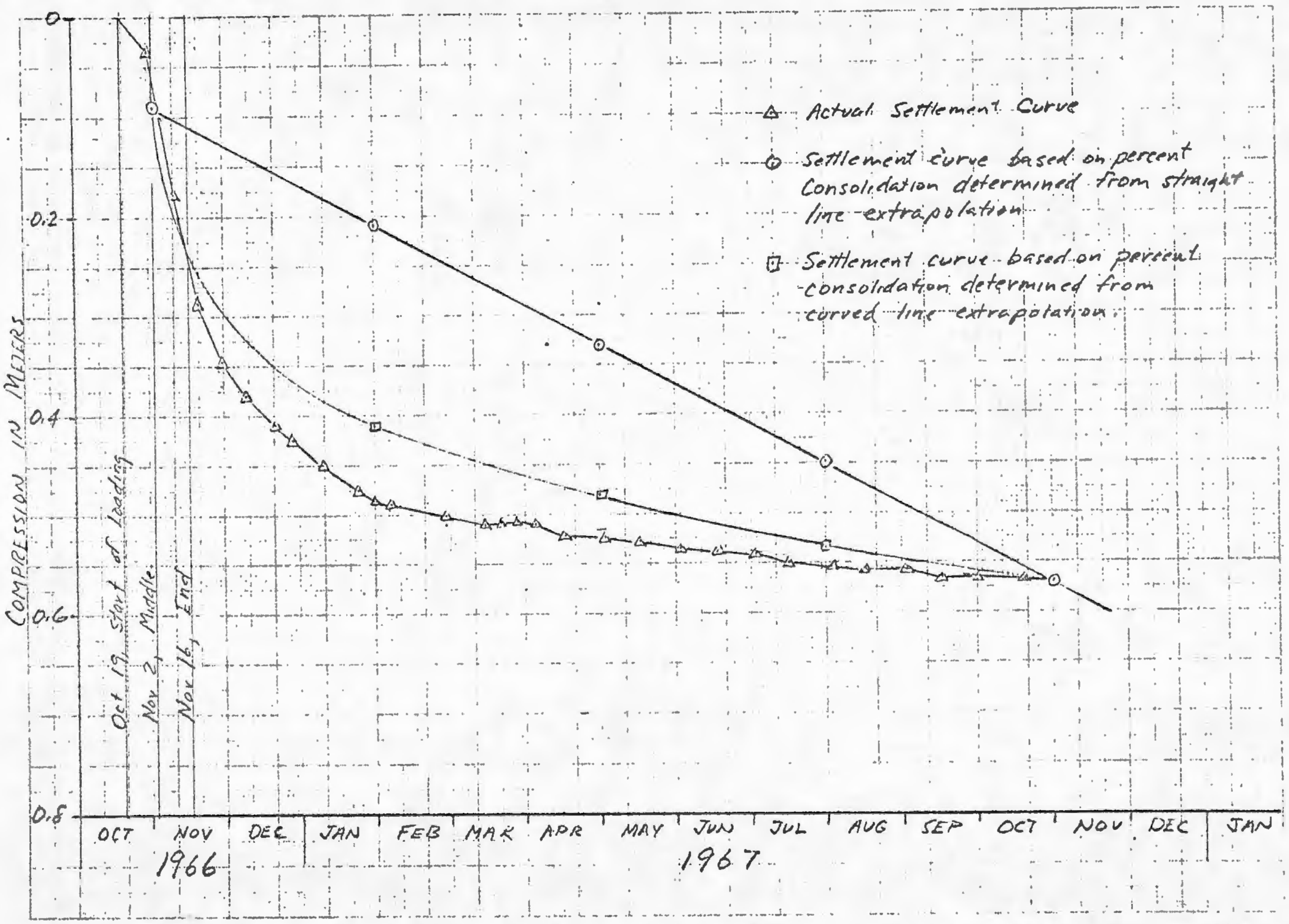

FIG III-6a COMPARISON OF ACTUAL SETTLEMENT CURVE AND CURVES BASED ON PERCENT CONSOLIDATION - CLAY I

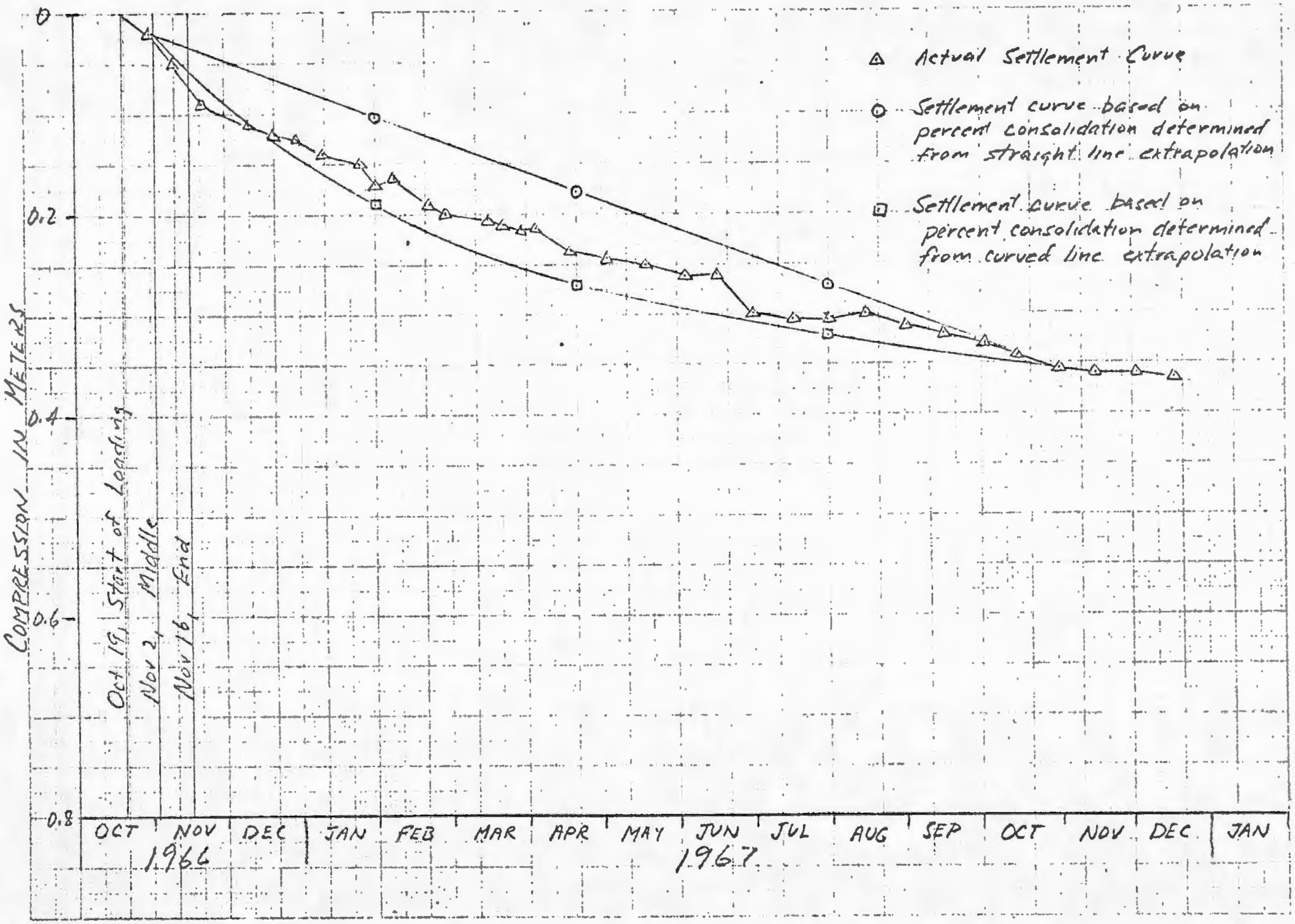

FIG III-66 COMPARISON OF ACTUAL SETTLEMENT CURVE AND CURVES BASED ON PERCENT CONSOLIDATION - CLAY II + III

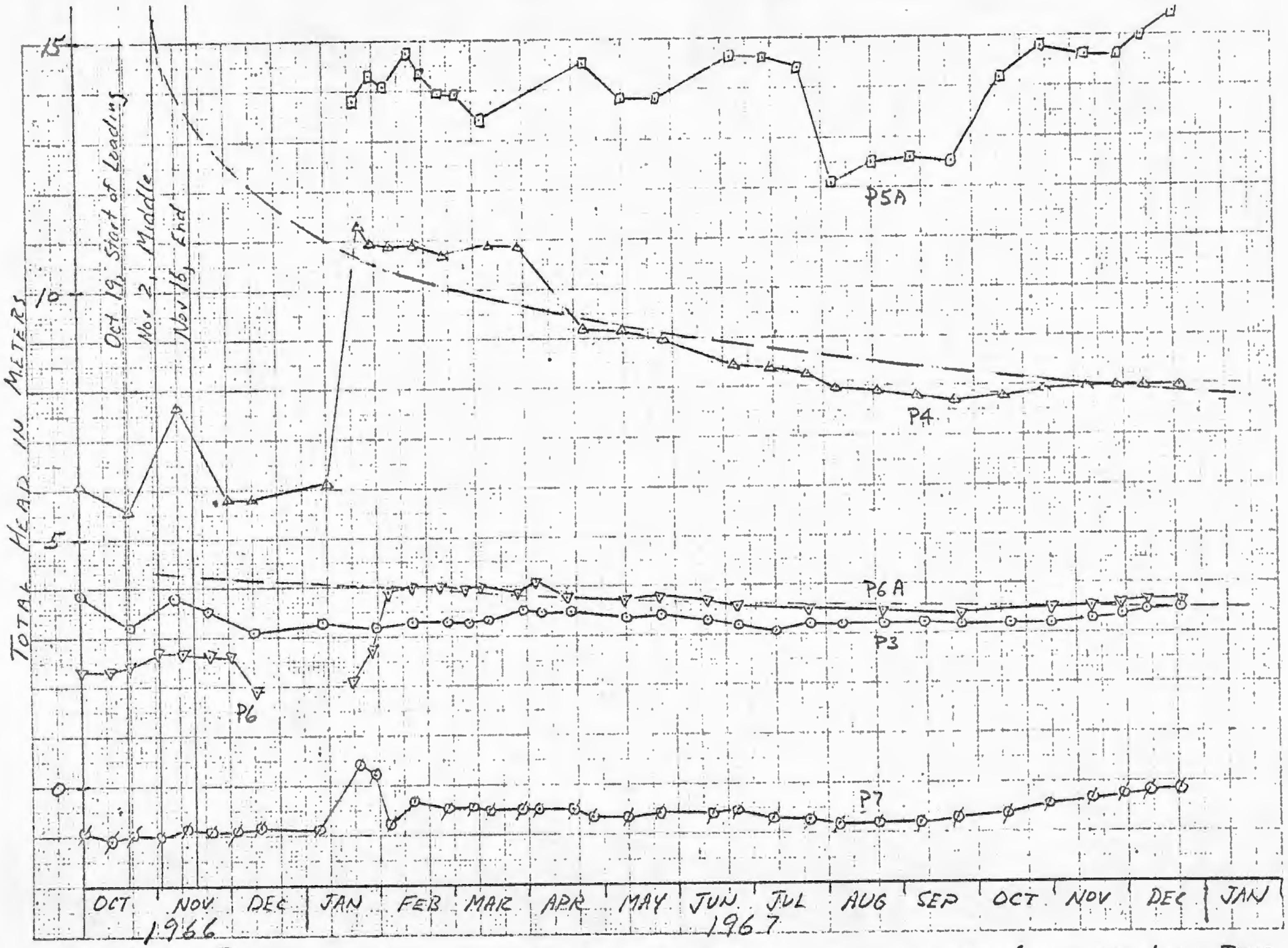

FIG III-7a PIEZOMETER READINGS AND CURVED LINE EXTRAPOLATION UNDER CENTER OF LOAD TEST

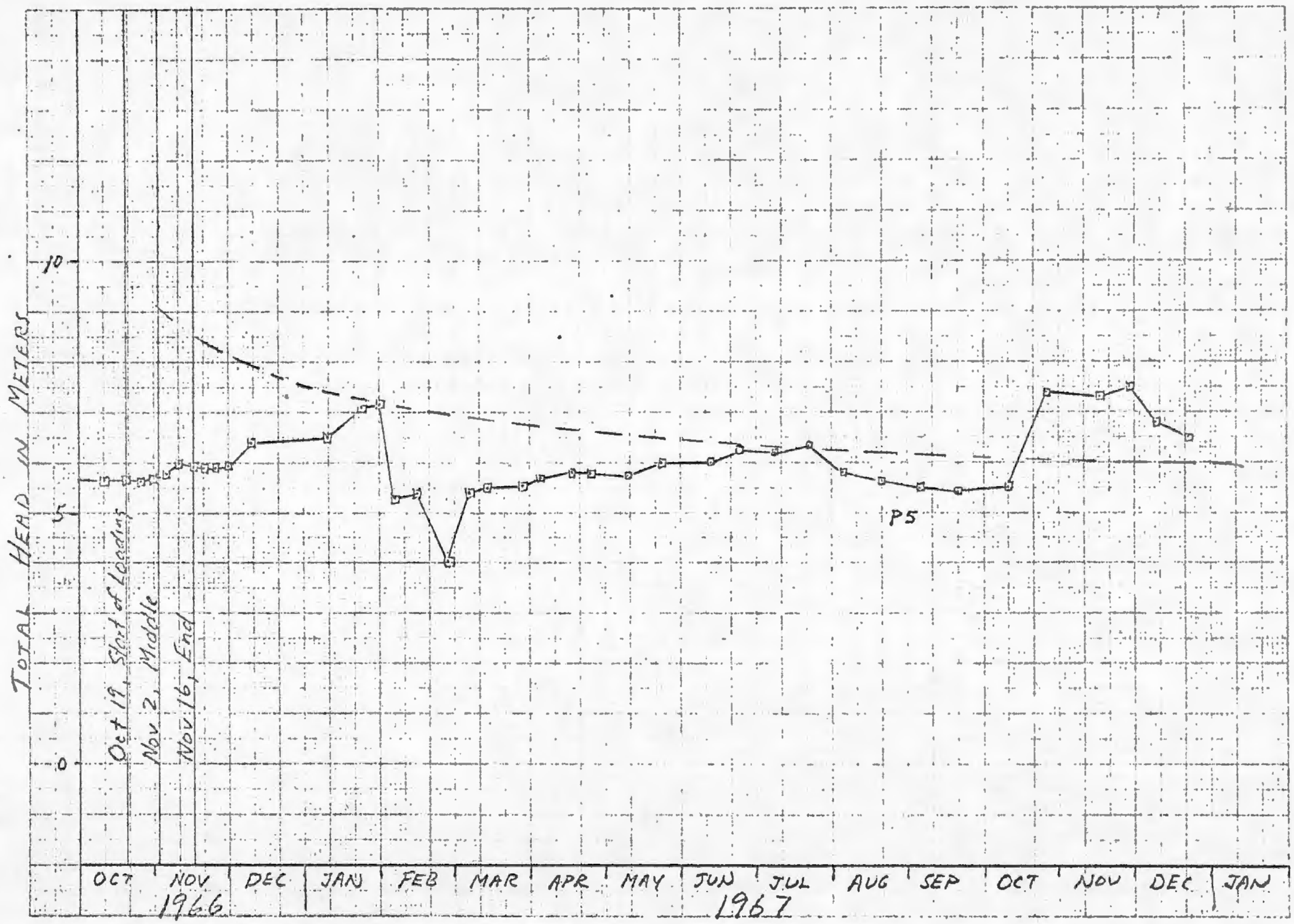

FIG III-76 PIEZOMETER READING AND CURVED LINE EXTRAPOLATION UNDER CENTER OF LOAD TEST

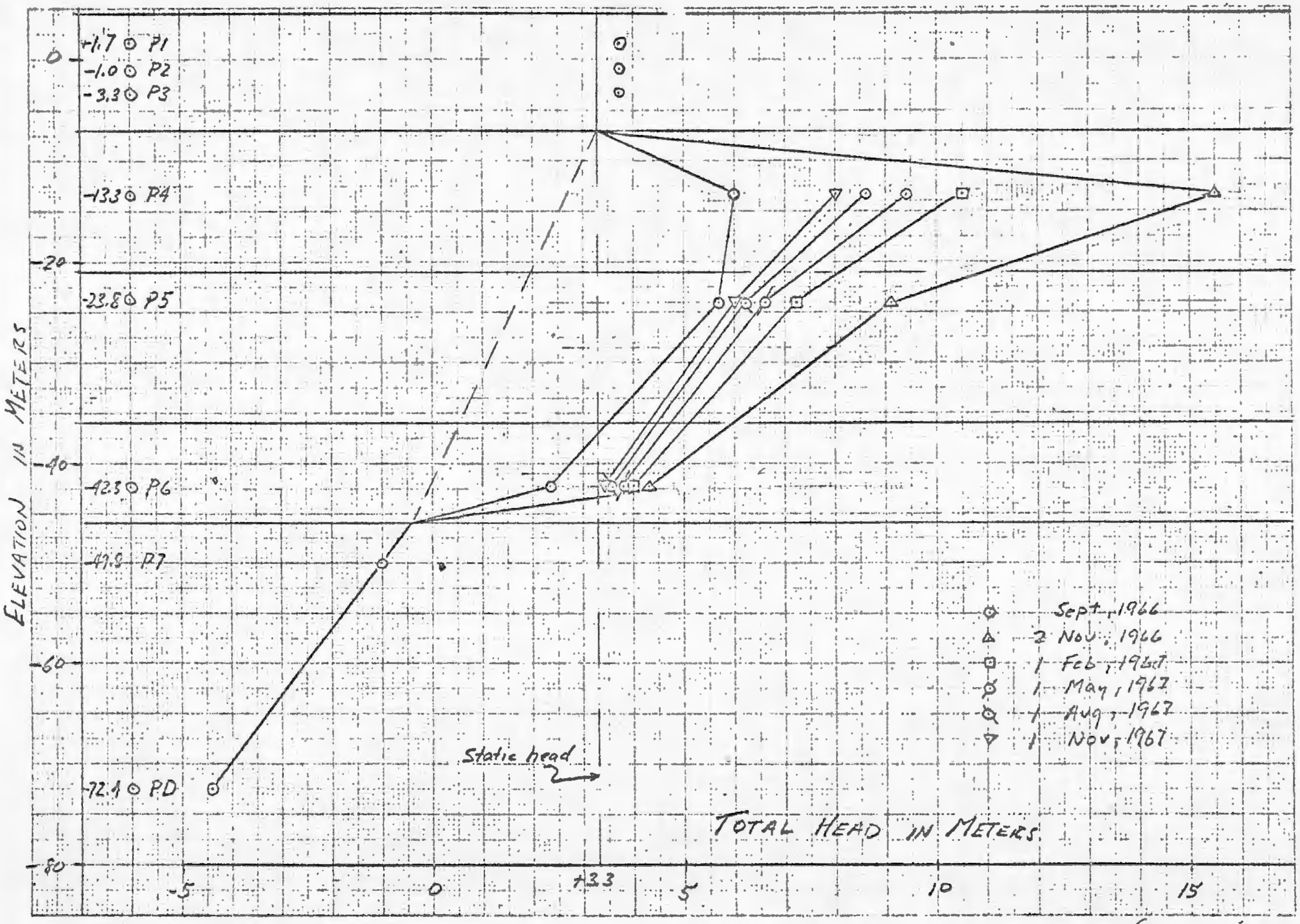

FIG III-8 PORE PRESSURE DISTRIBUTION UNDER CENTER OF LOAD TEST (REVISED)

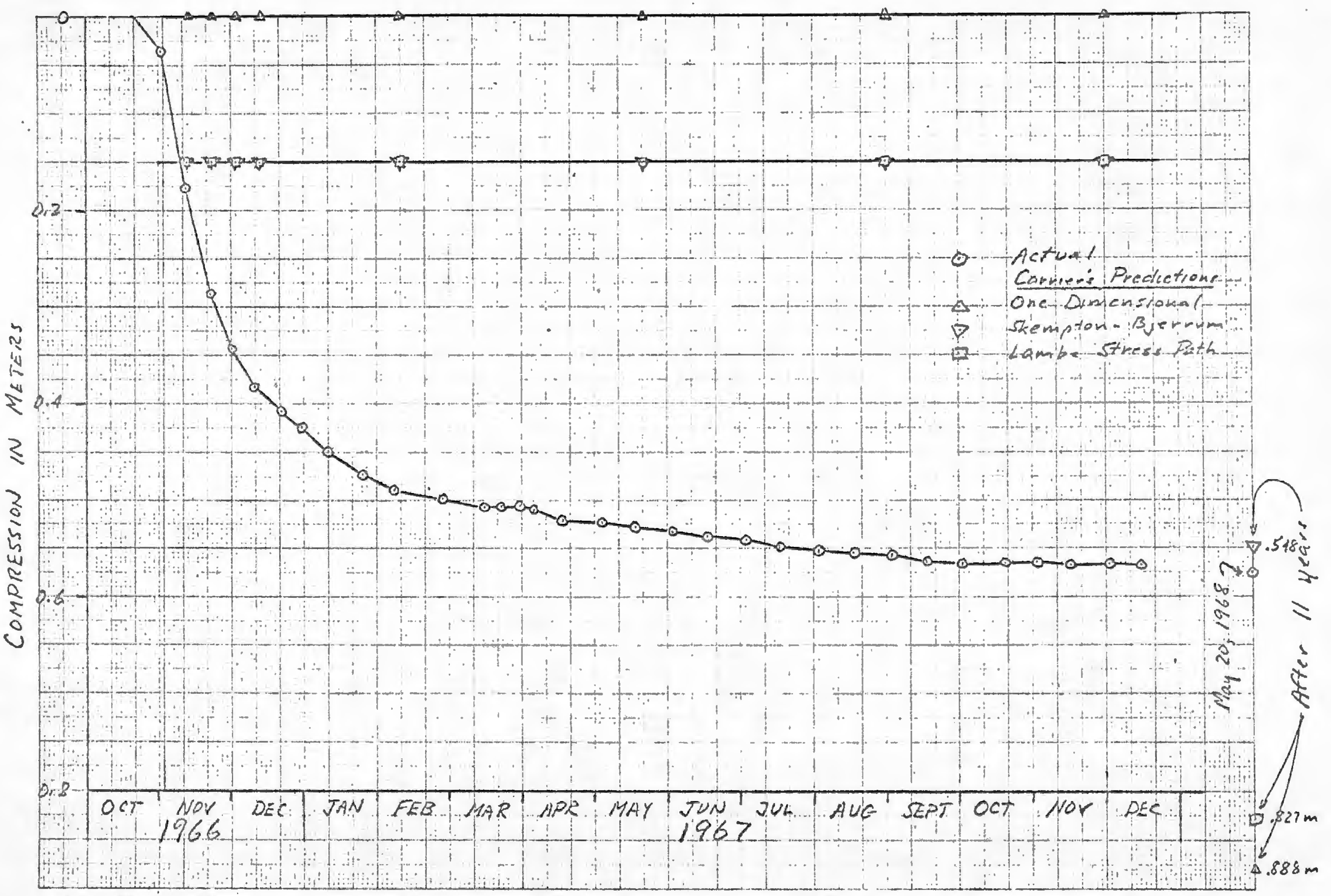

FIG IV-1a COMPARISON OF PREDICTED AND MEASURED RATE AND MAGNITUDE OF SETTLEMENT - CLAY I

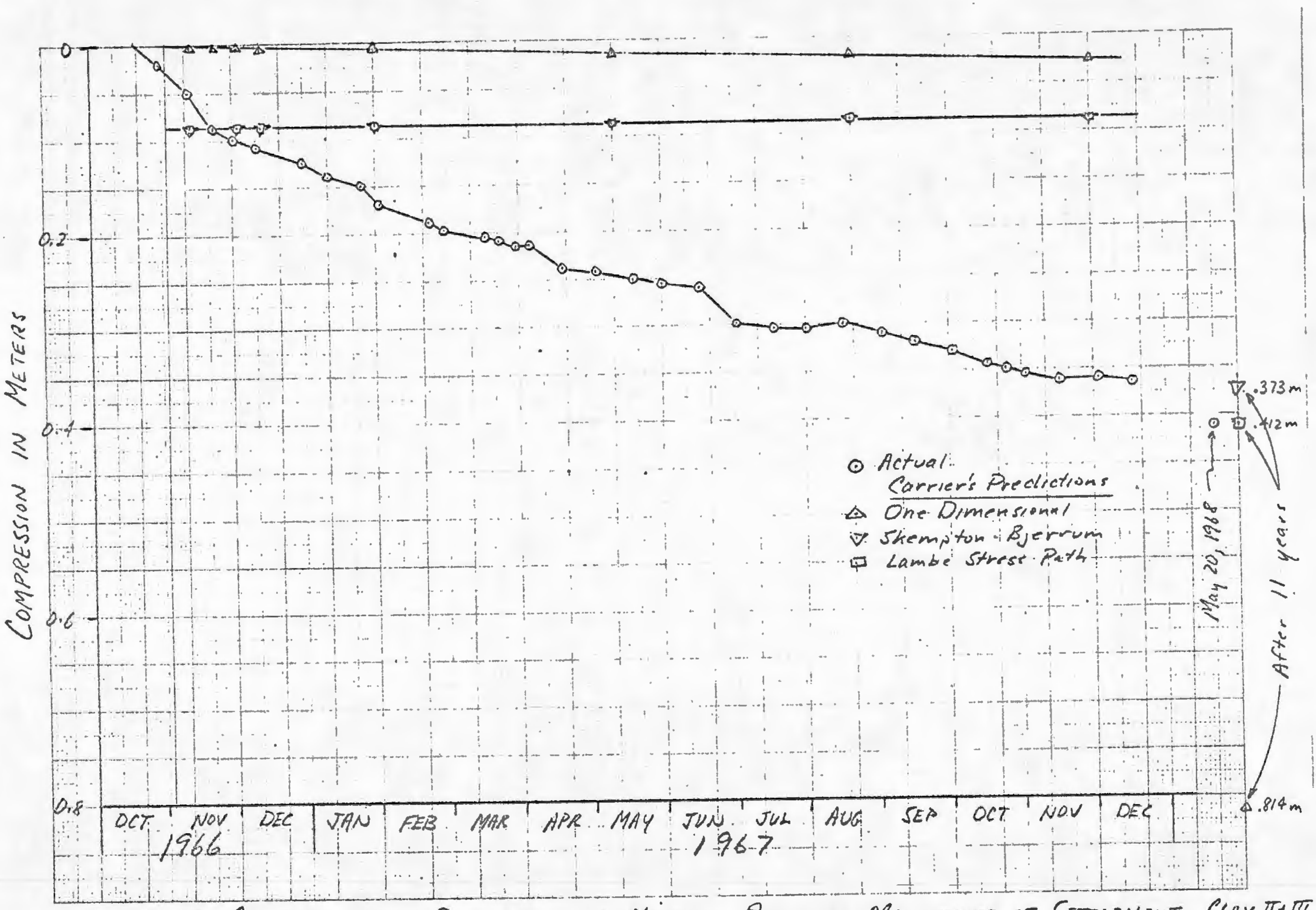

FIG IV-16 COMPARISON OF PREDICTED AND MEASURED RATE AND MAGNITUDE OF SETTLEMENT - CLAY II + III

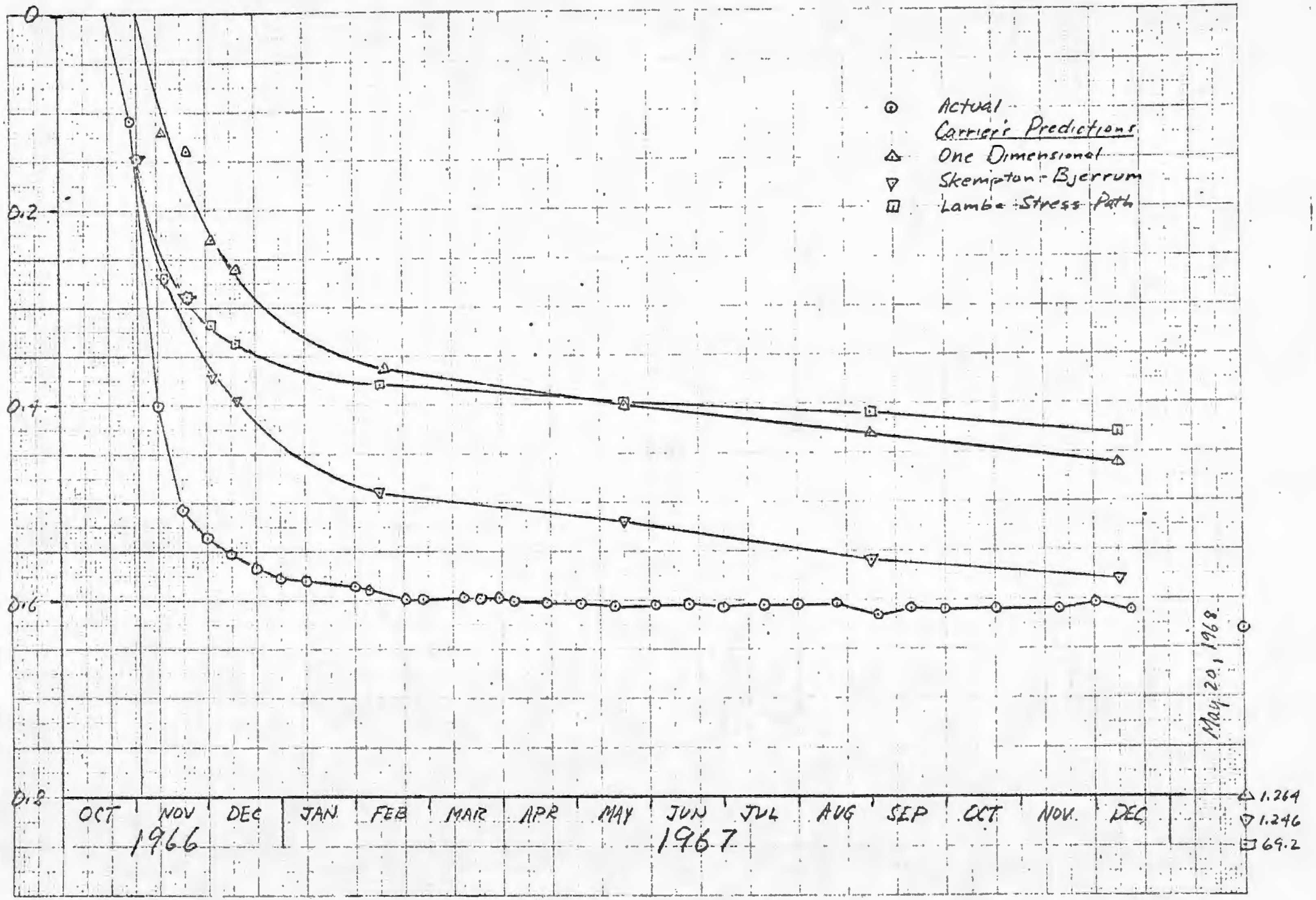

FIG IV-1c COMPARISON OF PREDICTED AND 'MEASURED' RATE AND MAGNITUDE OF SETTLEMENT - FILL

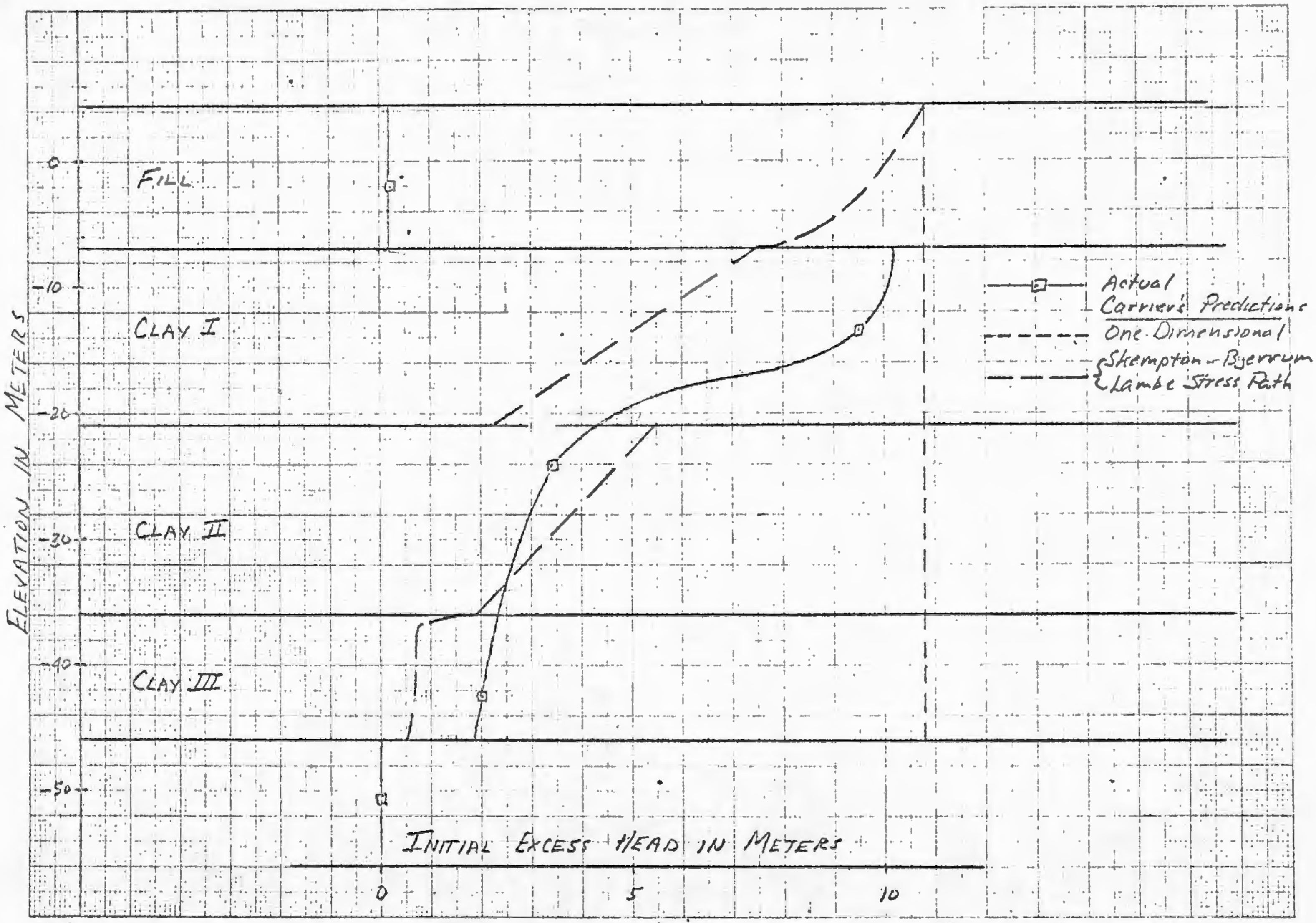

FIG IV-2 COMPARISON OF PREDICTED AND 'MEASURED' INITIAL EXCESS PORE PRESSURE

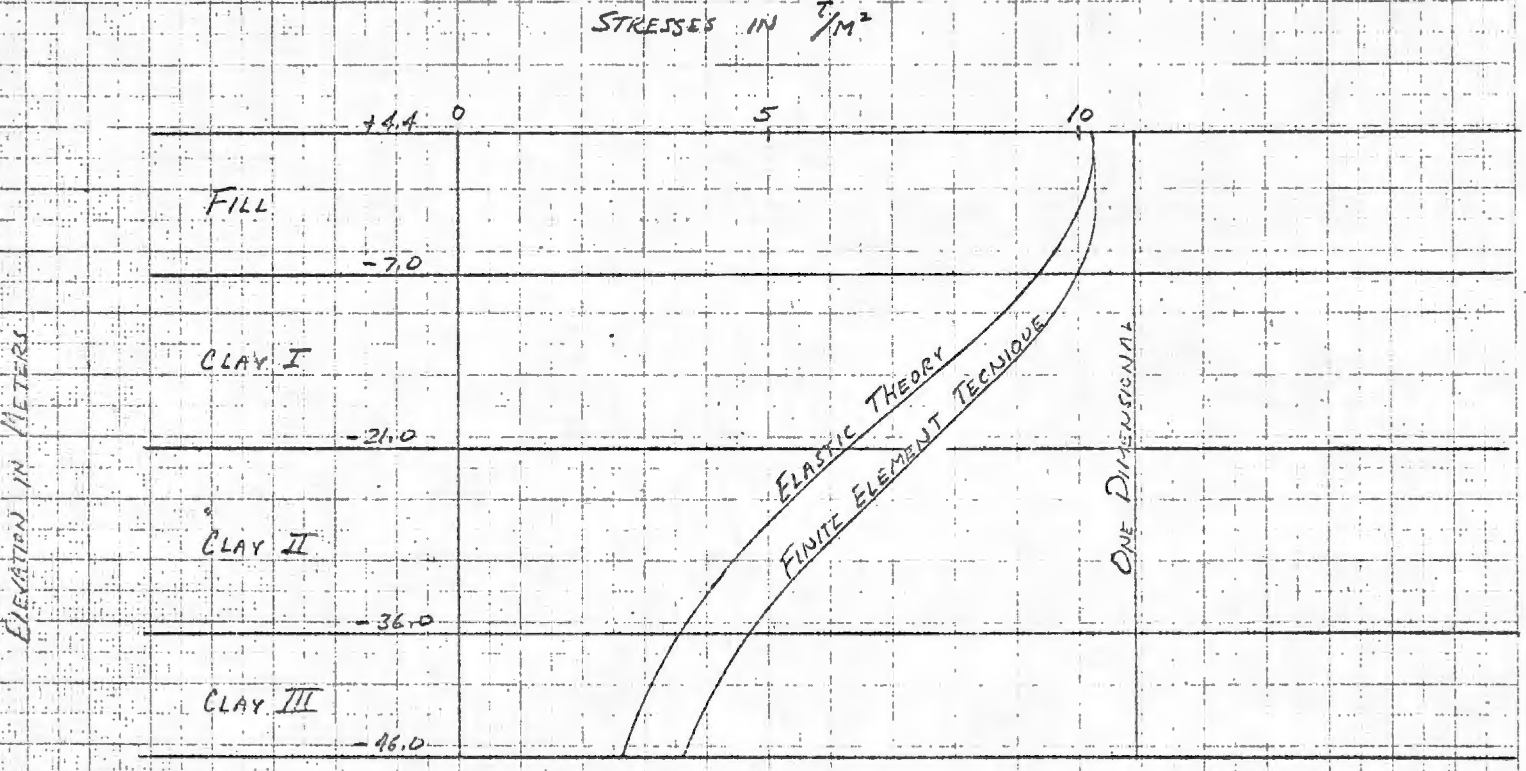

FIG IV-3 VERTICAL STRESS INCREMENTS COMPUTED BY DIFFERENT METHODS UNDER TEST EMBANKMENT

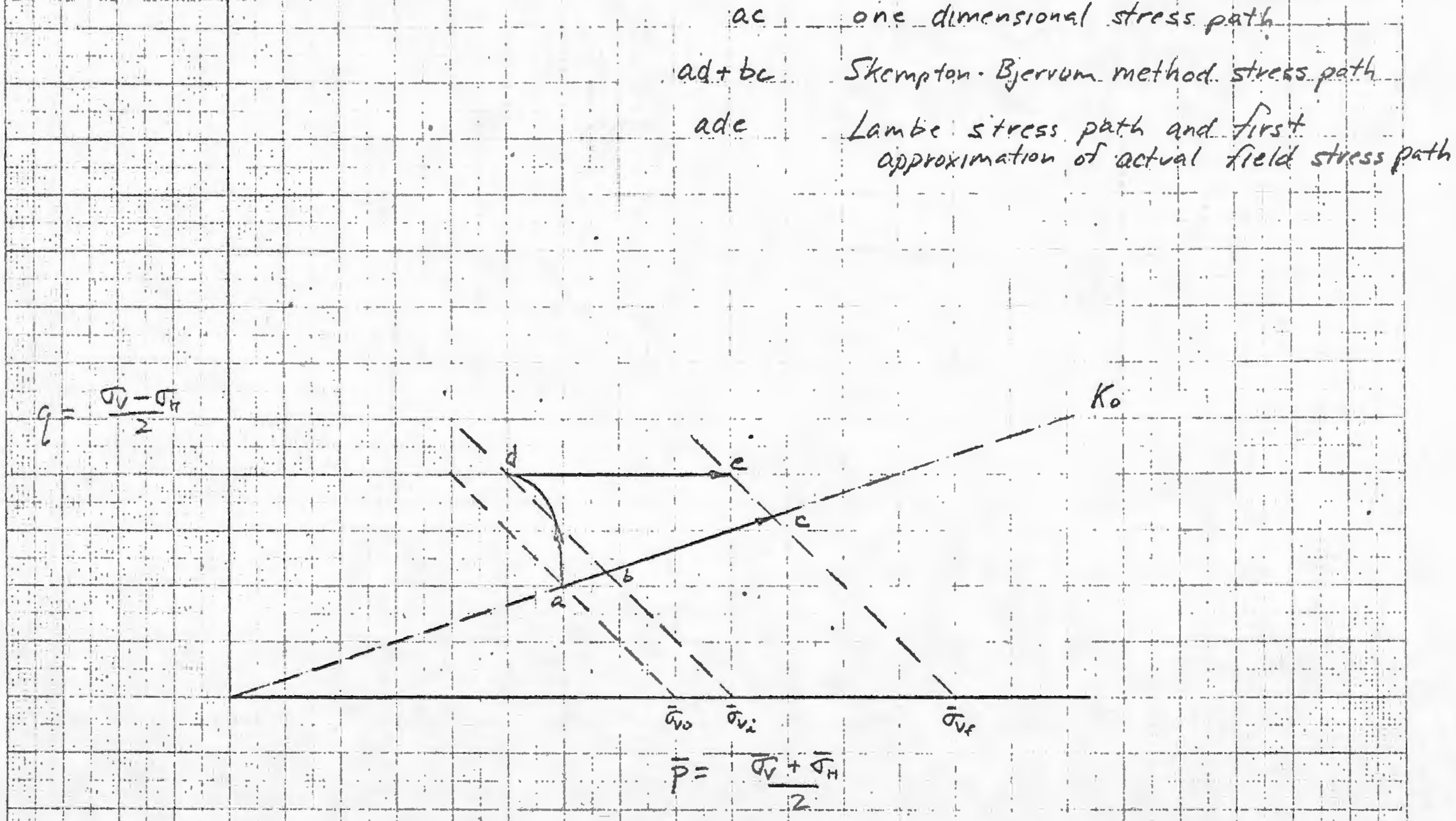
ac one dimensional stress path
ad + bc Skempton - Bjerrum method stress path
ade Lambe stress path and first approximation of actual field stress path
$q = \frac{\bar{\sigma}_V - \bar{\sigma}_H}{2}$
K_o
d
e
c
b
a
$\bar{\sigma}_{vo}$
$\bar{\sigma}_{vi}$
$\bar{\sigma}_{vf}$
$\bar{p} = \frac{\bar{\sigma}_V + \bar{\sigma}_H}{2}$

FIG IV-4 COMPARISON OF STRESS PATHS USED IN DIFFERENT PREDICTION METHODS WITH ACTUAL FIELD STRESS PATH

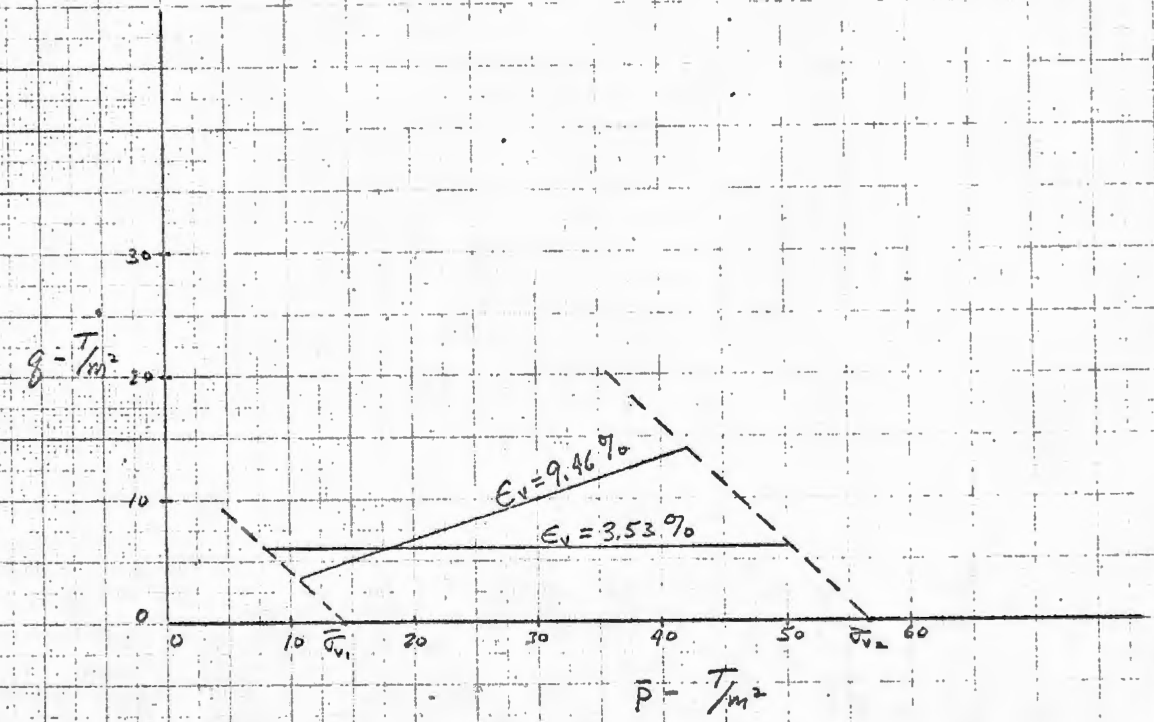

FIG. II-5 COMPARISON OF STRAINS ALONG DIFFERENT STRESS PATHS (FILL)

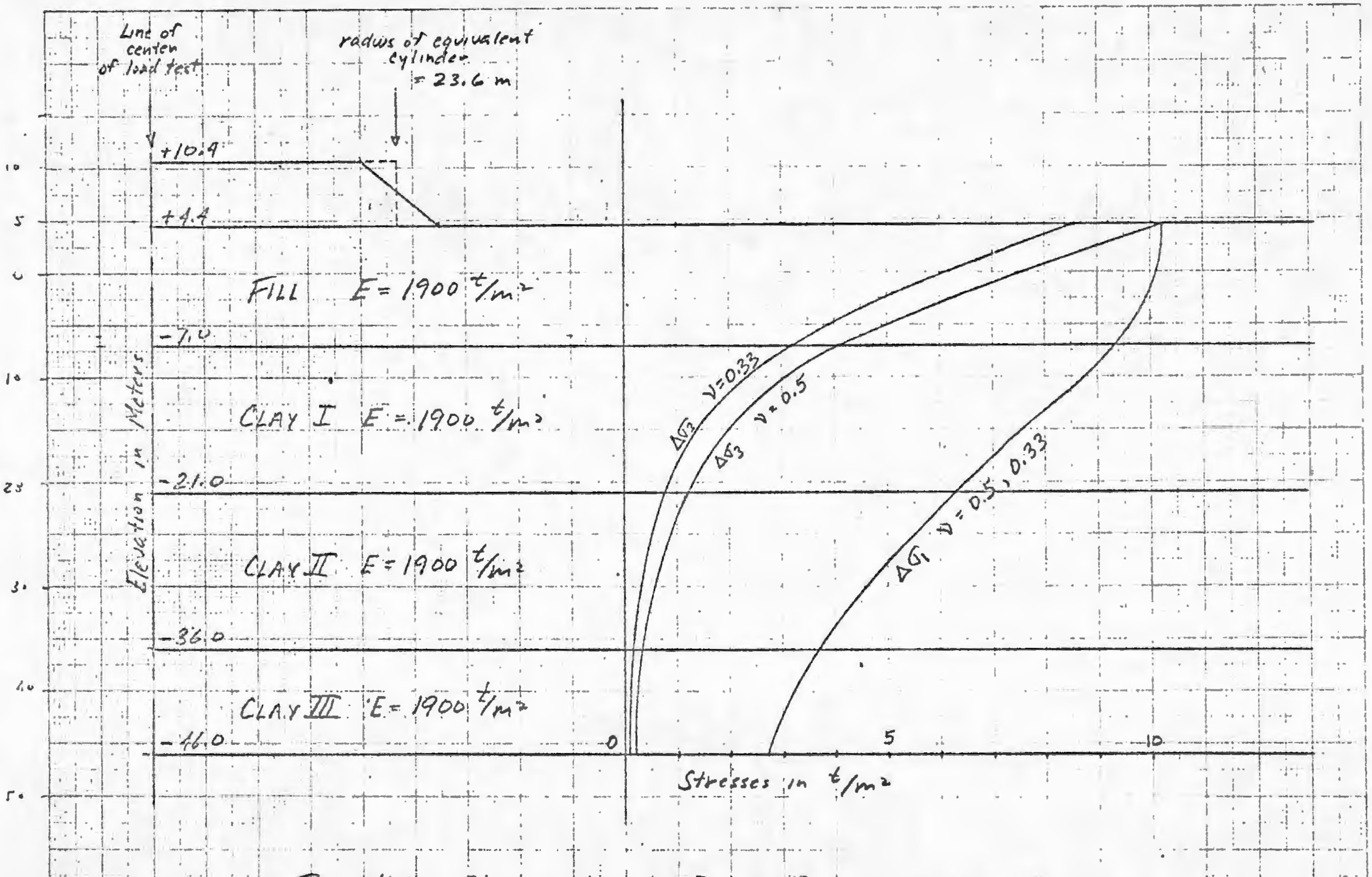

FIG. V-1 ELASTIC STRESS DISTRIBUTIONS UNDER CENTER-LINE OF LOAD TEST

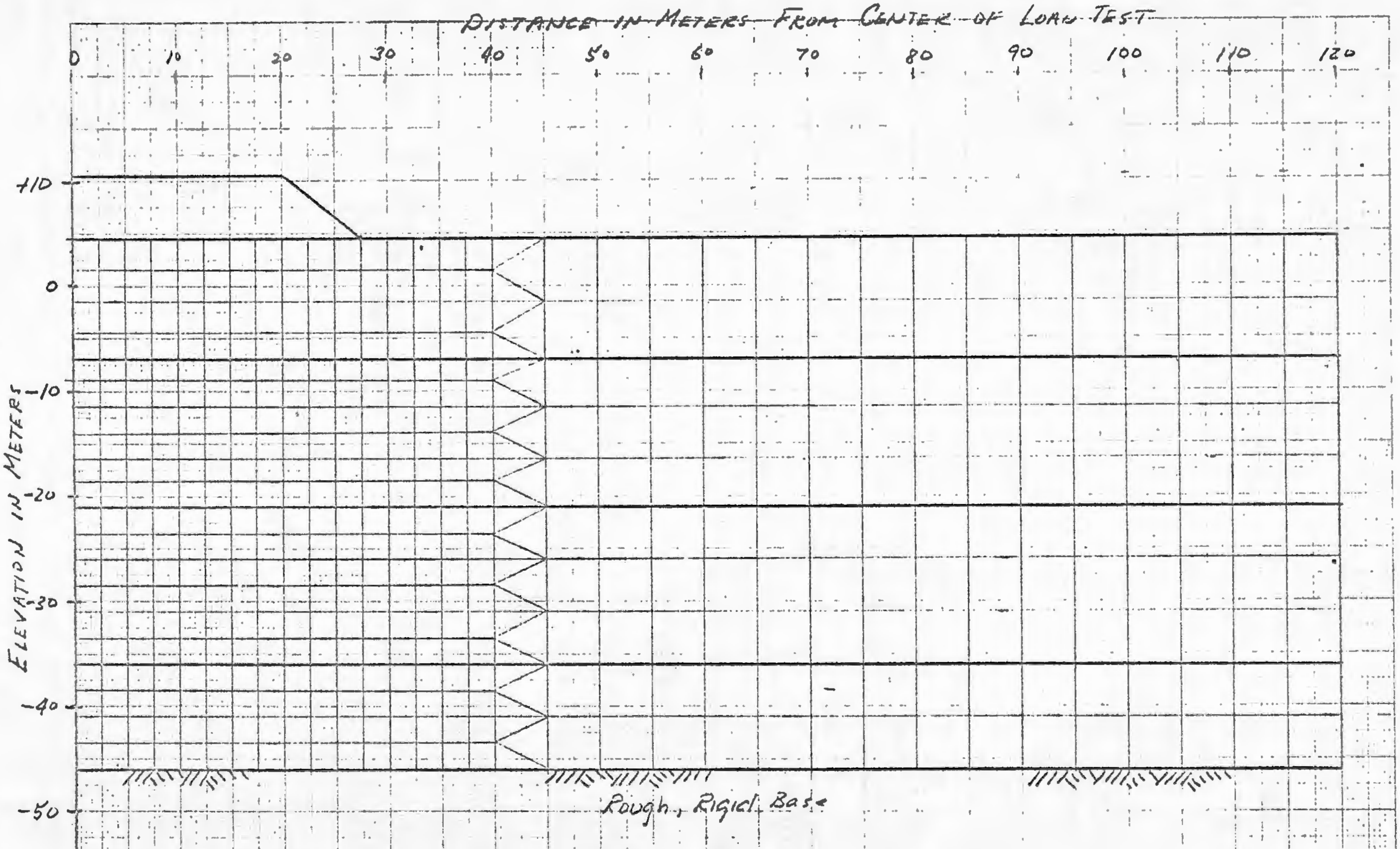

FIG V-2 MESH USED IN FINITE ELEMENT ANALYSIS.

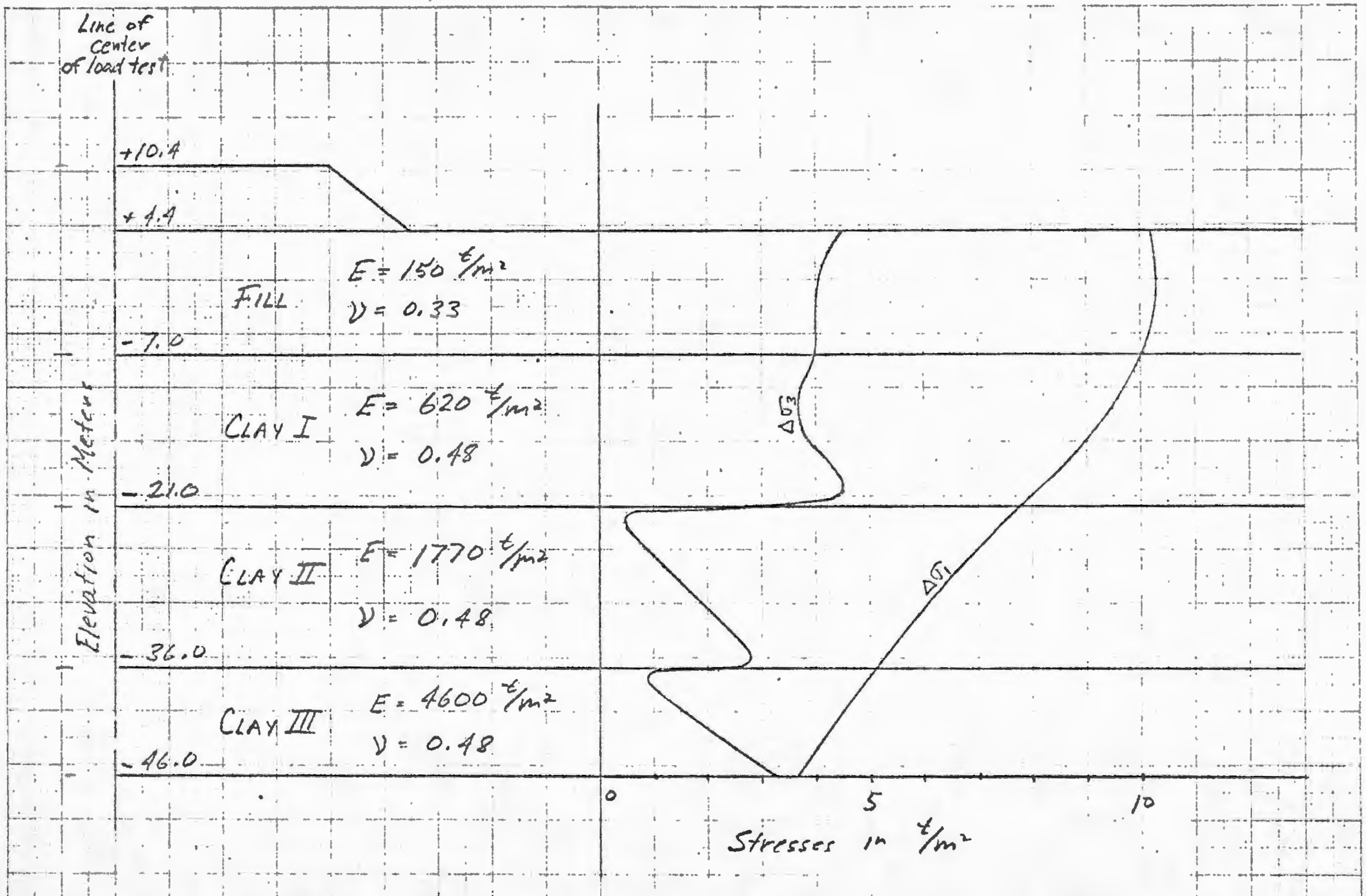

FIG V-3a. STRESS DISTRIBUTION UNDER CENTER LINE OF LOAD TEST USING FINITE ELEMENT TECHNIQUE AND UNDRAINED MODULI

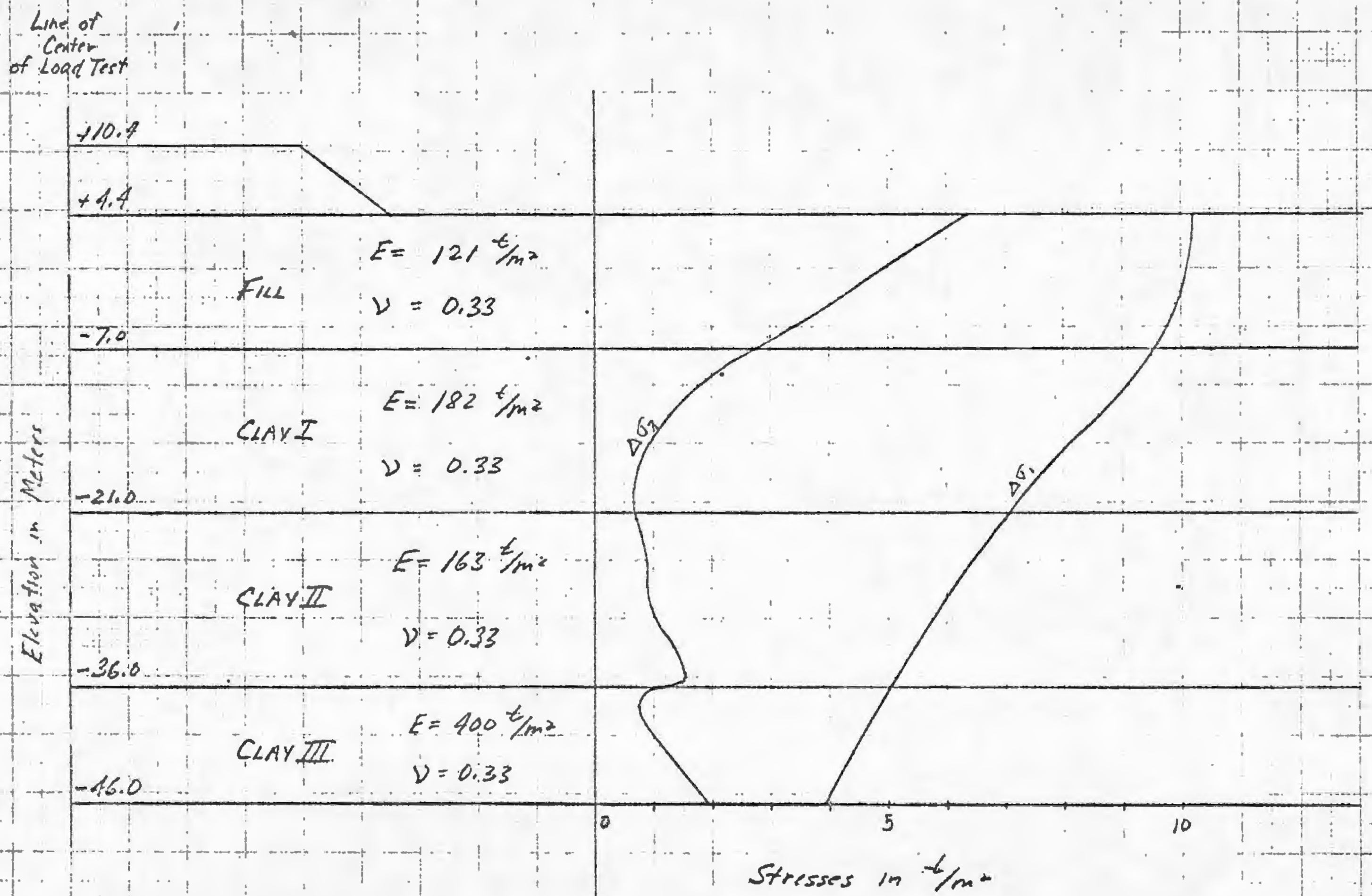

FIG V-3b STRESS DISTRIBUTION UNDER CENTER LINE OF LOAD TEST USING FINITE ELEMENT TECHNIQUE AND DRAINED MODULI

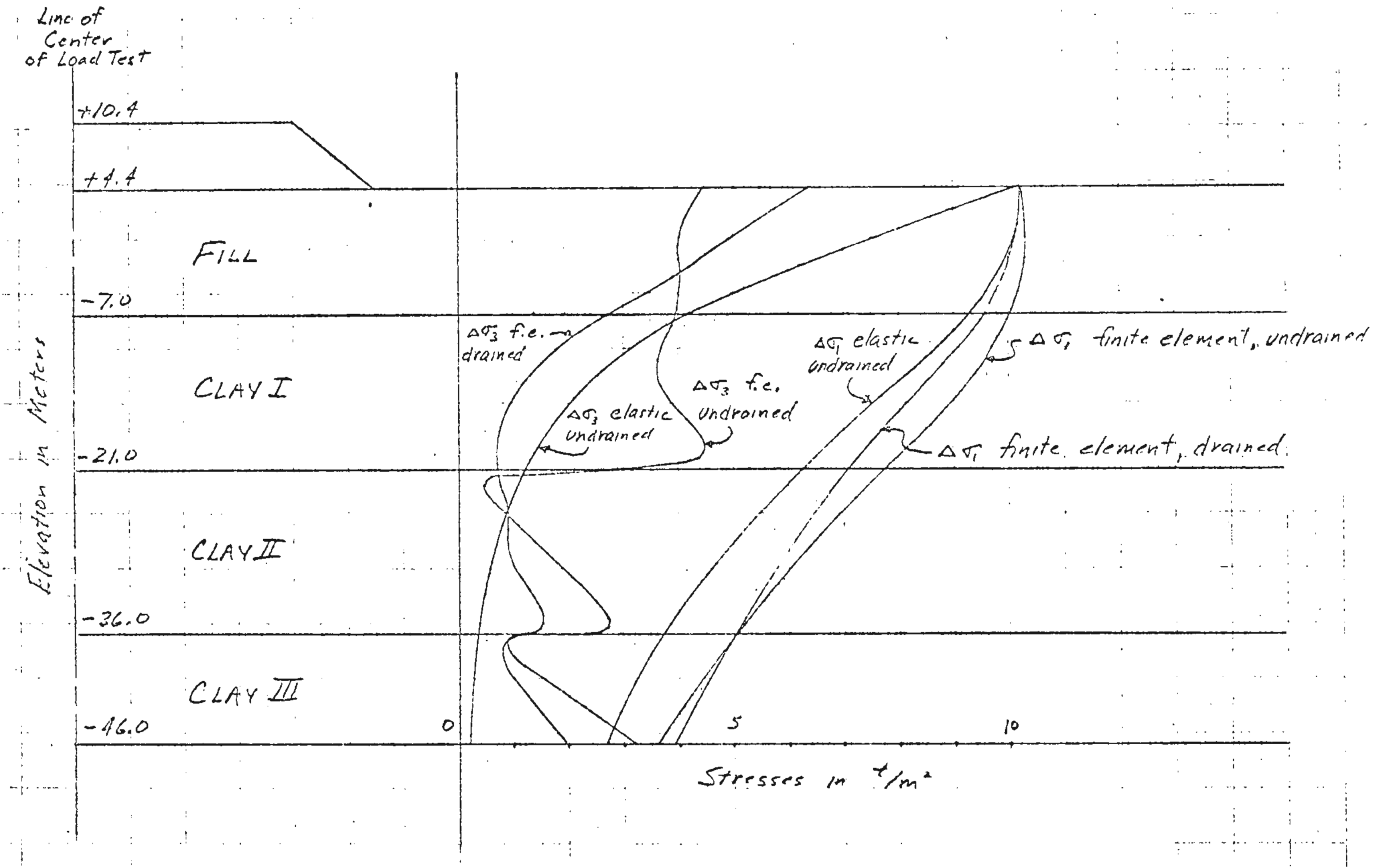

FIG. V-4 COMPARISON OF STRESS DISTRIBUTIONS UNDER CENTER-LINE OF LOAD TEST

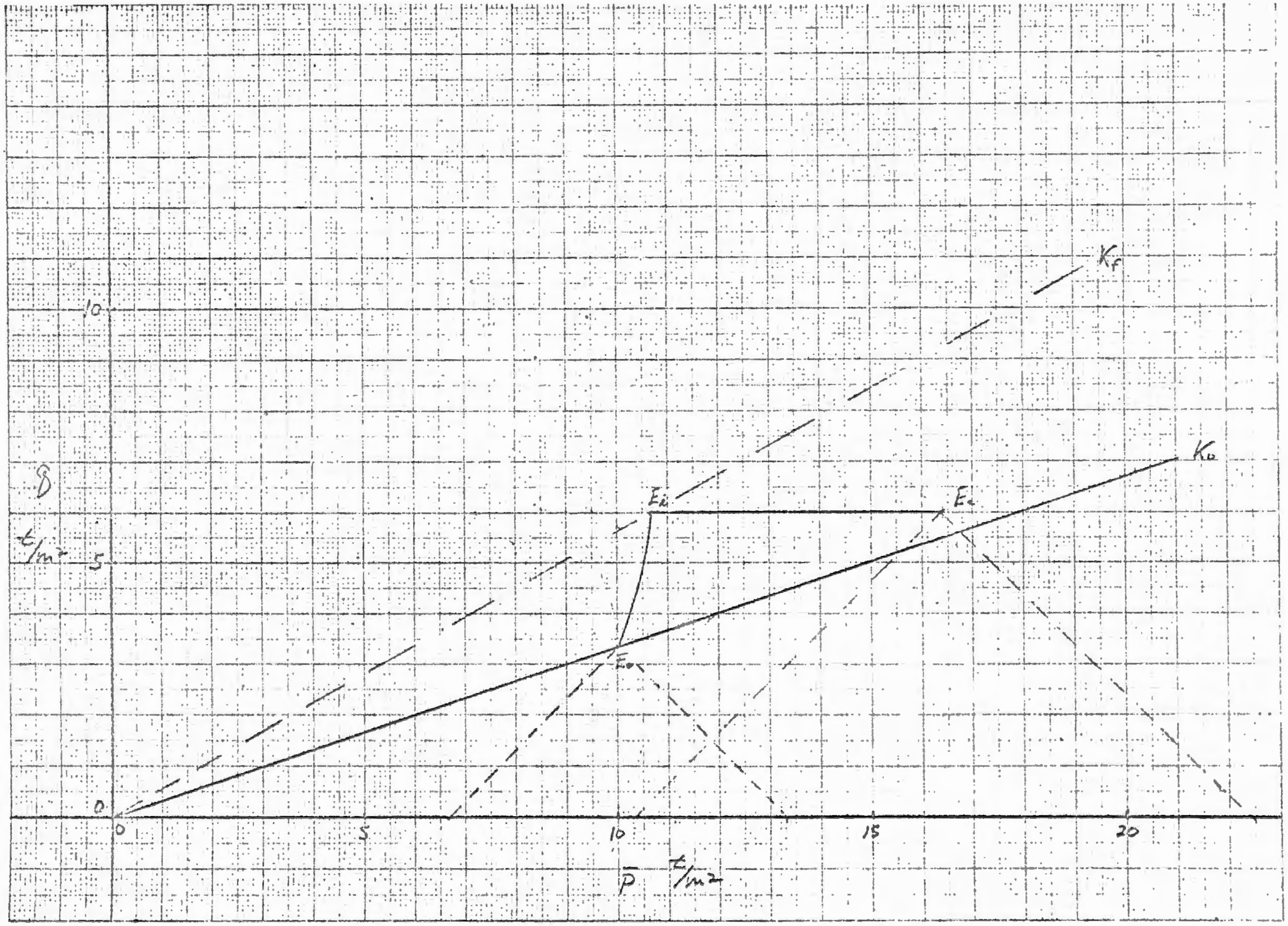

FIG VII-10 EFFECTIVE STRESS PATH IN CENTER OF CLAY I UNDER ℄ OF LOAD TEST

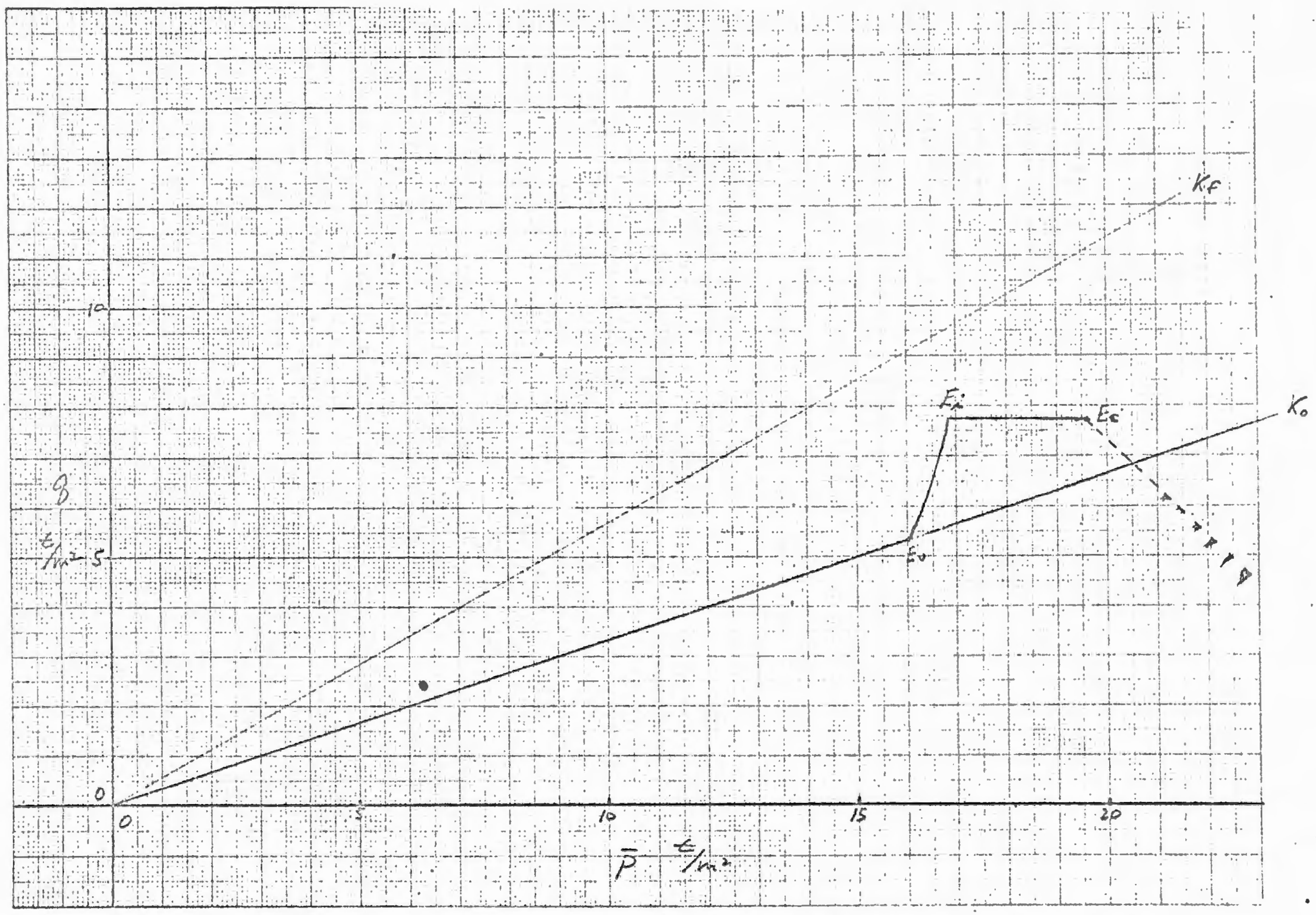

FIG VI-16 EFFECTIVE STRESS PATH IN CENTER OF CLAY II UNDER ℄ OF LOAD TEST

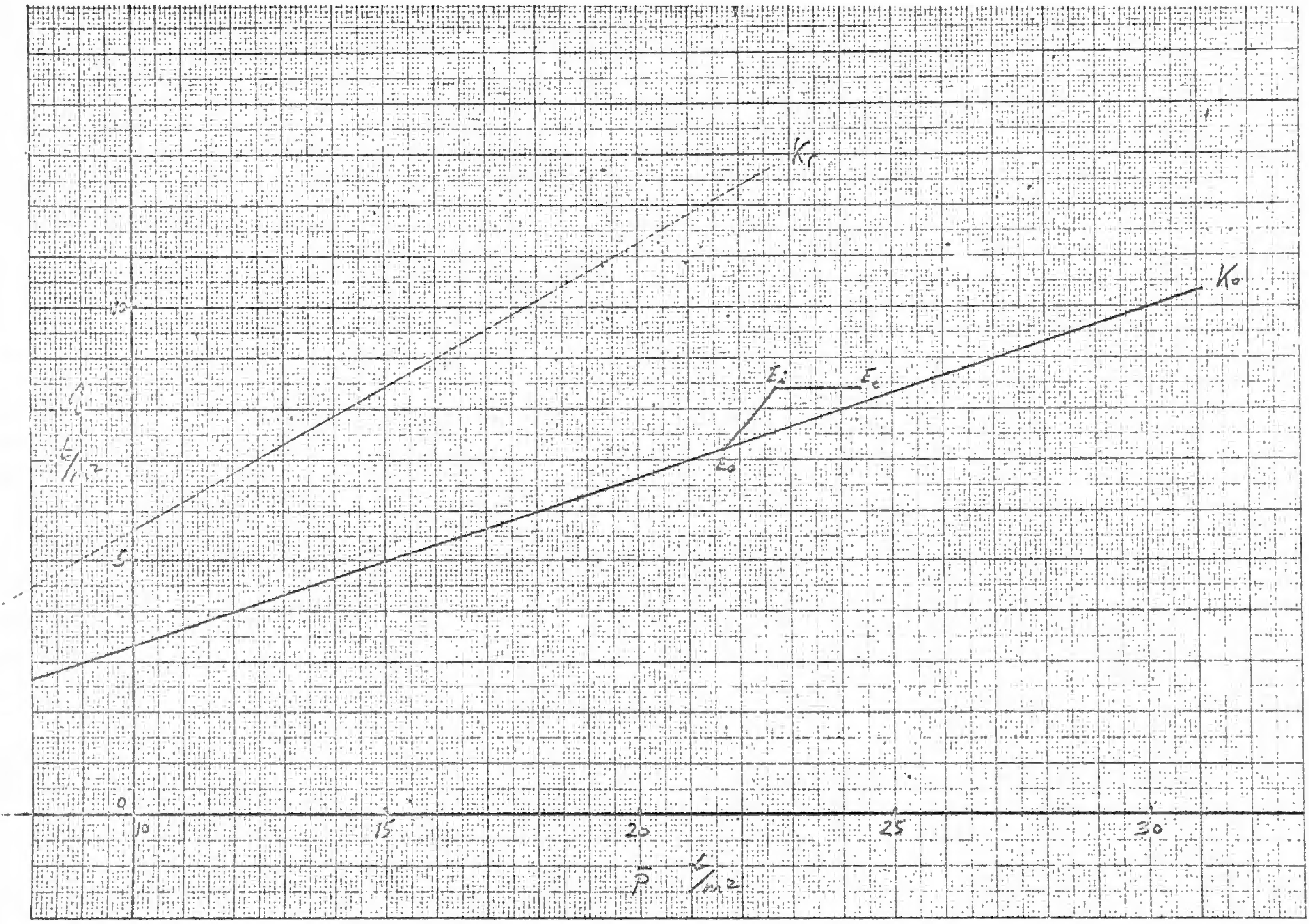

FIG VI-1c EFFECTIVE STRESS PATH IN CENTER OF CLAY III UNDER ℄ OF LOAD TEST

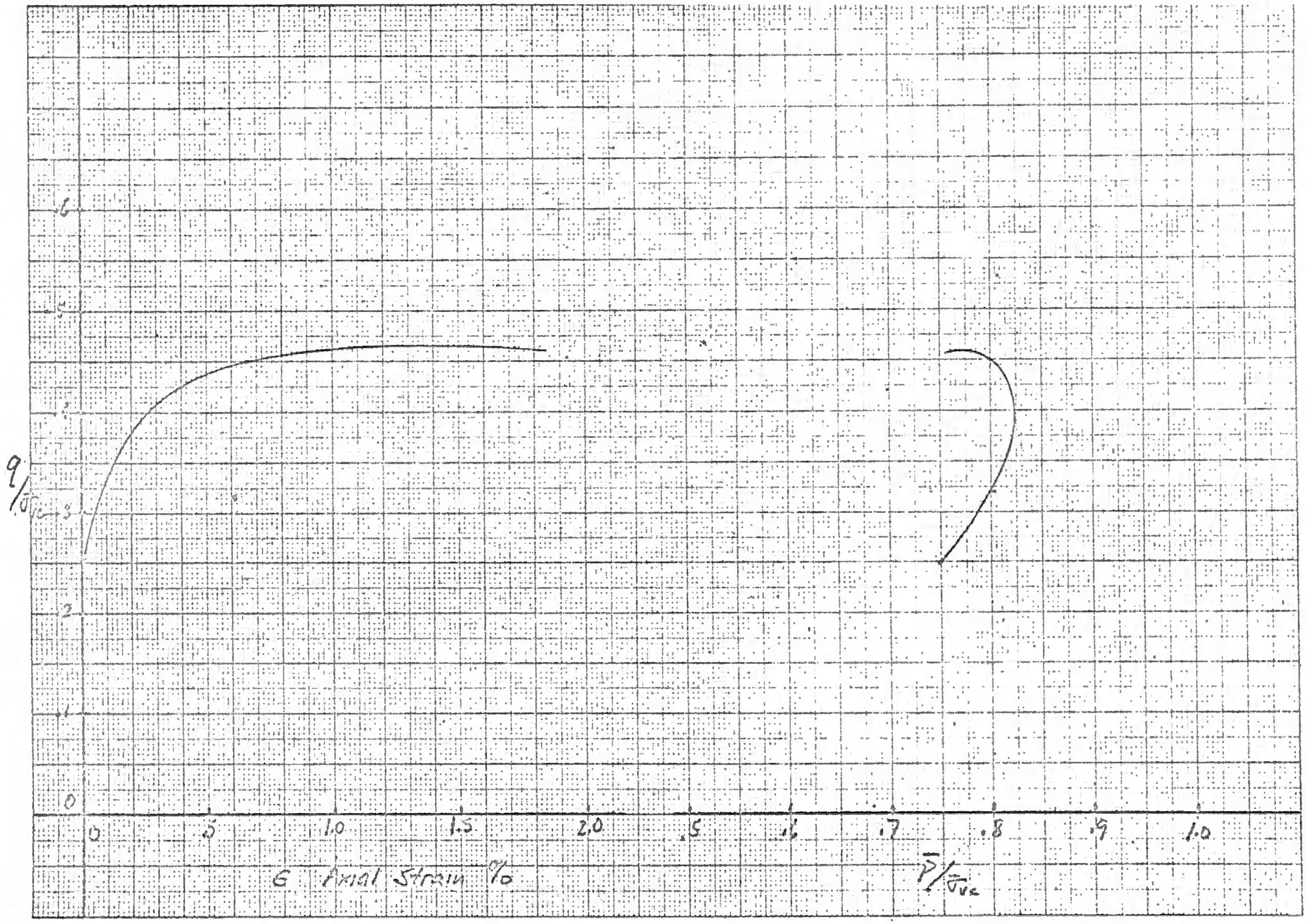

FIG VI-2a AVERAGES OF NORMALIZED DATA FOR CLAY I FROM TRIAXIAL TESTS REPORTED BY CARRIER (1966)

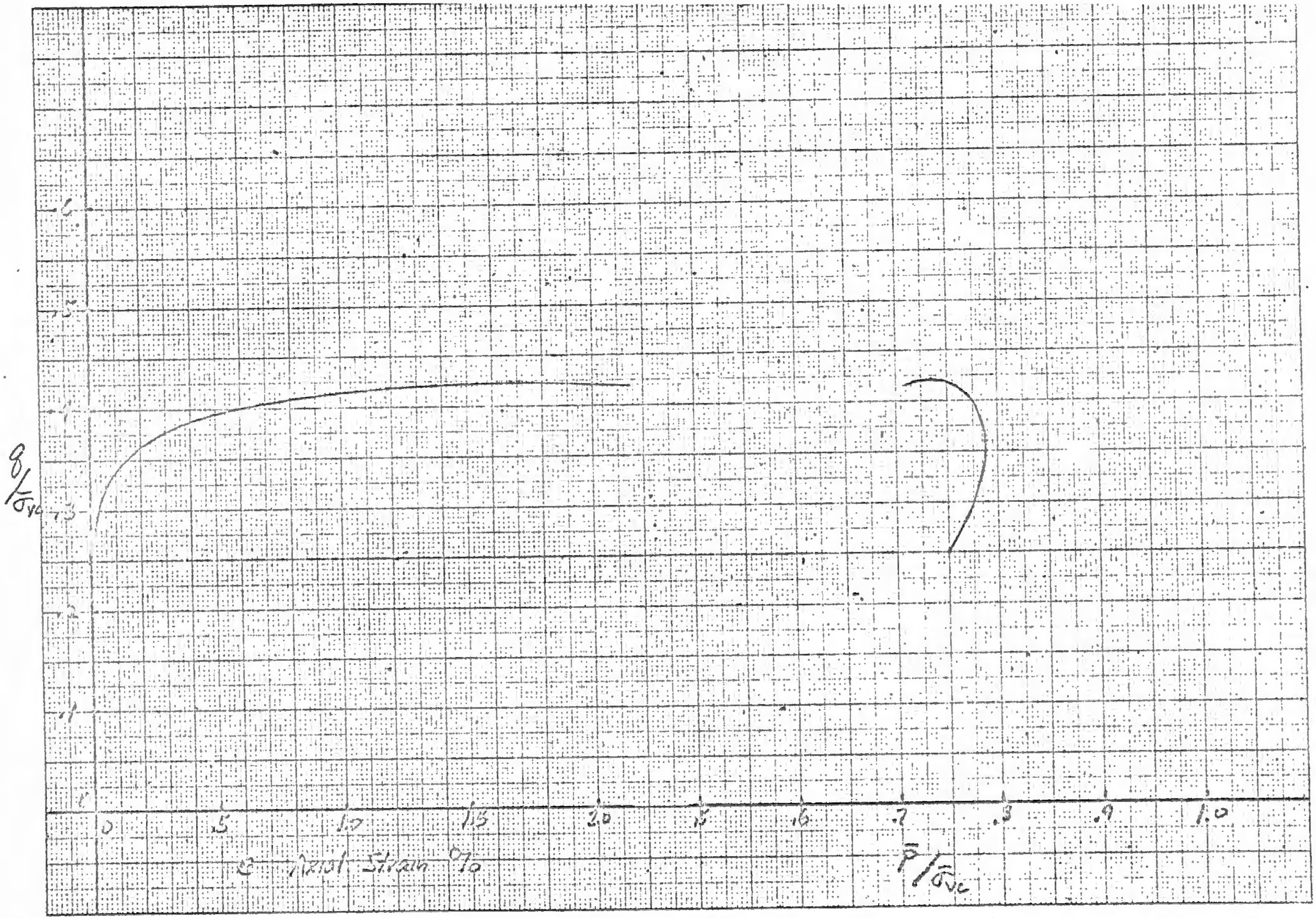

FIG VI-26 AVERAGES OF NORMALIZED DATA FOR CLAY II FROM TRIAXIAL TESTS REPORTED BY CARRIER (1966)

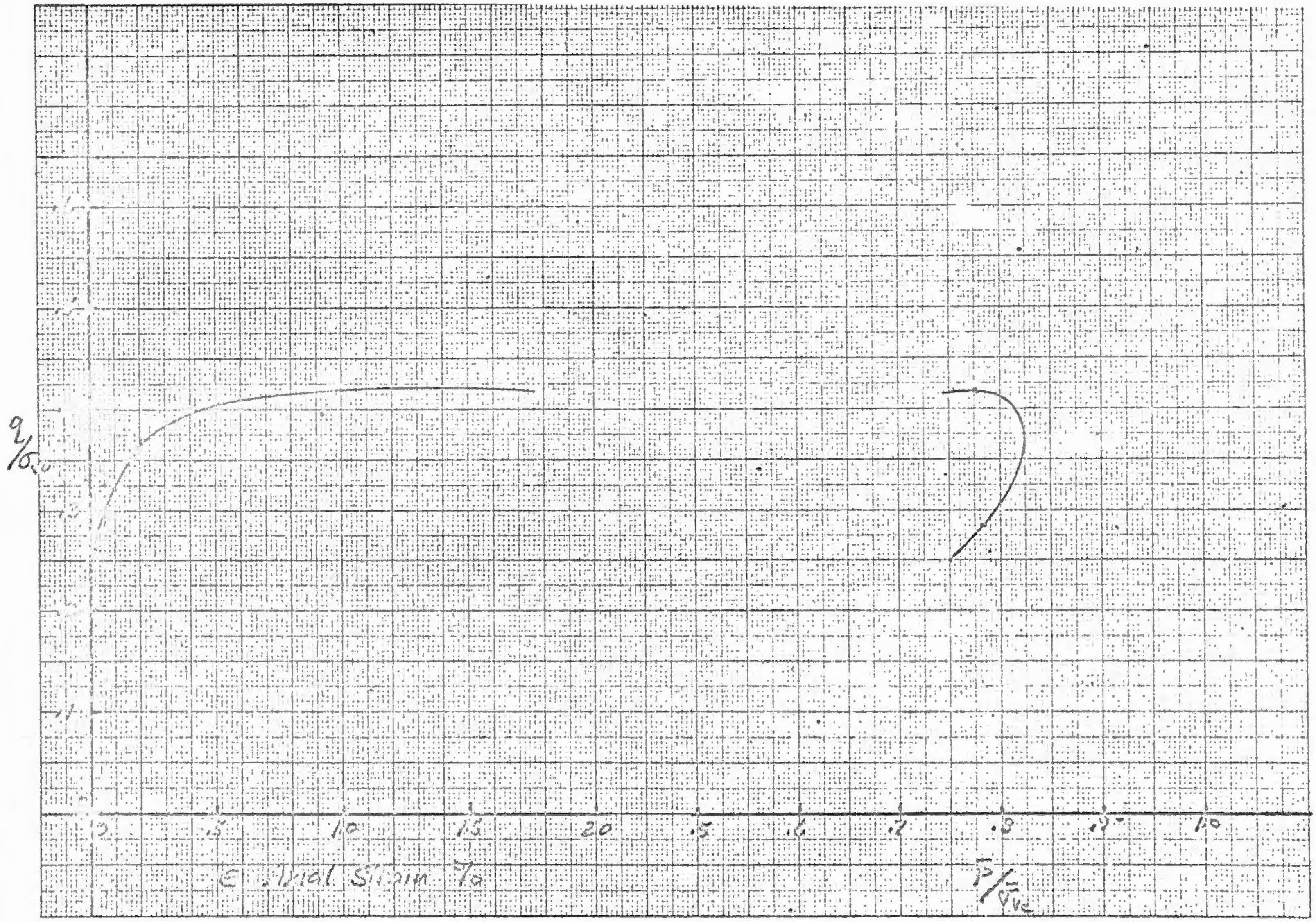

FIG VI-2c AVERAGES OF NORMALIZED DATA FOR CLAY III FROM TRIAXIAL TESTS REPORTED BY CARRIER (1966)

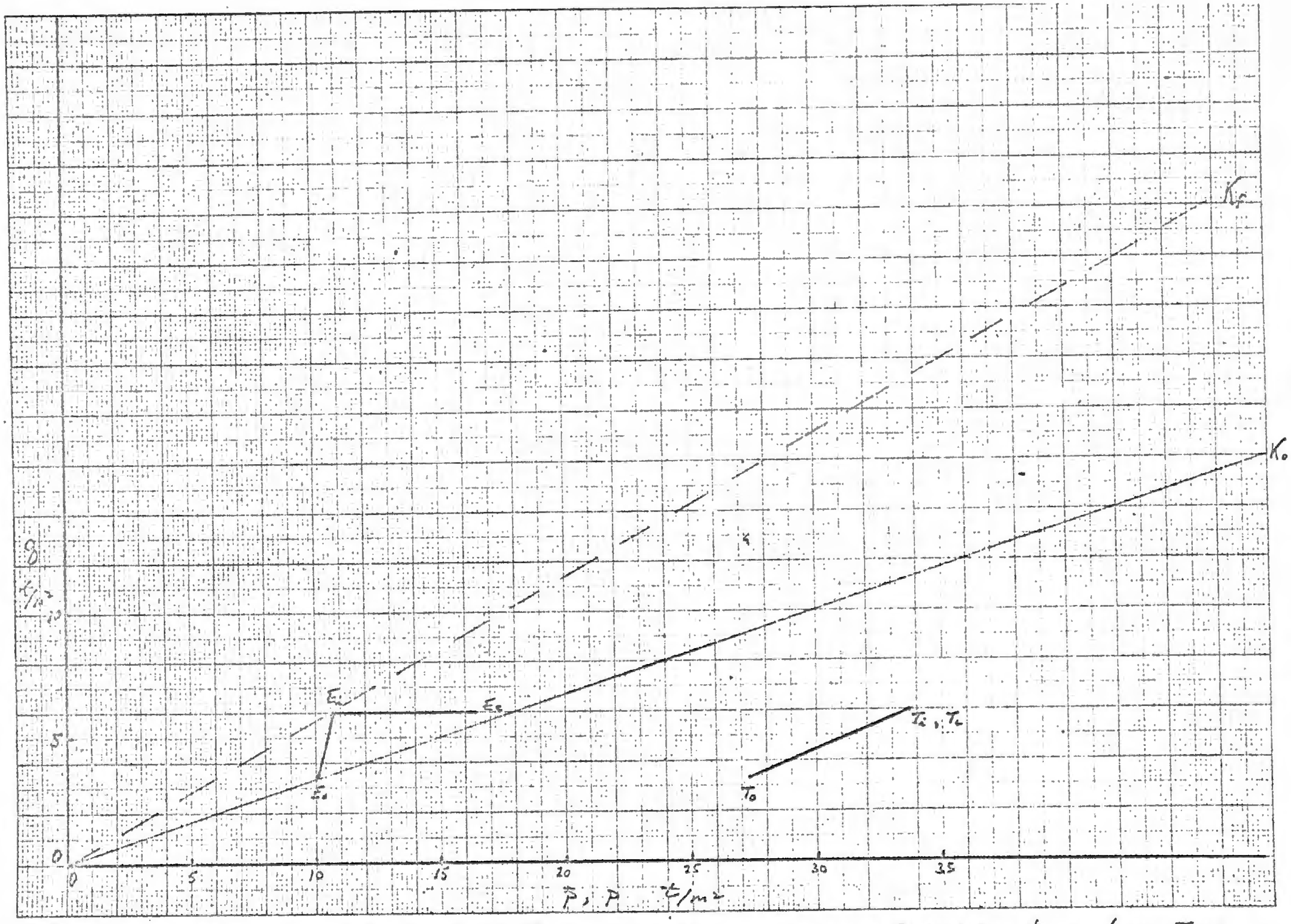

FIG VI-3 EFFECTIVE AND TOTAL STRESS PATHS FOR MIDDLE OF CLAY I UNDER ℄ OF LOAD TEST

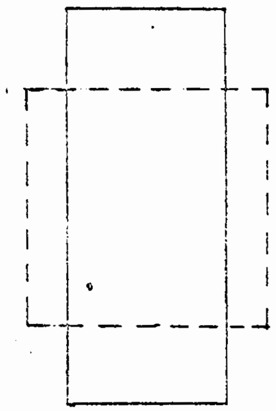

FIG VI-4a SOIL ELEMENT UNDER UNDRAINED SHEAR UNDERGOES SHAPE CHANGE BUT NO VOLUME CHANG

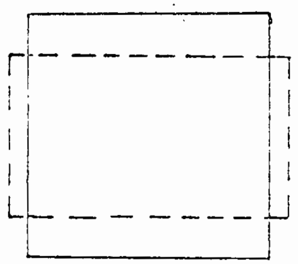

FIG VI-4b SOIL ELEMENT UNDER DRAINED CONSOLIDATION UNDERGOES SHAPE CHANGE AND VOLUME CHANGE

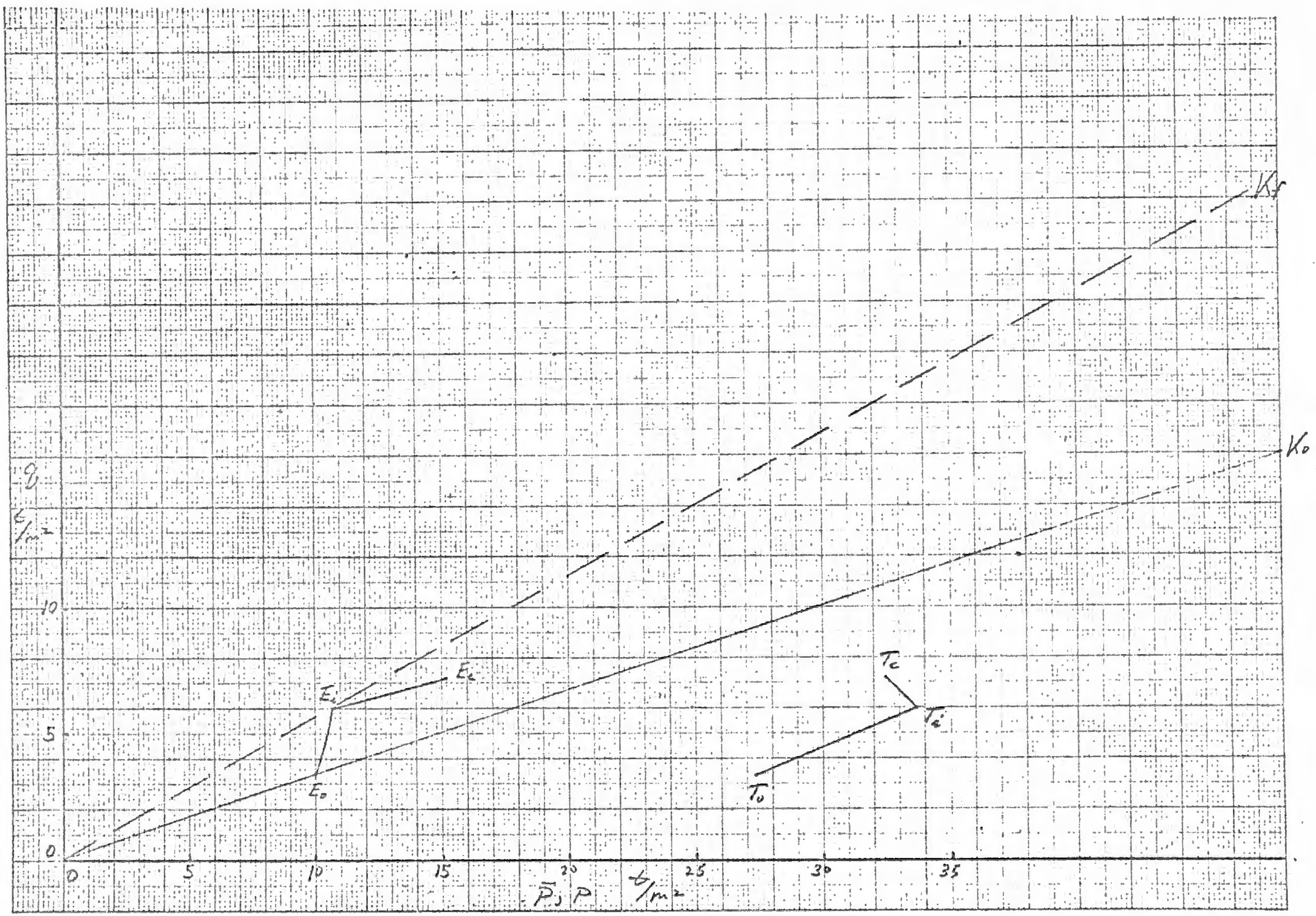

FIG VI-5 REVISED EFFECTIVE AND TOTAL STRESS PATHS FOR MIDDLE OF CLAY I UNDER ℄ OF LOAD TEST

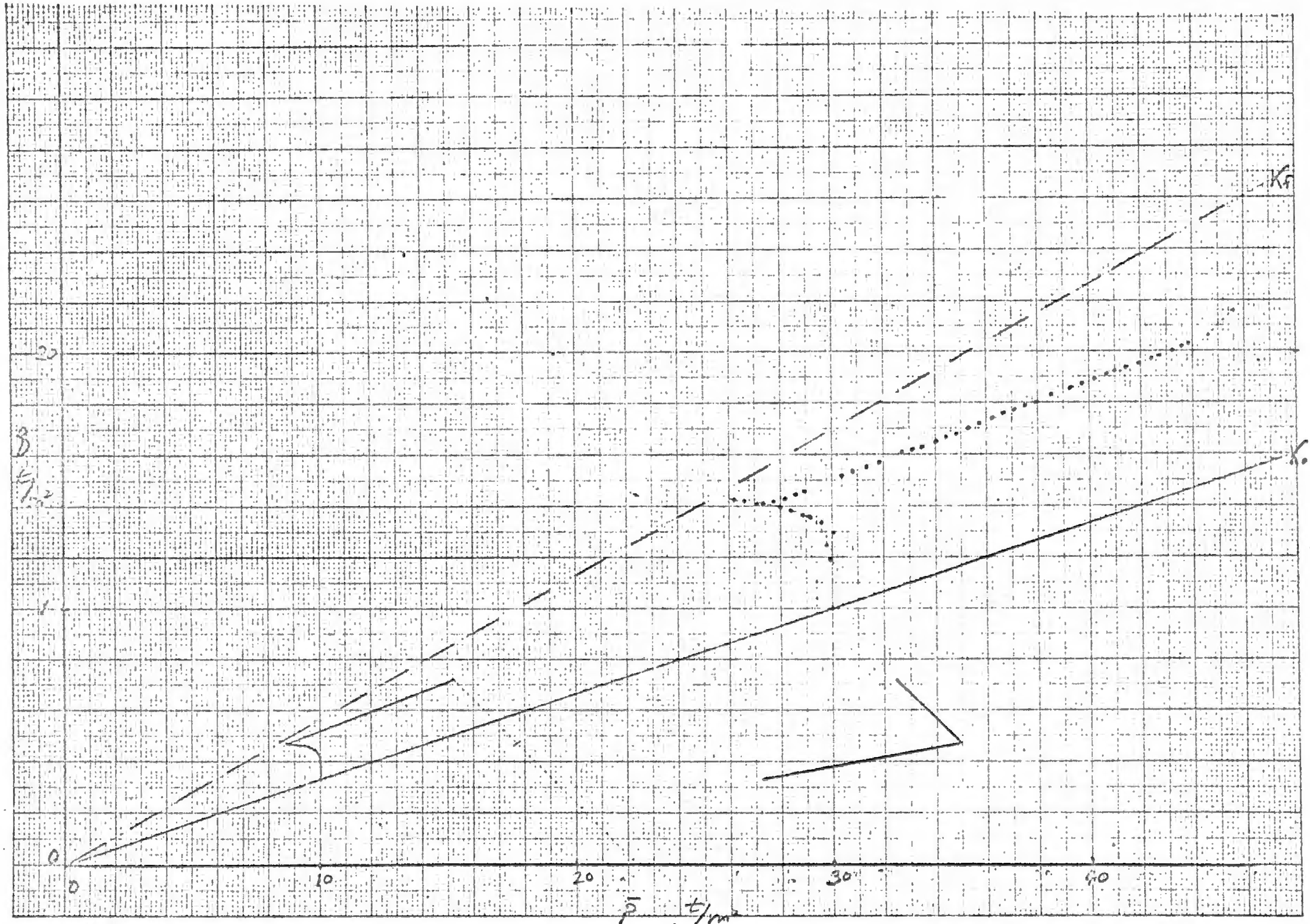

FIG VI-6 BEST ESTIMATE OF EFFECTIVE AND TOTAL STRESS PATH IN FIELD FOR CLAY I AND LAB. STRESS PATH

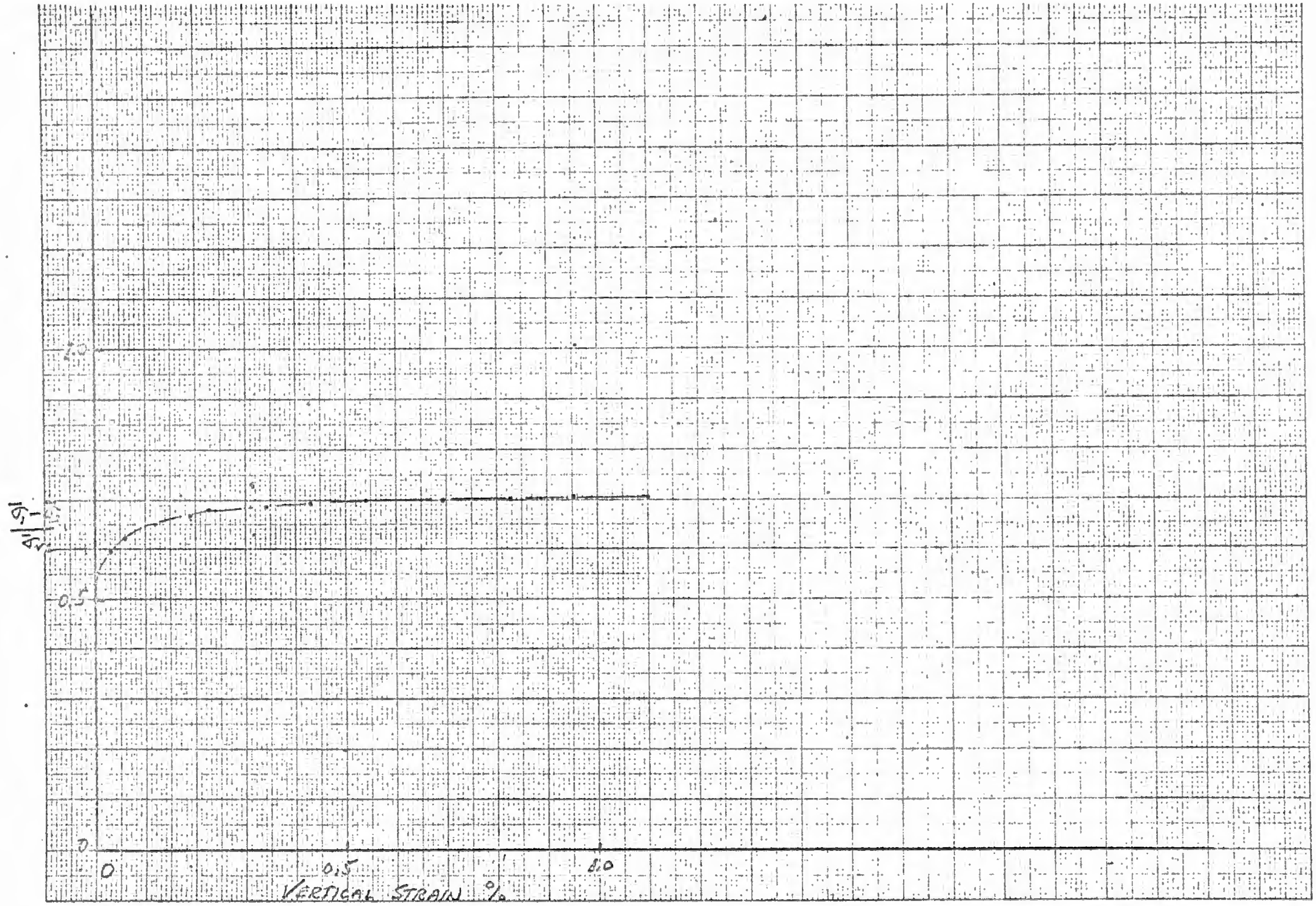

TABLE VI-7 NORMALIZED STRESS DIFFERENCE VS VERTICAL STRAIN - UNDRAINED PORTION OF STRESS PATH TEST

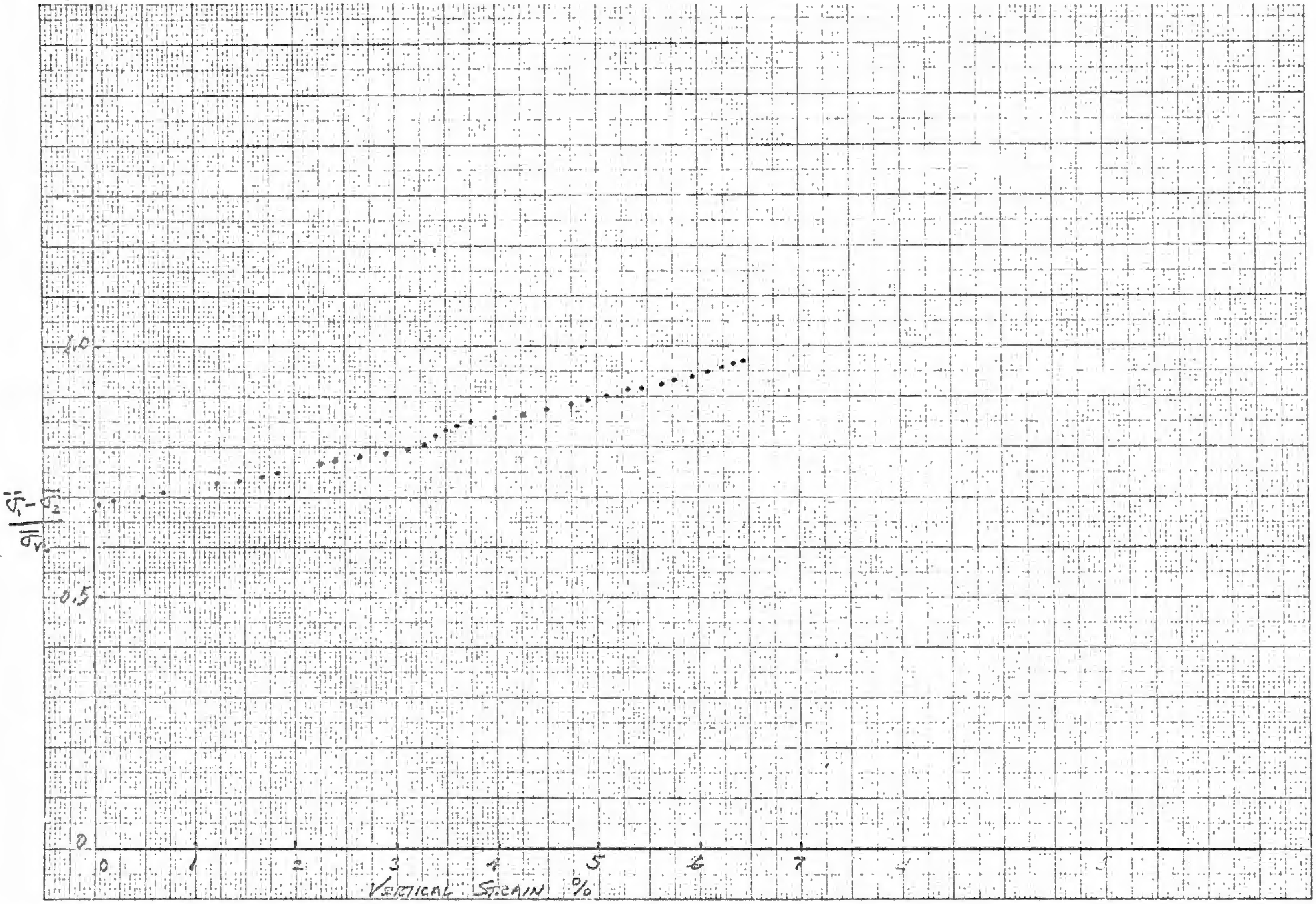

TABLE VI-8 NORMALIZED STRESS DIFFERENCE VS VERTICAL STRAIN - DRAINED PORTION OF STRESS PATH TEST.

LIST OF TABLES

TABLE NO.		PAGE
III-1	Immediate Settlement and Consolidation Settlement After 36 Days	98
III-2	Initial Excess Pore Pressures (First Estimate)	99
III-3	Percent Consolidation (First Estimate)	100
III-4	Initial Excess Pore Pressures (Revised)	101
III-5	Percent Consolidation (Revised)	102
IV-1	Comparison of Predicted and Measured Immediate Settlements	103
IV-2	Comparison of Estimated and Predicted Magnitudes of Compression	104
V-1a	Undrained Moduli and Poisson's Ratio As Determined by Wong (1968)	105
V-1b	Drained Moduli and Poisson's Ratio as Determined by Wong (1968)	106
VI-1	Initial Excess Pore Pressure and Compression as Predicted by One-Dimensional Analysis Using the Finite Element Technique and Elastic Theory	107
VI-2	A Factors Used in the Skempton-Bjerrum Method	108
VI-3	Initial Excess Pore Pressure and Compression as Predicted by the Skempton-Bjerrum Method Using the Finite Element Technique	109
VI-4	Values Used in Constant Shear Stress Paths	110
VI-5	Values Used for Undrained Portion of Constant Total Stress Path	111
VI-6	Initial Excess Pore Pressure and Compression as Predicted by the Lambe Stress Path Method Using the Finite Element Technique	112
VI-7	Values Used in Changing Total Stress Path - Clay I	113

TABLE NO. PAGE

VI-8 Initial Excess Pore Pressure and Compression of Clay I as Predicted by Lambe Stress Path Method 114

VII-1 Summary of Initial Excess Pore Pressures and Compressions 115

	ρ_i (METERS)	ρ_c 36 days (METERS)	ρ_{Total} 36 days (METERS)
NO TREATMENT			
FILL	0.24	0.315	0.555
CLAY I	0.075	0.305	0.380
CLAY II+III	0.04	0.07	0.11
TOTALS	0.355	0.690	1.045
PAPER DRAIN			
FILL	0.24	0.27	0.51
CLAY I	0.10	0.31	0.41
CLAY II+III	0.04	0.085	0.125
TOTALS	0.38	0.665	1.045
AVERAGE			
FILL	0.24	0.293	0.533
CLAY I	0.088	0.307	0.395
CLAY II+III	0.04	0.077	0.117
TOTALS	.368	0.677	1.045

TABLE III-1 IMMEDIATE SETTLEMENT AND CONSOLIDATION SETTLEMENT AFTER THIRTY SIX DAYS

PIEZOMETER	ELEVATION (METERS)	SOIL	Δu_i (METERS)
UNDER CENTER OF LOAD TEST			
P1, 2, 3	+1.7, -1.0, -3.3	FILL	≈ 0
P4	-13.3	CLAY I	11.6 - 6.0 = 5.6
P5A	-23.8	CLAY II	14.5 - 5.7 = 8.8
P6A	-42.3	CLAY III	4.2 - 2.3 = 1.9
P7	-49.8	DENSE SAND, CLAY	≈ 0
TWELVE METERS FROM CENTER OF LOAD TEST			
P8, 9, 10	-14.0	CLAY I	12.7 - 6.0 = 6.7

TABLE III-2 INITIAL EXCESS PORE PRESSURES
(FIRST ESTIMATE)

	CLAY I -14.0m	CLAY II -28.5m	CLAY III -41.0m
UNDER LOAD TEST			
3 MONTHS	17.3	5.6	13.0
6 MONTHS	34.5	9.9	21.8
9 MONTHS	51.7	15.5	26.0
1 YEAR	69.0	18.3	30.4
TO STEADY STATE			
3 MONTHS	13.5	3.1	6.0
1 YEAR	47.8	12.5	15.5

TABLE III-3 PERCENT CONSOLIDATION
(FIRST ESTIMATE)

PIEZOMETER	ELEVATION (METERS)	SOIL	Δu_i (METERS)
UNDER CENTER OF LOAD TEST			
P1.2,3	+1.7,-1.0,-3.3	FILL	≈ 0
P4	-13.3	CLAY I	15.5 - 6.0 = 9.5
P5	-23.8	CLAY II	9.1 - 5.7 = 3.4
P6A	-42.3	CLAY III	4.3 - 2.3 = 2.0
P7	-49.8	DENSE SAND, CLAY	≈ 0
TWELVE · METERS FROM CENTER OF LOAD TEST			
P8, 9, 10	-14.0	CLAY I	15.5 - 6.0 = 9.5

TABLE III-4 INITIAL EXCESS PORE PRESSURES (REVISED)

	CLAY I -14.0 m	CLAY II -28.5 m	CLAY III -41.0 m
UNDER LOAD TEST			
3 MONTHS	53.0	50.0	15.0
6 MONTHS	64.0	66.7	25.0
9 MONTHS	73.0	76.6	35.0
1 YEAR	79.0	83.0	43.3
TO STEADY STATE			
3 MONTHS	42.0	17.5	16.3
1 YEAR	58.5	33.4	28.6

TABLE III-5 PERCENT CONSOLIDATION
(REVISED)

PREDICTED (CARRIER) (Centimeters)		MEASURED (centimeters)	
		Paper Drain Section	No Treatment Section
FILL			
One Dimensional	0	24.0	24.0
Skempton-Bjerrum	14.7		
Lambe Stress Path	14.7		
CLAY I			
One Dimensional	0	10.0	7.5
Skempton-Bjerrum	15.0		
Lambe Stress Path	15.0		
CLAY II		CLAY II + III	
One Dimensional	0	4.0	4.0
Skempton-Bjerrum	8.2		
Lambe Stress Path	8.2		
CLAY II			
One Dimensional	0		
Skempton Bjerrum	0.5		
Lambe Stress Path	0.5		
CLAY II + III			
One Dimensional	0		
Skempton-Bjerrum	8.7		
Lambe Stress Path	8.7		

TABLE IV-1 COMPARISON OF PREDICTED AND MEASURED IMMEDIATE SETTLEMENTS

	CLAY I (Meters)		CLAY II+III (Meters)
ESTIMATED FROM FIELD DATA	0.72		0.48
PREDICTED BY CARRIER (1966)			
ONE DIMENSIONAL ANALYSIS	0.89		0.81
SKEMPTON - BJERRUM METHOD	0.55		0.37
LAMBE STRESS PATH METHOD	0.83		0.41

TABLE IV-2 COMPARISON OF ESTIMATED AND PREDICTED MAGNITUDES OF COMPRESSION

	MODULI DETERMINED FROM STRESS LEVEL AND FINITE ELEMENT TECH (T/m^2)		MODULI BACKFIGURED FROM LOAD TEST (T/m^2)		POISSON'S RATIO
	CIU TESTS	CAU TESTS	CIU TESTS	CAU TESTS	
FILL	—	—	—	150 (drained)	0.33 (drained)
CLAY I	1360	740	715	620	0.5
CLAY II	3000	1290	2320	1770	0.5
CLAY III	4380	4380	4420	4600	0.5

TABLE V-1a UNDRAINED MODULI AND POISSON'S RATIO AS DETERMINED BY WONG (1968)

	MODULI DETERMINED BY ELASTIC THEORY (T/m^2)	
	POISSON'S RATIO = 0.33	POISSON'S RATIO = 0.00
FILL	81	121
CLAY I	121	182
CLAY II	107	163
CLAY III	237	400

TABLE V-16 DRAINED MODULI AND POISSON'S RATIO AS DETERMINED BY WONG (1968)

	FINITE ELEMENT				ELASTIC THEORY			
LAYER	FILL	CLAY I	CLAY II	CLAY III	FILL	CLAY I	CLAY II	CLAY III
C_c	0.49	0.67	1.25	0.45	0.49	0.67	1.25	0.45
e_o	1.50	1.80	2.40	1.27	1.50	1.80	2.40	1.27
H (m)	11.4	14	15	10	11.4	14	15	10
$\bar{\sigma}_{vo}$ (t/m^2)	5.3	13.3	21.3	28.9	5.3	13.3	21.3	28.9
$\Delta\bar{\sigma}_v$ (t/m^2)	10.2	9.1	6.3	4.4	10.0	7.7	4.9	3.2
Δu (m)	10.2	9.1	6.3	4.4	10.0	7.7	4.9	3.2
ρ_c (m)	1.04	0.75	0.61	0.12	1.03	0.66	0.49	0.10

TABLE VI-1 INITIAL EXCESS PORE PRESSURE AND COMPRESSION AS PREDICTED BY ONE DIMENSIONAL ANALYSIS USING THE FINITE ELEMENT TECHNIQUE AND ELASTIC THEORY

LAYER	FILL	CLAY I	CLAY II	CLAY III
(UNDRAINED) STRAIN % (LOAD TEST)	2.10	0.64	0.20	0.10
A FACTOR ($\overline{\text{CIU}}$ TESTS)	—	0.62	0.47	0.59
A FACTOR ($\overline{\text{CAU}}$ TESTS)	—	0.47	0.35	0.29

TABLE VI-2 A FACTORS USED IN THE SKEMPTON BJERRUM METHOD

	$\overline{CIU}$				$\overline{CAU}$			
LAYER	FILL	CLAY I	CLAY II	CLAY III	FILL	CLAY I	CLAY II	CLAY III
H (m)	11.4	14.0	15.0	10.0	11.4	14.0	15.0	10.0
A		0.62	0.47	0.59		0.47	0.35	0.29
$\Delta\bar{\sigma}_1$ (t/m^2)	10.2	9.1	6.3	4.4	10.2	9.1	6.3	4.4
$\Delta\bar{\sigma}_3$ (t/m^2)	4.1	3.7	1.5	1.9	4.1	3.7	1.5	1.9
$\Delta u = \Delta\sigma_3 + A(\Delta\sigma_1 - \Delta\sigma_3)$ (m)		7.05	3.75	3.37		6.24	3.18	2.63
M_v		.00553	.00590	.00258		.00540	.00590	.00263
$\rho_c = H M_v \Delta u$ (m)		.545	.332	.087		.471	.281	.069

TABLE VI-3 INITIAL EXCESS PORE PRESSURE AND COMPRESSION AS PREDICTED BY THE SKEMPTON BJERRUM METHOD USING THE FINITE ELEMENT TECHNIQUE

LAYER	FILL	CLAY I	CLAY II	CLAY III
K_0	0.5	0.5	0.5	0.5
$\bar{\sigma}_{v0}$ (t/m^2)	5.3	13.3	21.3	28.9
$\bar{\sigma}_{h0} = K_0 \bar{\sigma}_{v0}$ (t/m^2)	2.65	6.65	10.65	14.45
$\Delta\bar{\sigma}_1$ (t/m^2)	10.2	9.1	6.3	4.4
$\Delta\bar{\sigma}_3$ (t/m^2)	4.1	3.7	1.5	1.9
$\bar{\sigma}_{vf}$ (t/m^2)	15.5	22.4	27.6	33.3
$\bar{\sigma}_{hf}$ (t/m^2)	6.75	10.35	12.15	16.35
$\bar{p}_f$ (t/m^2)	11.13	16.33	19.88	24.83
q_f (t/m^2)	4.38	5.98	7.73	8.48
$\bar{p}_0$ (t/m^2)	3.98	10.0	16.0	21.7
q_0 (t/m^2)	1.32	3.3	5.3	7.2

TABLE VI-4 VALUES USED IN CONSTANT SHEAR STRESS PATHS (FIGS. VI-1a, b, c)

LAYER	CLAY I	CLAY II	CLAY III
VERTICAL STRAINS (%)	0,64	0,20	0.10
$q/\bar{\sigma}_{vc}$ figs VI-2a,b,c	0,45	0,33	0,29
$\bar{p}/\bar{\sigma}_{vc}$ figs VI-2a,b,c	0.80	0.79	0.79
$\bar{\sigma}_{vc}$ (t/m^2)	13,3	21,3	28,9
q (t/m^2)	6.0	7.7	8,4
$\bar{p}$ (t/m^2)	10,65	16.8	22.7

TABLE VI-5 VALUES USED FOR UNDRAINED PORTION OF CONSTANT TOTAL STRESS PATH (FIGS. VI-1a, b, c)

LAYER	CLAY I	CLAY II	CLAY III
$\Delta u = \bar{P}_f - \bar{P}_i$ (m)	5.68	2.80	1.68
$\bar{P}_f / \bar{P}_i$	1.57	1.17	1.08
VERTICAL STRAIN (%)	5.75	1.40	NO DATA
H (m)	14	15	10
ρ_c (m)	.805	.21	—

TABLE VI-6 INITIAL EXCESS PORE PRESSURE AND COMPRESSION AS PREDICTED BY THE LAMBE STRESS PATH METHOD USING THE FINITE ELEMENT TECHNIQUE (FIGS VI-1a, b, c)

LAYER	K_o	$\bar{\sigma}_{vo}$ (t/m^2)	$\bar{\sigma}_{ho}$ (t/m^2)	p_o (t/m^2)	q_o (t/m^2)	$\Delta\sigma_1$ (t/m^2)	$\Delta\sigma_3$ (t/m^2)	$\bar{\sigma}_{vf}$ (t/m^2)	$\bar{\sigma}_{hf}$ (t/m^2)	$\bar{p}_f$ (t/m^2)	q_f (t/m^2)
CLAY I	0.5	13.3	6.65	10.0	3.3	9.1	1.3	22.4	7.95	15.18	7.23

TABLE VI-7 VALUES USED IN CHANGING TOTAL STRESS PATH - CLAY I
(FIG VI-5)

LAYER	Δu (m)	VERTICAL STRAIN (%)	H (m)	ρ_c (m)
CLAY I	9.1	6.46	14	.905

TABLE VI-8 INITIAL EXCESS PORE PRESSURE AND COMPRESSION OF CLAY I AS PREDICTED BY LAMBE STRESS PATH METHOD (FIG VI-6)

	CLAY I		CLAY II		CLAY III		CLAY II+III
	Δu (m)	ρ_c (m)	Δu (m)	ρ_c (m)	Δu (m)	ρ_c (m)	ρ_c (m)
A. MEASURED (FIELD)	9.5	.72	2.9		2.0		.48
B. CARRIER'S PREDICTIONS							
I ONE DIMENSIONAL	10.8	.89	10.8		10.8		.81
II. SKEMPTON-BJERRUM							
a. ELASTIC THEORY	4.8	.55	3.8		0.7		.37
III. LAMBE STRESS PATH							
a. ELASTIC THEORY	4.8	.83	3.8		0.7		.41
C. AUTHOR'S PREDICTIONS							
I ONE DIMENSIONAL							
a. ELASTIC THEORY	7.7	.66	4.9	.49	3.2	.10	.59
b. FINITE ELEMENT	9.1	.75	6.3	.61	4.4	.12	.73
II SKEMPTON-BJERRUM							
a. FINITE ELEMENT							
1. $\overline{CAU}$	7.05	.55	3.8	.33	3.4	.09	.42
III LAMBE STRESS PATH							
a. FINITE ELEMENT							
1. CONSTANT TOTAL STRESS	5.68	.81	2.8	.21	1.7		
2. CHANGING TOTAL STRESS	9.1	.91					

TABLE VII-1 SUMMARY OF INITIAL EXCESS PORE PRESSURES AND COMPRESSIONS

LIST OF REFERENCES

1. Carrier, W.D., "Settlement Analysis of the Toa Industrial Site, Kawasaki, Japan", thesis presented to Massachusetts Institute of Technology, at Cambridge, Mass., in partial fulfillment of the requirements for the degree Master of Science in Civil Engineering, September, 1966.

2. Guertin, J.D., "Stability and Settlement Analysis of an Embankment on Clay", thesis presented to the Massachusetts Institute of Technology, at Cambridge, Mass., in partial fulfillment of the requirements for the degree Master of Science in Civil Engineering, June 1967.

3. Kajima Construction Co., Ltd., and Oyo Chishitsu Chosa Jimusho, Load Test in Tonen's Area B, Ukijima-Cho, Kawasaki City, Report prepared for Toa Nenryo Kogyo Co., Ltd., and Dr. T. W. Lambe, Consultant, December 30, 1966.

4. Ladd, C.C., "Stress-Strain Modulus of Clay in Undrained Shear", Journal of the Soil Mechanics and Foundation Division, ASCE, Vol. 90, No. SM5, Proc. Paper 4039, September, 1964.

5. Ladd, C.C., "Stress-Strain Behavior of Anisotropically Consolidated Clays During Undrained Shear", Proceedings, 6th International Conference on Soil Mechanics, Montreal, Canada, 1965.

6. Lambe, T.W., Soil Engineering Studies for the Kawasaki Industrial Site, Kawasaki, Japan, Consulting report prepared for the Esso Research and Engineering Company, October, 1962.

7. Lambe, T.W., "Methods of Estimating Settlements", Journal of the Soil Mechanics and Foundations Division, ASCE, Vol. 90, No. SM5, Proc. Paper 4060, September, 1964.

8. Lambe, T.W., "Stress Path Method", Journal of the Soil Mechanics and Foundations Division, ASCE, Vol. 93, No. SM6, Proc. Paper 5613, November, 1967.

9. Lambe, T.W., and Whitman, R.V., An Introduction to Soil Mechanics, Preliminary Edition, Wiley, New York, 1967.

10. Lambe, T.W., "Engineering Characteristics of Reclaimed Land", To be published, 1968.

11. Skempton, A.W., and Bjerrum, L., "A Contribution to the Settlement Analysis of Foundations on Clay", Geotechnique, 7, pp. 168-178.

12. Taylor, D.W., Fundamentals of Soil Mechanics, Wiley, New York, 1948.

13. Wong, I.H., "Foundation Studies of a Kawasaki, Japan, Industrial Site", thesis presented to Massachusetts Institute of Technology, at Cambridge, Mass., in partial fulfillment of the requirements for the degree Master of Science in Civil Engineering, June, 1968.